Endomembrane markers and stress: a functional study using Arabidopsis plants

João Pedro Oliveira Neves
Biologia Funcional e Biotecnologia de Plantas
Departamento de Biologia
2022

Supervisor
Cláudia Pereira, Invited auxiliary professor, GreenUPorto, FCUP

Co-supervisor
José Pissarra, Associate Professor, GreenUPorto, FCUP

Co-supervisor
Cristiano Soares, Post-doc researcher, GreenUPorto, FCUP

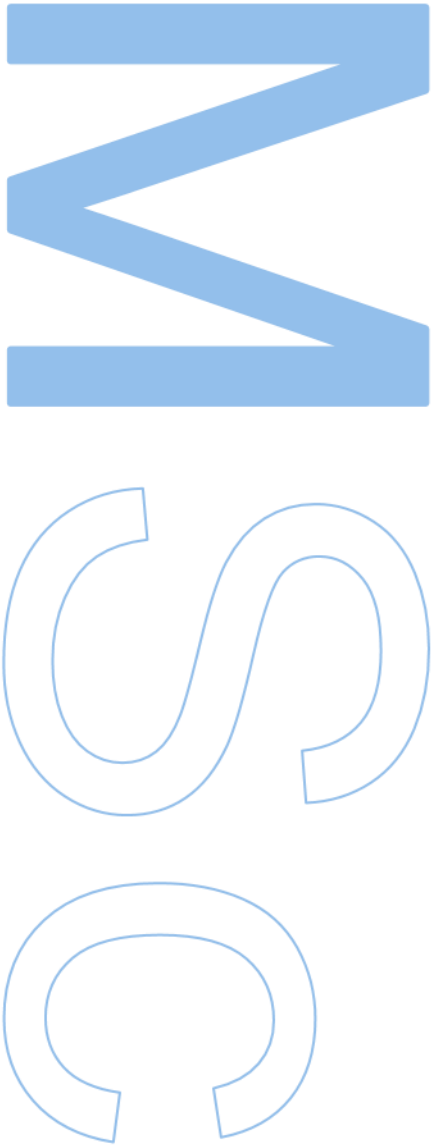


U.PORTO
FACULDADE DE CIÊNCIAS
UNIVERSIDADE DO PORTO

Sworn Statement

I, João Pedro Oliveira Neves, enrolled in the Master Degree Functional Biology and Plant Biotechnology at the Faculty of Sciences of the University of Porto hereby declare, in accordance with the provisions of paragraph a) of Article 14 of the Code of Ethical Conduct of the University of Porto, that the content of this dissertation/ internship report/ project [choose accordingly] reflects perspectives, research work and my own interpretations at the time of its submission.

By submitting this dissertation/ internship report/ project [choose accordingly], I also declare that it contains the results of my own research work and contributions that have not been previously submitted to this or any other institution.

I further declare that all references to other authors fully comply with the rules of attribution and are referenced in the text by citation and identified in the bibliographic references section. This dissertation/ internship report/ project [choose accordingly] does not include any content whose reproduction is protected by copyright laws.

I am aware that the practice of plagiarism and self-plagiarism constitute a form of academic offense.

Acknowledgements

“Nothing new that is really interesting comes without collaboration”

- James D. Watson

A great year as passed, full of new experiences and challenges to overcome. I start my dissertation with this quote because without the persons I will mention this work could not be fulfilled, and this is my way to show my appreciation for their contribution.

Starting with Dr. Cláudia Pereira, the person that received me in PSI Lab 4 years ago and since then has been a pleasure and an honour to be part of the team leaded by her. Cláudia always made me feel that I had my own project, allowing me to fail, gain autonomy, gain critic spirit, and most of all scientific rigour. This would not be possible without her patience, appreciation, trust and numerous advice. All of it led me to where I am today, with the confidence to go further with my scientific career, and the necessary confidence to publish these results. For all of this, I am most grateful!

Second to Professor José Pissarra for having received me with open arms in the laboratory, for your kindness, for the effort in improving my scientific communication skills, for all the knowledge shared, and for always having an open door. For all of it, I am most grateful!

To Professor Ana Séneca and Professor Susana Pereira, for all the knowledge shared, for the kind words, and for all the guidance that helped me to reach this stage. To you professors, thank you!

To Cristiano Soares (Cris) and Bruno Sousa, my co-orientator and my lab tutor in all the biochemistry assays. Without the way you received me in your laboratory, the availability, the patience to check every result and repeat the assays if necessary, and for all the friendship and good moments lived in 2.62, I am thankful for that!

To my lab brother and housemate, Miguel, for all the patience, the adventures, the knowledge share, the help when I felt more overloaded, and the most important of all, for being one of my biggest friends. Italy would not be the same without you, and you are one of the reasons that it is so memorable. I hope we can keep working together for many years and keep with the incredible dynamic that we have. For all of it, I am most grateful!

To Professor Gian Pietro DiSansebastiano for receiving me in his laboratory, for all the knowledge passed, for the hospitality. I am really grateful to have known you and having the opportunity to work with you. Grazzie professor!

I am also really grateful to had the opportunity of working with Monica, and thank you for your patience in protoplast protocol.

To my Italian friends, Grabiele, Piergiorgio, Makarena and Chiara for all the great moments that we have passed. I hope to back to Lecce, even if just to meet you guys, because I miss you. Grazzie per tutti!

To my master companions, Alejandro Pedro Nadais e Carla Alejandro, for all the support during these 2 years of the master, for making all the group works look better than what they were, and the most important of all, for being great friends. To you thank you!

To my “intern” and big friend, Monteiro, for all the companionship, dedication and help in the lab. I hope to still be part of your scientific career and see you grow and reach where you intend to be. To you my friend I owe you a big thank you!

To PSI Lab team, Tatiana, Inês, Diana, Vanessa, Marta for all the great moments we pass in the lab, and for all your help. I am glad to be part of an incredible team! To you, thank you!

To Plant Stress Lab team, Maria, Sofia, Filipa, Mafalda, for receiving me in such a great environment, for all the help and for the vast reggaeton/funk playlists played in the lab, allowing me to extend my musical horizons. To you, thank you!

To Zé and David, two brothers in arms, for all the support and kind words when I felt overwhelmed with lab work, or just life. To you I owe you a big thank you!

To my family, especially my parents, for making what I am today. Without your will to let me follow my objectives and dreams, without your values, without your belief in me, without all discussions, and without all the love, I would not be here today. Gratitude is not enough to express how I feel for all you did for me.

To all of you, thank you for being part of my life, without you I would not be here today. I hope you keep up with me in my next challenges!

Resumo

De modo a enfrentar condições ambientais adversas, capazes de afetar o crescimento e o desenvolvimento vegetal, as plantas necessitam de se adaptar. Nesse sentido, estes organismos conseguem alterar o seu padrão de desenvolvimento, modulando processos celulares, tais como o trânsito de proteínas e a ativação de sinais envolvidos na resposta ao stresse. Apesar de existirem inúmeros estudos focados na resposta fisiológica das plantas ao stresse, pouca atenção tem sido dada aos processos moleculares que controlam estas adaptações. Um estudo prévio no nosso laboratório demonstrou que diversas proteínas do sistema endomembranar se comportam de maneira distinta em plantas sob stress abiótico. Tendo isto em conta, o objetivo deste projeto consistiu em caracterizar plantas mutantes, por ausência de algumas daquelas proteínas, quando expostas a condições ambientais adversas. Para isso foram selecionados mutantes de *Arabidospsis* com inserções de T-DNA em genes alvo, realizaram-se estudos de exposição aguda a condições de stresse abiótico (salinidade, osmótico, oxidativo e toxicidade por metais) de modo a comparar as respostas fisiológicas (padrão de crescimento e pigmentos fotossintéticos), bioquímicas (marcadores de stresse oxidativo e defesa antioxidante – AOX) e moleculares (expressão de genes envolvidos em vias de trânsito intracelular) entre os vários genótipos. Foram utilizadas linhas knock-down, homozigóticas para os genes que codificam as proteínas VSR2 e EXO70. A primeira proteína desempenha um papel no trânsito para o vacúolo lítico, enquanto a segunda é uma subunidade fundamental para a formação do exocisto. Os resultados obtidos mostram que as duas linhas mutantes (*vsr2* e *exo70)* se comportam de formas distintas, entre elas e em relação a plantas silvestres, sendo que no mutante *vsr2* não se observa um aumento da expressão dos efetores do trânsito de proteínas para o vacúolo de armazenamento proteico, como era esperado, e mostra uma preferência pela resposta enzimática ao stress por parte do sistema antioxidante. Em contrapartida, no mutante *exo70*, alterações morfológicas são mais notórias nas plantas, como um atraso no desenvolvimento, assim como um investimento em mecanismos não enzimáticos por parte do sistema antioxidante, permitindo confirmar o exocisto como uma importante estrutura na tolerância/adaptação ao stress. Desta forma é possível observar que diferentes efetores do sistema endomembranar têm diferentes papéis no combate ao stress, e que se comportam de forma diferente quando um deles está oprimido. De notar que este é um trabalho pioneiro, visto que tenta conjugar uma resposta molecular, através do estudo de efetores

do sistema endomembranar com a resposta do sistema antioxidante, que desempenha um papel direto na resposta ao stress.

Palavras-chave: Stress abiótico; Trânsito vacuolar; Exocisto; Sistema antioxidante; SNAREs

Abstract

To cope adverse environmental conditions, capable of affecting plant growth and vegetal development, plants must adapt to overcome. To do it, these organisms can alter their development pattern by modulating cellular processes, such as protein trafficking and the activation of stress-responsive signals. Despite the huge number of studies regarding plant stress physiology, little attention has been given to the molecular mechanisms controlling these rearrangements. A previous study from our laboratory showed that some endomembrane system effectors have a differential expression upon exposure to abiotic stress conditions. Thereby, this project focused on the characterization of plants lacking these key players when exposed to abiotic stress conditions. To accomplish this, Arabidopsis mutants with T-DNA insertions in the genes of interest were selected, and an acute exposition of several abiotic conditions (saline, osmotic, oxidative, and metal-induced toxicity) was performed, to compare the ecophysiologic (growth pattern, photosynthetic pigments), biochemical (oxidative stress markers, and AOX defence) and molecular responses (expression of genes involved in protein sorting) between the genotypes. Two knockdown homozygous lines were obtained for VSR2 and EXO70 proteins. The first is an intermediate player in the Litic Vacuole trafficking and the second one is involved in the exocyst formation. The results obtained show that the two mutant lines (*vsr2* and *exo70)* behave differently, between them and in relation to wild type plants, and in the *vsr2* mutant there was no increase in the trafficking of proteins to the protein storage vacuole, as expected, and showed a preference for the enzymatic response to stress by the antioxidant system. On the other hand, in the *exo70* mutant, morphological changes were more noticeable in plants, such as a delay in development, as well as an investment in non-enzymatic mechanisms by the antioxidant system, allowing the confirmation of the exocyst as an important structure in tolerance/adaptation to the stress. In this way it's possible to observe that different endomembrane system effectors play different roles in stress response and behave differently when another player is oppressed. It should be noted that this is a pioneering work, as it attempts to combine a molecular response, through the study of effectors of the endomembrane system, with the response of the antioxidant system, which plays a direct role in the response to stress.

Keywords: Abiotic stress; Vacuolar trafficking; Exocyst; Antioxidant system; SNAREs

Table of Contents

List of Figures

List of Tables

List of Abbreviations and Acronyms

AIM	Short linear motif
AOX	Antioxidant
APX	Ascorbate peroxidase
AsA	Ascorbic acid
ATG	Autophagy-related
BSA	Bovine serum albumin
C	Control
CAT	Catalase
Chi	Chitinase A
Chl	chlorophyll
COPI	Coat protein complex I
COPII	Coat protein complex II
Ct	Cycle threshold
DTNB	5,5-dithio-bis-(2-nitrobenzoic acid)
DV	Dense vesicles
EDTA	Ethylenediaminetetraacetic acid
EE	Early endosome
ER	Endoplasmic reticulum
ERAD	ER-associated degradation
ERMEC	ER Microtubule-related Export Compartments
ETC	Eletron transport chain
EXPO	Exocyst-positive organelle
Fw	Fresh weight
GA	Golgi apparatus
gDNA	Genomic DNA
Gen	Gentamycin
GR	Glutathione reductase
GSH	Glutathione
GSSG	Oxidesed glutathione
H1	Lower concentration of osmotic stress
H2	Higher concentration of osmotic stress
Kan	Kanamycin
LB	Luria broth medium
LP	Lipid Peroxidation
LSP	Leaderless secretory protein
LV	Lytic vacuole
MDHA	Monodehydroascorbate
MNA	Methyl Nadic Anhydrin
MS	Murashige and Skoog medium
MVB	Multi-vesicular body
NaPIPES	Sodium 1,4-piperazine-diethane sulfonic acid
NASC	Nottingham Arabidopsis Stock Centre
OD_{600}	Optic density at 600 nm
ON	Overnight
Ox	Oxidative stress

PA	Protease associated domain
PAC	Precursor accumulating vesicles
PB	Protein Bodies
PCR	Polymerase chain reaction
PM	Plasma membrane
PMSF	Phenylmethylsulphonyl fluoride
Pro	Proline
PSI	Plant Specific insert
PSV	Protein storage vacuole
PVC	Pre-vacuolar Compartment
PVPP	Polyvinylpolypyrrolidone
qPCR	Quantitative PCR
RFP	Red fluorescente protein
RMR	Receptor homology-transmembrane-RING H2 proteins
RT	Room temperature
ROS	Reactive oxygen species
S1	Salt stress
SDS	Sodium dodecyl sulfate
SIGnAL	Salk institute Genomic Analysis Laboratory
SN	Supernatant
SNARE	Soluble N-ethylmaleimide-Sensitive Factor Attachment Protein Receptor
SOD	Superoxide dismutase
SYP	Syntaxins
TBA	Thiobarbituric acid
TCA	Trichloroacetic acid
TEM	Transmission electron microscopy
TET	Tetracycline
TGN	Trans-Golgi network
TIP	Tonoplast intrinsic protein
UPR	Unfolded protein response
VPS	Vacuolar protein sorting
VSD	Vacuolar sorting determinants
VSR	Vacuolar sorting receptor
VTI	Vesicular transport V-SNAREs
Zn	Metal induced stress

1. Introduction

Climate change is a major threat to crop development since it impacts multiple aspects of the agricultural systems, such as water availability, soil fertility, pathogen spread and host susceptibility. The combination of these factors can cause crop failures, leading to food insecurity in times where the demand for agricultural products keeps on the rising (Abberton et al., 2016; Mousavi-Derazmahalleh et al., 2019). Thereby, plants are in a constant changing environment, which often becomes unfavourable to their development (Zhu, 2016). Plants, as sessile organisms and most susceptible to abiotic stress conditions (Zhu, 2016; Mousavi-Derazmahalleh et al., 2019), have been evolving to be capable of adapting and taking advantage of these situations through multiple signalling pathways that lead to physiological adjustments, such as protein accumulation, alteration of the development patterns, and antioxidant system activation (Zhu, 2016; Kalinowska and Isono, 2018; Soares et al., 2019).

1.1 Abiotic Stress

1.1.1 Salt and drought stress

Soil salinity is one of the most common problems in modern agriculture since one-third of the lands irrigated are affected by salinisation. Besides anthropic action, one of the main causes behind world salinization is the rising levels of groundwater contaminated with high salt content (Rengasamy, 2006; Zhao et al., 2020). Salt stress is a complex mechanism that affects almost every developmental aspect of plants, both at the subcellular and phenotypic levels, being these effects damaging for the plant homeostasis (Abbasi et al., 2016). Thereby, the adaptations to this adverse situation, which generates the ability to tolerate high salinity, vary between and within species (Munns and Tester, 2008; Zhao et al., 2020). The effects of salt stress has two stages: initially, osmotic stress occurs, which typically is not a problem for plants (Zhu, 2016); however, a prolonged state under these conditions leads to nutritional imbalance, specific ion effect, membrane disorganisation, generation of toxic metabolites, inhibition of photosynthesis and generation of reactive oxygen species (ROS), which lead to cell and plant death (Abbasi et al., 2016; Zhao et al., 2020).

The osmotic stress induced by salt lowers the external water potential, resulting in a minor water uptake, compromising the natural development of the plant, since the turgor pressure will be shifted and the membrane permeability decreased (Munns

and Tester, 2008; Abbasi et al., 2016; Zhao et al., 2020). Besides this, stomata will close in response to the deficient water uptake, inhibiting photosynthetic activity (Abbasi et al., 2016; Zhao et al., 2020). Another effect of salt stress is the ionic imbalance that is originated due to a higher concentration of Na^+ and Cl^- in the soil, which will conduct to a higher concentration of these ions in the metabolic activities, resulting in the inhibition of certain enzymes and inefficient mineral nutrients uptake (Shabala and Cuin, 2008; Abbasi et al., 2016; Wu et al., 2018; Zhao et al., 2020). Furthermore, the high amount of Na^+ will provoke changes in plant organelles, such as: plant cell wall, by affecting the chemical properties of this structure; apoplast, by the alkalinisation of this pathway; and chloroplasts, by the reduction of CO_2 uptake, which will result in thylakoid membrane damage, oxidative stress and reduced photosynthetic efficiency (Shomer et al., 2003; Zhu et al., 2010; Suo et al., 2017; Zhao et al., 2020).

1.1.2 Metal-induced stress

Although metals occur naturally in soil and living organisms (Kintlová et al., 2017), since the beginning of the industrial era, the contamination of agricultural lands by metals has increased due to extensive mining, industrial activities and improper agricultural practices. Currently, soil contamination by metals, especially in agricultural areas, is a major threat to ecosystems health and functions (Wang et al., 2015; Piotto et al., 2018). Some metals are important micronutrients for plants, such as zinc (Zn) and copper (Cu), being required for the organisms' normal development and physiological status (Taiz et al., 2017; Branco-Neves et al., 2017; Kintlová et al., 2017). However, when above a certain threshold, they become phytotoxic, inducing stressful conditions for plant development by interfering with aminoacidic chains, which lead to physiological disturbances, including decreased growth, enhanced senescence and abnormal photosynthetic apparatus (Wang et al., 2015; Branco-Neves et al., 2017; Sousa et al., 2020; Soares et al., 2016). The response of plants to metal toxicity is very flexible and involves a complex transcriptional reprogramming of auxin-related genes, leading to a shift in the timing and localisation of auxin accumulation, which results in a reshaping and optimisation of the development of the plant (Wang et al., 2015). Besides this, though not all metals are redox-active compounds, it is recognized that metal-induced toxicity is often related to oxidative damage and disturbances in the plant antioxidant (AOX) system (Fidalgo et al., 2013; Branco-Neves et al., 2017; Sousa et al., 2020; 2022).

1.1.3 Oxidative stress and AOX system

Upon exposure to stress, multiple changes in the plant metabolism occur. One of the most common is the overaccumulation of ROS, the generation of which is enhanced in response to different biotic and abiotic stresses (Mittler, 2017; Soares et al., 2019). Anyhow, ROS play an antagonist role related to their concentration in plant cells: at low concentrations, they serve as important intracellular signals, however, at higher concentrations, they become phytotoxic and capable of interacting with all kinds of organic molecules, jeopardizing plant cell homeostasis. To prevent an unregulated increase of these compounds, plants developed an efficient AOX system to keep the redox state of the cells under control. When there is a disproportion between ROS production and their elimination, oxidative stress situation takes place, leading to cellular and subcellular damage (Gill and Tuteja, 2010; Sharma et al., 2012). There are four main species of ROS produced by two main phenomena: transference of energy to the molecular oxygen (O_2), leading to the production of singlet oxygen ($^1O_2$); and transference of one, two or three electrons to O_2, giving rise to the superoxide anion ($O_2^{\cdot -}$), hydrogen peroxide (H_2O_2) and hydroxyl radical (·OH), respectively (Demidchik, 2015). The singlet oxygen ($^1O_2$) is induced under strong light conditions and, when at high concentrations, it is capable of damaging the photosystems, reacting with other biological molecules, activating lipid peroxidation (LP) and oxidise important macromolecules (Soares et al., 2019). On its turn, the superoxide anion ($O_2^{\cdot -}$) is the first to be produced, and it is generally associated with the electron transport chains (ETCs) in the chloroplasts; however, it can be generated in other organelles, such as mitochondria. Although this molecule is incapable of directly interacting with organic molecules, its toxicity should not be overlooked, as it can lead to the formation, together with H_2O_2, of a much more dangerous ROS (Gill and Tuteja, 2010). Hydrogen peroxide (H_2O_2) is one of the most stable ROS, which can result in a more severe oxidative stress condition. Its production is associated with ETCs in several organelles, and it has a high toxicity due to its chemical nature since it does not have unpaired electrons and, therefore, it is able to cross biological membranes and act downstream of its producing sites (Demidchik, 2015). Lastly, the hydroxyl radical (·OH), considered as the most harmful and reactive one, is produced by the interaction between O_2.- and H_2O_2 in the presence of redox-active metals, such as Cu and Cd, in a reaction named as Haber-Weiss (Soares et al., 2019). Since it has a short half-life, the sites of action of this molecule are closely located to the

production site, however, it can cause severe damage to all organic molecules. Besides this, there is not an enzymatic mechanism responsible for its degradation and metabolism, which can lead to cell death (Sharma et al., 2012).

To keep the redox status of the cell, the AOX system must act effectively. This system comprises both non-enzymatic and enzymatic components. The non-enzymatic one is formed by diverse molecules and low mass metabolites, such as ascorbic acid (AsA), glutathione (GSH), proline (Pro), and phenolic compounds (Soares et al., 2019). These molecules can directly neutralise, transform, or remove ROS, allowing the cell to sense and keep the redox homeostasis. However, the efficiency of these AOX players depends on a conjuncture of factors like the type of stress, time-length of exposure, intensity, plant species, genotype, organ affected, among other physiological traits (Gill and Tuteja, 2010).

Pro, a proteinogenic amino acid well-known for its features as an osmolyte (Hayat et al., 2012), acts in two ways as an AOX molecule: by preventing ROS production acting as an electron sink; and by scavenging ROS by converting ·OH into γ-aminobutyric acid. Alongside, GSH can also react with all the ROS, except for the 1O2, thus functioning as a radical scavenger (Soares et al., 2019). Moreover, GSH is an important cellular redox buffer, as the ratio between GSH and its oxidised form (GSSG) can provide an overall picture of the cell redox status. GSH and GSSG levels are tightly coordinated by the action of glutathione reductase (GR; EC 1.6.4.2) (Sharma et al., 2012). Besides this, GSH functions are also linked to protein synthesis, enzymatic regulation, and expression of stress-responsive genes (Soares et al., 2019). Working in tandem with GSH, ascorbic acid (AsA), also known as vitamin C, is the most abundant metabolite in plant cells. It can interact with the different ROS by neutralising their effects or being used as an electron donor in enzymatic reactions, leading to reductions in ROS content due to the activity of ascorbate peroxidase (APX; EC 1.11.1.11). Moreover, together with GSH, it is one of the main metabolites of the AsA-GSH cycle, one of the main biochemical pathways in the redox metabolism (Soares et al., 2019). However, it should also be noted high amounts of this metabolite, conjugated with high amounts of H2O2 might act as a ROS enhancer as it stimulates the Fenton reaction [a reaction between Fe (II) and H2O2 to yield hydroxyl radicals (·OH)], the last step of the Waber-Weiss reaction.

On their turn, and working together with the AOX metabolites, the enzymatic components give a complex and multifaceted protection mechanism to maintain the cell homeostasis by avoiding oxidative-induced damage and supporting plant

development (Soares et al., 2019). This enzymatic part comprises three major enzymes: superoxide dismutase (SOD; EC 1.15.1.1), catalase (CAT; EC 1.11.1.6) and APX. Superoxide dismutase (SOD) is considered the first to act because it catalyses dismutation reactions that will detoxify O2.-, the first produced ROS, arising the production of O2 and H2O2. In fact, studies show that SOD is an efficient tool to increase abiotic and biotic stress tolerance, given its high AOX activity (Soares et al., 2019). Catalase (CAT) is responsible for mediating the neutralization of H2O2 into H2O and O2. This enzyme does not require any reducing power, making it one of the central scavengers of ROS. However, its efficiency is reduced, as it is only activated when high amounts of H2O2 are present. Similarly, to CAT, APX catalyses the reaction in which H2O2 is converted into H2O and monodehydroascorbate (MDHA), using reducing power provided by AsA. This enzyme is the first response to the increase of H2O2, due to its high affinity to this ROS, also representing a role in the management of signalling events (Soares et al., 2019).

Overall, the interdependence between non-enzymatic and enzymatic AOX players provided plants a sophisticated network of defence, allowing them to proper balance ROS production and avoid cellular damages (Figure 1). However, as stated before, given the magnitude (e.g., intensity, frequency) of the stress exposure, not always the AOX system is capable ensuring the redox homeostasis.

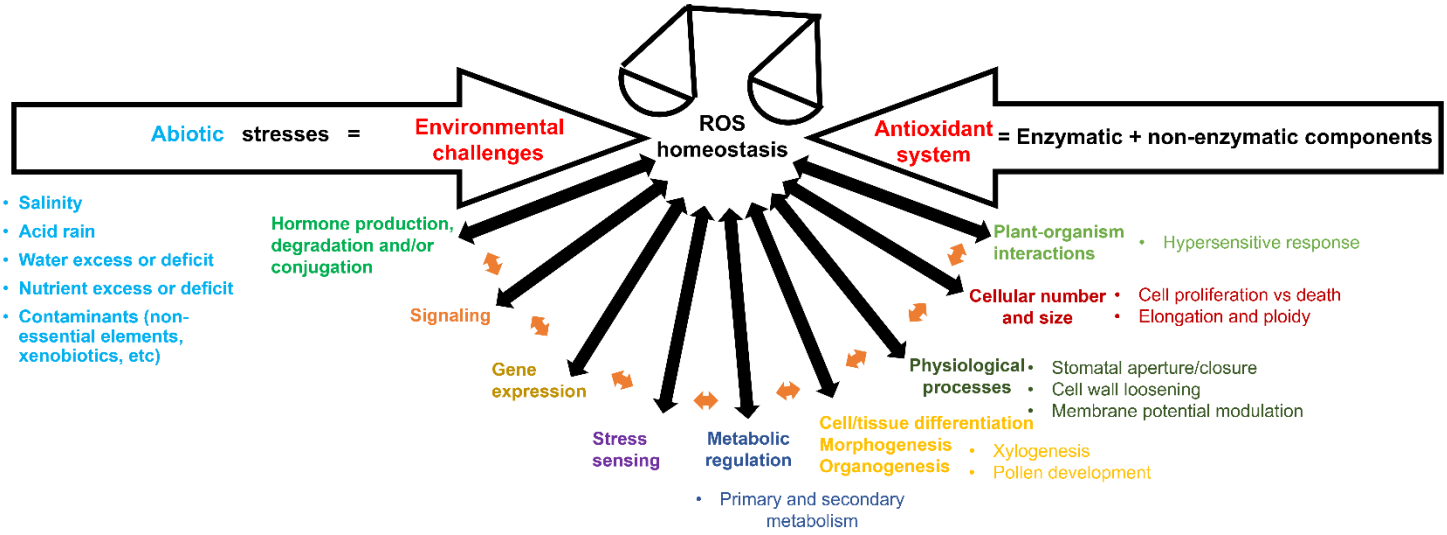

Figure 1 - Overview of the redox homeostasis in plant cells, focusing on the interplaying between the generation of ROS, as a result of both abiotic stresses, and their control by the plant AOX system. Adapted from Soares et.al (2019)

1.2 Endomembrane system

Plant cells, as eukaryotic cells, present a complex intracellular membrane network - the endomembrane system - composed of several membranous compartments. The endomembrane system is characterised by the presence of the nuclear envelope, endoplasmic reticulum (ER), Golgi apparatus (GA), the trans-Golgi network or early endosome (TGN/EE), the pre-vacuolar compartment/multi-vesicular body (PVC/MVB), the vacuole and the plasma membrane (PM). Although these organelles have distinct functions, the communication and protein transport between them is crucial for cell survival because they help to maintain cellular homeostasis and support cellular proliferation and polarisation. This linkage between organelles is achieved by small membranous structures, called vesicles, and they are responsible for delivering cargos from an organelle to another, by fusing their membranes with the membrane of the accepting organelle. The fusion process is only possible due to a mechanism that involves specialised transmembrane proteins that have a factor sensitive to soluble N-ethylmaleimide and are named SNAREs (Soluble N-ethylmaleimide-Sensitive Factor Attachment Protein Receptor) (Kwon et al., 2020; Zhu et al., 2020; Aniento et al., 2022).

1.2.1 Endoplasmic reticulum (ER)

The ER is the starting point for proteins entering the endomembrane system (Wang et al., 2017a; Pereira and Di Sansebastiano, 2021). This organelle is formed by a system of tubules (abundant in highly vacuolated cells) and cisterns (abundant in meristematic cells), with functions that comprise the biosynthesis of phospholipids, the synthesis and glycosylation of proteins, the folding and maturation of proteins and their quality control, calcium homeostasis, and the accumulation of reserve substances (Staehelin, 1997; Stefano and Brandizzi, 2018; Pereira and Di Sansebastiano, 2021). The despatch of the cargo to other organelles of the endomembrane system is done by the fusion between tubules and the interconversion of the cisternae into tubules, being the ER in continuous reshaping, reason why it can be classified as extremely plastic (Kriechbaumer and Brandizzi, 2020; Pereira and Di Sansebastiano, 2021).

As the beginning of the endomembrane system transport, the ER is in a privileged position to recognise external signals and coordinate cellular responses to challenging environmental conditions (Liu and Li, 2019; Sampaio et al., 2022). Upon stressful situations, one of the first processes being affected is protein folding, an event that takes place in the ER, causing protein misfolding or the accumulation of unfolded proteins, which is characterised as ER stress (Howell, 2013; Zhu, 2016; Wang et al., 2020). This

situation is recognised by specific sensor proteins located in the ER membrane that will lead to the activation of the ER stress response, which is translated into unfolded protein response (UPR) (Walter and Ron, 2011). The ER stress response consists of the expression of genes encoding chaperones and other proteins important for enhancing protein folding capacity, ER-associated degradation (ERAD), or the suppression of processes like protein translation to reduce the amount of synthesised proteins loaded into the ER (Walter and Ron, 2011; Zhu, 2016). These alterations help to restore ER homeostasis and the normal functionality of the endomembrane system (Walter and Ron, 2011; Liu and Howell, 2016; Zhu, 2016; Sampaio et al., 2022).

1.2.2 Golgi apparatus

The GA is a key point in the secretory system where proteins take their course to other organelles, representing a central node in several protein sorting pathways (Pereira and Di Sansebastiano, 2021). In plant cells, the GA is composed of several Golgi stacks called dictyosomes, which consist of many discrete stacks with a polarised architecture, forming small stacks along the cytoplasm (Dupree and Sherrier, 1998a; Hawes and Satiat-Jeunemaitre, 2005; Kang et al., 2022). They are polarised structures with three different sub-compartments that are biochemically distinct: *cis*-Golgi, medial-Golgi and trans-Golgi (Dupree and Sherrier, 1998b; Hawes and Satiat-Jeunemaitre, 2005; Zhu et al., 2020; Pereira and Di Sansebastiano, 2021). The GA is involved in the synthesis of complex polysaccharides of the cell wall matrix and wall glycolipids, in the glycosylation process of membrane proteins destined to the cell wall and proteins that will be stored as a reserve (Driouich et al., 1993; Pereira and Di Sansebastiano, 2021). The maintenance of the dictyosome structure is guaranteed by an anterograde and retrograde membrane flow, where the retrograde mediated by COPI vesicles is responsible for the retention of biosynthetic enzymes and other proteins, while the anterograde mediated by COPII vesicles is responsible for the distribution of proteins to the secretory pathway (Wang et al., 2017b; Brandizzi, 2018; Pereira and Di Sansebastiano, 2021).

1.2.3 The Vacuole

Plant cells contain more than one type of vacuole, different from mammalian cells and yeasts (Paris et al., 1996). Vacuoles accomplish several essential functions for plant survival and proper development, through the storage of solutes, by being a hydrostatic skeleton due to the water uptake. Also they provide the necessary force beneath the cell growth, in combination with the cytoskeleton, and are responsible for the changes in the cell volume (Viotti et al., 2013; Zhu et al., 2020; Zhang et al., 2021). Thereby, the thriving

of land plants is correlated with the existence of this organelle, as it improves the plasticity of the plant cell by improving the changes in the availability of essential nutrients, detoxifying the cytosol in the presence of harmful molecules, and by being part of abiotic and biotic defence mechanisms. Besides this, they function as lysosomes due to the presence of hydrolytic enzymes (Viotti et al., 2013). Based on this set of functions, the vacuoles are divided into two types: the lytic vacuole (LV); and the protein storage vacuole (PSV) (Paris et al., 1996). The first one is mainly found in vegetative cells (Viotti et al., 2013; Zhang et al., 2021) and it is equivalent to animal lysosomes as it shares the same protein degradation functions, besides the degradation of other compounds and macromolecules, and has an acid pH (Rogers, 2008; Jiang and Rogers, 2018; Zhu et al., 2020). The PSV is mainly found in storage tissues such as seeds, cotyledons and endosperm and presents a neutral pH in order to store reserve proteins (Jiang et al., 2000; Zouhar et al., 2010; Zhu et al., 2020). The existence of these two types of vacuoles is not mutually exclusive since they can transform into each other depending on the physiological conditions, functioning as a plant flexibility mechanism (Zhang et al., 2021; Sampaio et al., 2022). In fact, during germination of soybean and pumpkin, the PSV undergoes a dedifferentiation by the degradation of a specific tonoplast intrinsic protein (TIP), the α-TIP (PSV characteristic TIP). In response, there is an internalisation of the tonoplast and the formation of a new tonoplast with γ-TIP, that is considered an LV marker (Bolte et al., 2011).

Several studies point to the importance of the vacuole in the abiotic stress response since this organelle is associated with the maintenance of the turgor pressure and the accumulation of toxic molecules (Mimura et al., 2003; Queval et al., 2011; Tang et al., 2015). Tang and collaborators (2015) address a role for the vacuole in ion detoxification to avoid cell death under environmental stress by the interaction between Calcineurin B-like and protein kinases when there is a Mg^{2+} excess. Another study involving oxidative stress shows that the vacuole accumulates great levels of GSSG to protect the cell from an excessively positive shift in cytosolic glutathione redox potential (Queval et al., 2011). Furthermore, we recently showed that under several abiotic stresses, the protein sorting is shifted from the LV to the PSV, providing more evidence that the LV and PSV are key players in the combat against adverse environmental conditions (Neves et al. 2021).

1.2.4 Exocyst-Positive Organelle

Exocytosis is one of the fundamental processes for cell survival, being involved in the regulation of several key factors in cell development such as cell

polarity/morphogenesis, protein recycling, cell wall biogenesis, and interactions during adverse environmental conditions, being characterised by some authors as an important regulatory hub of the endomembrane dynamics (Žárský et al., 2013). The exocyst-positive organelle (EXPO) is a double-membrane organelle responsible for the transport of cargos to the plasma membrane. The EXPO is part of the unconventional protein secretion (UPS) routes, since the model proposed for its mode of action required the sequestrum of cytosolic leaderless secretory proteins (LSP), that will be then fused with the PM (Wang et al., 2010; Ding et al., 2014; Robinson et al., 2016; Wang et al., 2017b). The EXPO is a complex formed by proteins of the EXO70 family, that is responsible for the formation of the exocyst. In land plants, this family is encoded by a large number of EXO70 paralogues (23 in Arabidopsis), while in other eukaryotic organisms, there is only one (Synek et al., 2006; Cvrčková et al., 2012). This trait can be explained by the different needs that plant cells present compared with other eukaryotic cells, like cell-specific exocytosis within differentiating plant tissues and exocytosis related to biotic and abiotic stress responses (Synek et al., 2006; Li et al., 2010; Žárský et al., 2013). (Žárský et al., 2013; Wang et al., 2017b). The first exocyst subunit described in Arabidopsis was AtExo70E2. This marker is fundamental for the assembly of the exocyst since it is the one that recruits the other subunits. However, the mechanism behind this process is still undefined (Wang et al., 2017b). In a recent study, we demonstrated that, under abiotic stress conditions, the expression of the gene that encodes AtEXO70E2 is highly upregulated (Neves et al., 2021). This represents a hint that under adverse environmental conditions, EXPO-mediated exocytosis is enhanced showing that the UPS responses are more pronounced and may play a role in plant defence system.

1.2.5 Autophagosome

Autophagy is an important process to maintain cell homeostasis by degrading proteins and organelles and promoting intracellular recycling. The autophagosome is the organelle responsible for autophagy (Su et al., 2020). Its formation involves several autophagy-related (ATG) family proteins that are divided according to their functional groups: ATG1/ATG13 kinase initiates the autophagosome formation; ATG9 promotes the expansion of this organelle; and ATG8/ATG12 ubiquitin-like conjugation system mediates the autophagosome expansion and maturation (Kim et al., 2012; Wang et al., 2018). ATG8, through its short linear motif (AIM), interacts with several proteins and SNARES that will allow the right development of the autophagosome and its fusion with the vacuole membrane. Thereby, these ATG family proteins play key roles in

compartmentalisation of autophagic degradation, and due to their interactions with several proteins, allow for a selective autophagic mechanism (Aniento et al., 2022).

1.3 Protein trafficking routes

Due to the complexity of the eukaryotic cell, and the consequent compartmentalisation of cellular functions, each organelle has specific biochemical characteristics, which result in a specific identity. Despite this, they must communicate to maintain the subcellular functions and homeostasis. This network is comprised of membrane-bound transport carriers, known as vesicles. Vesicular transport is mediated by several endomembrane system effectors that are responsible for the bud of the vesicle from the donor compartment and fusion to the acceptor compartment; also they are responsible for the specificity of the transport directing the vesicle to the right compartment. This transport may be conducted through conventional or unconventional routes (Figure 2), depending on numerous conditions, such as environmental ones (Zhu et al., 2020; Pereira and Di Sansebastiano, 2021). In this chapter, both routes will be explored:

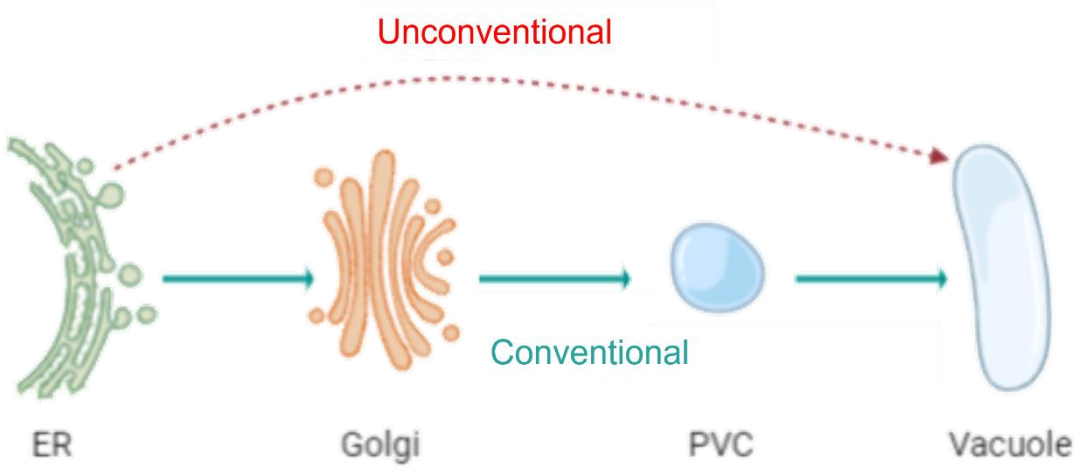

Figure 2 – Schematic representation of conventional and unconventional vacuolar trafficking routes Abreviatures: ER- Endoplasmic Reticulum; PVC – Pre-vacuolar compartment

1.3.1 Conventional protein sorting

In the conventional secretory pathway, soluble proteins are translocated to ER lumen, and if they are not retained in this stage, they will be transported to the Golgi for further processing events. This type of transport, anterograde, is mediated by vesicles COPII (coat protein complex II) (Wang et al., 2017b; Zhu et al., 2020; Pereira and Di Sansebastiano, 2021). After the maturation process in the Golgi, proteins require a positive sorting at the Trans-Golgi Network (TGN) to continue their path to the vacuoles

which is assisted by vacuolar sorting receptors (VSRs). Afterwards, cargo proteins will be fused with the pre-vacuolar compartment (PVC), and VSRs will be recycled back to TGN. Then, PVC will be fused with the tonoplast thanks to N-ethyl-maleimide-sensitive fusion attachment protein receptors (SNAREs) and tethering complexes (Zhu et al., 2020; Pereira and Di Sansebastiano, 2021; Aniento et al., 2022).

However, because plants have two different types of vacuoles (LVs and PSVs), and although they can coexist, the transport pathways for each can be separated (Figure 3) (Sanmartín et al., 2007). While the transport to LV is mainly mediated by clathrin-coated vesicles and follows the described pathway (Sanmartín et al., 2007), the transport to PSV is based on multiple mechanisms like: sorting in dense vesicles (DVs) from *cis*-Golgi, mediated by VSRs (Robinson and Neuhaus, 2016); or via receptor homology-transmembrane-RING H2 proteins (RMRs) (Shen et al., 2011); autophagic fusion of protein bodies (PBs) (Zhu et al., 2020); and other unconventional routes that will be described later.

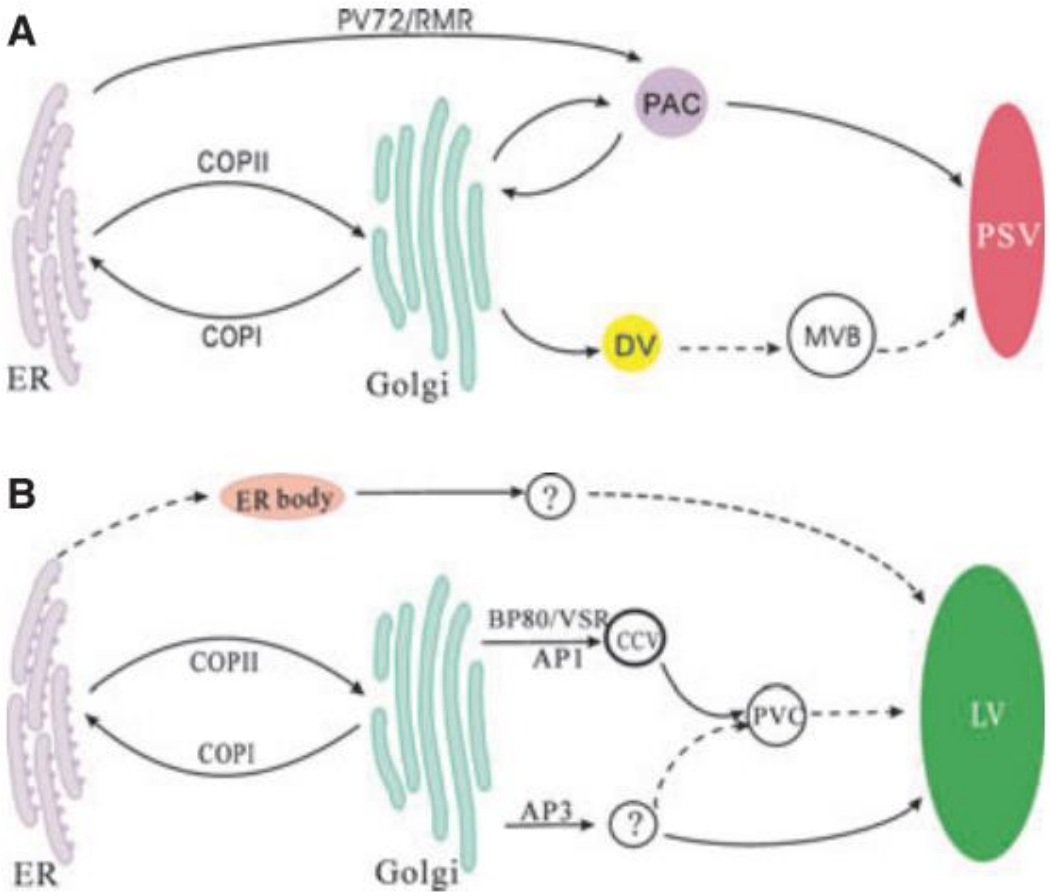

Figure 3 - Differences between PSV and LV sorting
A – Sorting process to PSV. Proteins sorted to PSV initiate their path in ER, and they can reach their final destination through two pathways: Golgi dependent or -independent pathways. Abbreviatures: MVB, multivesicular body; PAC, precursor-accumulating vesicle; PV72/ RMR, vacuole sorting receptor
B – Sorting process to LV. Proteins destined for the LV initiate their life in the ER and can be sorted to the LV through

Golgi-dependent or -independent pathways. Abbreviatures: CCV- Clhatrhirn coated vesicles; PVC- Pre-vacuolar compartment; LV -Lytic vacuole; Adapted from Xiang et al, (2013).

Since conventional and unconventional secretory pathways may involve separate routes, they must have different endomembrane system effectors working in the different vacuolar sorting pathways. Most of them work at TGN and PVC levels. VSRs and RMRs were already mentioned, and they are the proof that different routes have different endomembrane system effectors. VSRs are type I membrane proteins with a cytosolic motif and a large luminal domain (Ahmed et al., 2000; Lee et al., 2013; Xiang et al., 2013), that recognises NPIRL-like motifs in cargo proteins. Thereby, they recognise and bind to specific vacuolar sorting determinants (VSD) that will route the proteins to the respective vacuole (Xiang et al., 2013). VSR1, one of the seven members of VSR family in Arabidopsis, mediates the transport of specific storage cargo in seeds and vegetative tissue (Zouhar et al., 2010), and interacts with vacuolar protein sorting 35 (VPS35), another protein that mediates PSV route, at PVC level (Yamazaki et al., 2008; Xiang et al., 2013). In the LV route, VSR2 takes place and binds to proteins like barley aleurain and sporamin, typically LV proteins (daSilva et al., 2005; Kim et al., 2010; Xiang et al., 2013), and uses clathrin-coated vesicles (Lee et al., 2013). RMRs are type I integral membrane proteins that contain a typical *N*-terminal signal peptide, followed by protease-associated (PA) domain that allows for protein-protein interaction (Wang et al., 2011). What makes them different from the VSRs is the presence of zinc fingers domains in the *C*-terminal site. RMR1 in the cell is distributed through Golgi, TGN and PVC (Shen et al., 2011). This protein binds in a specific way to PSV sorting determinants (Wang et al., 2011), and the lack of this protein leads to the interruption of some storage proteins accumulation (Zouhar et al., 2010). RMR2 preferentially interacts with chitinase *C*-terminal peptide, which can be related to the PSV trafficking routes. To support this, RMR2 does not interact with aleurain, a LV protein (Wang et al., 2011).

Other proteins also participate in the vacuolar trafficking pathways, like vesicular transport V-SNAREs (VTI) family members or several families of plant syntaxins (SYP). VTI12 and VTI11 mediate the PSV and LV route, respectively (Sanmartín et al., 2007). VTI12 is involved in protein sorting and autophagic pathways (Surpin et al., 2003; Sanmartín et al., 2007). In protein sorting, it mediates a clathrin independent route, meaning that it mediates the transport to the PSV, and forms several complexes with SYP proteins like SYP41/SYP42 and SYP61 (SNvti12complex) at TGN levels (Bassham et al., 2000; Sanderfoot et al., 2001; Sanmartín et al., 2007). VTI11 has been associated with the clathrin dependent transport, which is in the LV route, and forms complexes with other SYP proteins, like SYP21/SYP22 and SYP52 (SNvti11complex) at PVC level and

tonoplast (Sanderfoot et al., 2001; Sanmartín et al., 2007; Shirakawa et al., 2010). These findings are also supported by co-localisation assays, where SYP51 was found to be a positive regulator of chitinase transport, while SYP52/SYP22 has the same function but for aleurain transport (Shirakawa et al., 2010; De Benedictis et al., 2013). Some SYP2 family members, like SYP23 and SYP21, do not have their biological roles clearly described; however, it is known that SYP23 lacks a transmembrane domain and localises to the cytosol (Shirakawa et al., 2010). VPS45 is another protein that is very important to vacuolar trafficking since it mediates the recycling of VSRs in TGN, allowing them to perform additional rounds of protein cargo sorting (Zouhar et al., 2009). VPS45 protein is also a regulatory protein for the SNvti12complex, since it is a positive regulator for the activity of this complex (Zouhar et al., 2009).

Under abiotic stress situations, cell sorting pathways are affected, and the cell adjusts these processes in order to take a chance to survive. Thereby, genes that encode proteins involved in PSV route are enhanced, while LV route is less preferable showing a preference for a more reserved state (Neves et al., 2021).

1.3.2 Unconventional pathways

Besides the conventional pathway, protein sorting may occur by other routes, where proteins are directly delivered from ER, occurring a Golgi bypass. Many of these routes are associated with development and stress-induced conditions because cells need to rapidly adapt their mechanisms to thrive (Pereira and Di Sansebastiano, 2021). Despite being often disregarded and seen as abnormalities occurring in specific conditions, these routes are gaining more interest as more examples have been reported and the mechanisms behind them are being disclosed (Pereira and Di Sansebastiano, 2021). The plant specific insert (PSI) is a vacuolar sorting domain that mediates an unconventional pathway to the vacuole bypassing the Golgi (Pereira et al., 2013). The *C*-terminus from Chitinase A is another example of a vacuolar signal that mediates Golgi bypass pathway to the vacuole (Stigliano et al., 2013; Stigliano et al., 2014). These two VSDs have been extensively studied in the past years and efforts have been made to characterise in more detail these unconventional routes. As so, new compartments are being described as part of these routes, such as ER Microtubule-related Export Compartments (ERMEC) (Pereira and Di Sansebastiano, 2021). ERMEC were discovered while studying the Chitinase A (Chi) routes. Recently, De Caroli and co-workers (2021) reported that, even when several cytoskeleton alterations were induced, the RFP-Chi still reached the vacuole. Thereby this new intermediate compartment was described as a compartment that emerges from the ER as microtubule dependent. There

are still other unconventional pathways to the PSV, such as the Golgi bypass mediated by precursor accumulating vesicles (PAC) that were observed with 2S albumin and 11S globulin in pumpkin seeds (Shimada et al., 1997; Shimada et al., 2002; Zhu et al., 2020).

Regarding all the information presented so far, unconventional pathways are another proof of how adaptive the plant cell can be, unravelling that a great amount of knowledge is yet to acquire.

1.4 Endomembrane modifications and stress

When the cell senses abiotic stress conditions, other processes involving the endomembrane system are also affected, including their natural morphology or chemical composition. The ER is the first organelle to be affected, by activating the unfolded protein responses (UPRs) and ER-derived autophagy (Koizumi et al., 2001; Liu and Bassham, 2012; Park and Park, 2019). Then the Golgi generates a large number of vesicles under stressful situations, being in a hypertrophic state (Neves et al., 2021). The LV has an adaptive response to the type of stress that the plant is submitted, for example, when there are excessive amounts of Mg^{2+}, certain kinases are activated to detoxify the excessive amount of ions (Tang et al., 2015). Also in the presence of ROS, the LV storages GSH as a mechanism to protect the cell from a shift in cytosolic glutathione redox potential (Queval et al., 2011). The PSV has an increase of cysteine proteases, which normally are responsible for the degradation of storage proteins during plant development, but studies demonstrated that they may be triggered by stress, enabling a new perspective of the cysteine proteases in stress response (Hayashi et al., 2001; Sampaio et al., 2022). Figure 4 represents the major changes observed in plants cells' endomembrane system and trafficking routes in plants under abiotic stress when compared to control (Neves et al, 2021). It is clear an increase in the number of vesicles associated with the Golgi and ER, differential expression of several genes involved in vesicle docking and fusion and a shift in protein sorting towards the PSV (Figure 4). As a whole, it is possible to conclude that endomembrane effectors play effective roles in cellular homeostasis under adverse conditions.

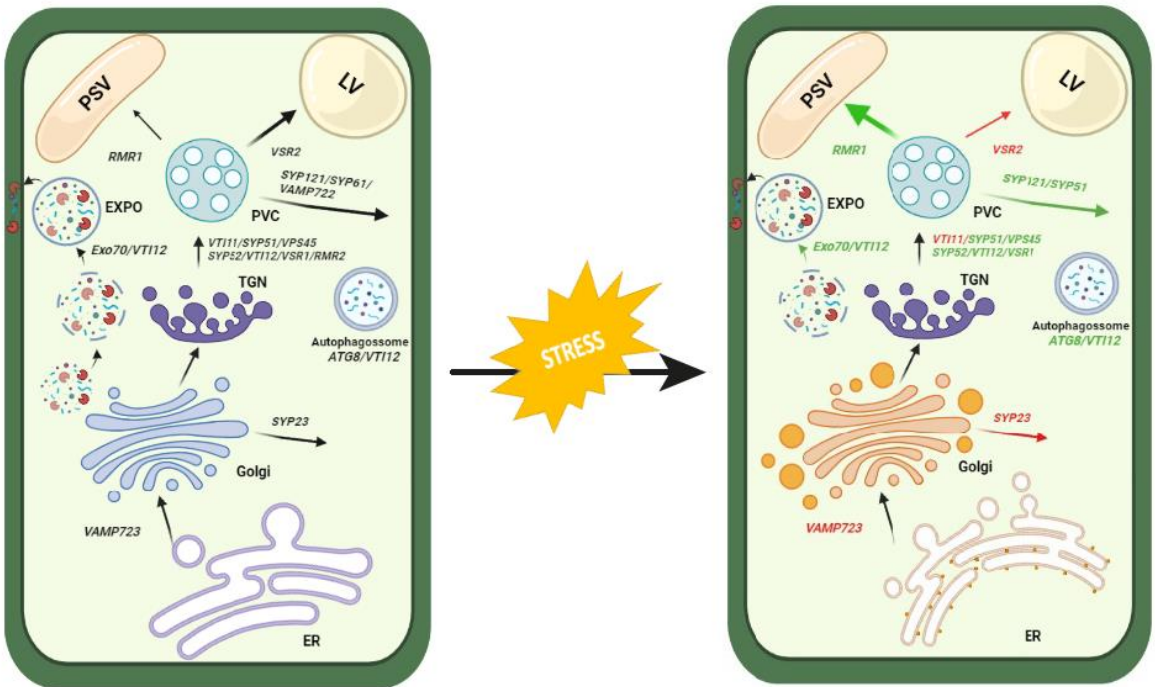

Figure 4 -Schematic representation of the plant cell in control versus stress conditions. From Neves et al. (2021). Under stress situations the morphological changes are observed in Golgi, it presents an hypertrophy and a higher vacuolization. Also the endomembrane system effectors alter their expression, being the green ones up-regulated and the red ones downregulated.

1.5 Aims

The impact of adverse environmental conditions in plants has been more studied in physiological terms, rather than at the molecular levels (protein trafficking), especially regarding the protein sorting mechanisms. This dissertation was carried out in frame with the recent line of work of the laboratory, which seeks to investigate how abiotic stress affects protein sorting mechanisms, namely the LV/PSV route and exocyst mediated sorting. Thereby, the aim of this work is to provide new insights into how proteins involved in protein sorting are relevant to the stress response. To accomplish it, we studied how protein trafficking is affected when some key players are absent, by the use of T-DNA *Arabidopsis thaliana* lines, and in combination with different abiotic stresses. These plants were analysed according to different perspectives to have an integrated vision on these processes: 1) Biometric parameters and biochemical characterization of the AOX status; 2) Expression analysis of endomembrane effectors from the same/related transport routes; 3) Localisation of trafficking-related proteins. The data acquired from these experiments will be used to better understand which endomembrane-system effectors play a relevant role in the stress response, leading to

an increase in knowledge of how protein sorting, and its players behave under stress conditions, and may be applied in field studies.

2. Methodology

2.1 *Arabidopsis thaliana* mutant lines genotyping

2.1.1 Germination and gDNA extraction

Arabidopsis thaliana (col 0) T-DNA lines for different endomembrane system effectors, shown in Table 1, were ordered from NASC (Nottingham Arabidopsis Stock Centre). Then, seeds were germinated in half-strength Murashige and Skoog medium (MS) (Duchefa), supplemented with 1.5% (w/v) sucrose and solidified with 0.7% (w/v) bacteriological agar. Prior to germination, seeds were maintained 48 h at 4 °C, in the dark, to promote stratification; after that, they were transferred to a growth chamber under a photoperiod of 16 h light/8 h dark, an average humidity of 50-60%, and a temperature of 21 °C, with a light quantity of 110 $\mu mol.m^{-2}.s$. When the seedlings reached the rosette state, they were used to extract gDNA according to a protocol adapted from Edwards and collaborators (1991). Briefly, a young leaf was pinched into a tube and grinded with a pestle. Then, 400 µL of extraction buffer, composed by 200 mM Tris-HCl pH 7.5, 250 mM sodium chloride (NaCl), 25 mM (ethylenediaminetetraacetic acid) EDTA and 0.5% (w/v) sodium dodecyl sulfate (SDS), were added, followed by a series of vortexing cycles. To pellet the debris, a centrifugation at max speed for 1 min took place. The supernatant (SN) was then transferred into a clean 1.5 mL tube, and 350 µL of isopropanol were added. After a short incubation (2 min) at room temperature (RT), a 5 min max speed centrifugation was performed to pellet the gDNA. The SN was removed, and the pellet was left to dry and finally dissolved in 50 µL of sterile deionized water.

Table 1 - *Arabidopsis thaliana* T-DNA lines used in this study

Target	Accession Numbers	NASC accession number	Reference
SYP23	AT4G17730	SAKL_018233	
VSR2	AT2G30290	SALK_038782	
VTI11	AT5G39510	SALK_044000	
VTI12	AT1G26670	SALK_069041	

SYP22	AT5G46860	SALK_076009	(Alonso et al., 2003)
RMR1	AT5G66160	SALK_088174	
RMR2	AT1G71980	SALK_010784	
SYP51	AT1G16240	SAIL_44_B11	
EXO70	AT5G61010	SAIL_637_D01	

2.1.2 Confirmation of T-DNA insertion

After obtaining the gDNA from the T-DNA lines, PCR assays were performed to confirm the presence of the T-DNA insertion. Thereby, primers were designed for each insertion with the program T-DNA Primer Design, from SIGnAL (Salk institute Genomic Analysis Laboratory; http://signal.salk.edu/tdnaprimers.2.html). Their sequences can be found in in Supplementary Table 1. Afterwards, the gDNA was amplified using NZYTaq II 2x Green Master Mix (NZYTech®), following the manufacture's guidelines, as described in Tables 2 and 3. Afterwards, the amplified products were analysed by electrophoresis in a horizontal system (Horizon 58, Life Technologies) at 100 V for 30-40 min, in a 1% (w/v) agarose gel prepared in 1x tris-acetate-EDTA (TAE – 40 mM Tris-HCl and 1 mM EDTA pH 8.3) buffer.

Table 2 - PCR Reaction for the screening of T-DNA Arabidopsis lines using NZYTaq II

Components	Concentration	Volume
Primer forward	0.5 µM	1.25 µL
Primer reverse	0.5 µM	1.25 µL
Template DNA	5 ng	variable
NZYTaq II 2x Green Master Mix	1x	25 µL
Nuclease-free water	-	variable
Final Volume	-	50

Table 3- PCR program used for the screening of T-DNA Arabidopsis lines

Steps		Temperature (°C)	Time
Initial Denaturation		95	3 min
35x	Denaturation	94	30 s
	Annealing	55	30 s
	Extension	72	15-30 s/kb
Final Extension		72	10 min
Hold		4	∞

2.2 Abiotic stress experiments

In order to test the effects of different abiotic stress factors, wildtype and T-DNA lines were grown under *in vitro* conditions in nutritive medium (see section 2.1:), supplemented with: 50 mM NaCl (saline stress), 50 and 100 mM mannitol (osmotic stress), 0.5 mM hydrogen peroxide (H_2O_2) (oxidative stress) and 150 µM zinc sulphate ($ZnSO_4.5H_2O$) (metal toxicity) (Table 4). The selection of the concentrations applied was based on our previous recent work (Neves et al., 2021) As previously detailed, after disinfection, seeds were maintained 48 h at 4 °C, in the dark, to promote stratification, and after that they were transferred to a growth chamber with controlled conditions (see section 2.1) for 10-12 days. Eight biological replicates were prepared for each stress situation, being each plate an biological replicate, as formerly described (Neves et al., 2021). Upon the growth period, seedlings from four replicates of each experimental group were immediately sampled for transmission electron microscopy (TEM) and biometric analysis, while the plant material from other 4 replicates was frozen in liquid nitrogen for further molecular and biochemical determinations.

Table 4 - Different conditions and stress inducers used to simulate abiotic stress

Stress Type	Nomenclature	Stress inducer	Concentration

Control	C	-	-
Saline	S1	Sodium Chloride (NaCl)	50 mM
Osmotic	H1	Mannitol	50 mM
	H2	Mannitol	100 mM
Oxidative	Ox	Hydrogen Peroxide (H_2O_2)	0.5 mM
Metal	Zn	Zinc Sulphate	150 µM

2.3 Transmission Electron Microscopy

The biological material used for this assay consisted of leaves of *Arabidopsis thaliana* wildtype and mutant-DNA lines mentioned in section 2.1.1. After sampling, they were cut in pieces with approximately 1-2 mm and fixated in 1.25% (w/v) sodium 1,4-piperazine-diethane sulfonic acid - NaPIPES - pH 7.2 with 2.5% (v/v) glutaraldehyde for 1 hour at RT. Afterwards, the samples were washed with 2.5% (w/v) NaPIPES, 3 times for 10 min each, and post-fixed in 4% (w/v) osmium tetroxide (OsO_4), prepared in 2.5% (w/v) NaPIPES, at RT for 2 h. The samples were then subjected to a series of dehydration, with increasing concentrations of ethanol and different incubation times: 10% (v/v) for 10 min; 20, 30 and 50% (v/v) for 15 min each; 70 and 100% (v/v) for 20 min. At the end of the last incubation, the ethanol was replaced by propylene oxide for 20 min. To proceed to impregnation, the Epoxi resin was prepared. To do so, 12 mL of Agar 100 resin was mixed with 13 mL Methyl Nadic Anhydrin (MNA) (Agar Scientific), stirred for 20 min, and then 0.5 mL of DMP-30 (Agar scientific) was added. The specimens started to be gradually infiltrated with increasing concentrations of the resin, diluted in propylene oxide, as follows: 10% (for 15 min), drop was added every 10 min until a 50% ratio, and let to incubate ON. Then the mixed was replaced by pure resin for 24 h 100% . The samples were then transferred to oriented molds, covered with resin, and let to polymerize at 60 °C overnight. The obtention of ultrathin sections (60-80 nm) was performed by using a diamond knife (Diatome) and the UC6 Ultramicrotome (Leica, Carnaxide, Portugal). The cuts were recovered to 400 mesh copper grids, post-stained with Uranyless EM Strain (Uranyless©) and with Reynolds Lead citrate 3% (Uranyless©) for 5 min each. After washing to remove excess stain, grids were to be observed in a Jeol JEM 1400 Transmission Electron Microscope, and the images were acquired with

an Orius DC200D camera (Gatan, Pleasanton, CA, USA), however due to a malfunction of the TEM camera this analysis will be performed as soon as the equipment is fully operational.

2.4 Biochemical assays

In order to assess the physiological and biochemical responses of the selected mutants, several biomarkers were characterized.

2.4.1 Pigments quantification

The quantification of total chlorophyll (chl) and carotenoids was performed according to Lichtenthaler (1987). Aliquots of 80 mg of tissue were homogenized with 80% (v/v) acetone. The homogenates were then centrifuged at 1 400 x *g* for 10 min and the SN was collected and maintained in the dark. The absorbance was read at 470, 647 and 663 nm. The levels of chl a, chl b and carotenoids were calculated from formulas derived by Lichtenthaler (1987) and the final results were presented in mg g^{-1} fw.

2.4.2 Determination of lipid peroxidation (LP)

Lipid peroxidation (LP) was evaluated in accordance to Heath and Packer (1968), through the quantification of malondialdehyde (MDA) levels, as it is an end product formed from polyunsaturated fatty acids peroxidation. Aliquots of 100 mg were homogenized in 0.1% (w/v) trichloroacetic acid (TCA) with the use of Bead Ruptor 12 (Omni International), a bead-miller homogenizer. To prevent overheating of the samples, three homogenization cycles (5 m s^{-1}; 20 s) were performed with a 1-min period on ice between each. Then, samples were centrifuged for 15 min at 10 000 x *g*. After recovering the SN, 1 mL of 0.5% (w/v) thiobarbituric acid (TBA) in 20% (w/v) TCA were added to 250 µL of SN. This mix was incubated for 30 min at 95 °C, followed by an incubation on ice for 15 min. An 8-minute centrifugation at 10000 x *g* was performed and the absorbance of the samples was measured at 532 and 600 nm. The latter result was subtracted to the first to avoid effects of non-specific turbidity and, by utilizing the extinction coefficient of 155 mM^{-1} cm^{-1}. MDA content was expressed as nmol/g of fresh weight (fw).

2.4.3 Quantification of H_2O_2

Hydrogen peroxide (H_2O_2) levels were quantified according to Alexieva and co-workers (2001), with few modifications for adapting to a microplate. Briefly, frozen aliquots of 100 mg of seedling tissue were homogenized in 1 mL of 0,1% TCA using a bead miller homogeniser (Bead Ruptor 12, OMNI International). To prevent overheating of the samples, three homogenization cycles (5 m s^{-1}; 20 s) were performed with a 1-min

period on ice between each. The homogenates were centrifuged at 12 000 *x g* for 15 min at 4 °C. The SN was used to perform the rest of the protocol, were 50 µL were removed and transferred to each well of the microplate. Then, 50 µL of PK buffer (100 mM, pH 7.0) and 200 µL of 1M KI (Potassium iodide) were added. The mix was left at RT for 1h, in obscurity, and the absorbance was read at 390 nm. The final results were expressed in $nmolg^{-1}$ fw, using 0.28 μMcm^{-1} as extinction coefficient.

2.4.4 Determination of proline (Pro) levels

The quantification of proline (Pro) levels was performed as described by Bates and co-workers (1973). Frozen seedling samples were homogenised in 3% (w/v) sulfosalicylic acid in the Bead Ruptor 12 (Omni International). To prevent overheating of the samples, three homogenization cycles (5 m s^{-1}; 20 s) were performed with a 1-min period on ice between each. Then, the homogenates were centrifuged at 16 000 x *g* for 10 min and the SN recovered. Afterwards, 200 µL of each sample was mixed with 200 µL of glacial acetic acid and 200 µL of acid ninhydrin. This was followed by an incubation at 95 °C for 1 h. After the samples were cooled out on ice, 1 mL of toluene was added and the mixture was vortexed for 15 s to separate a red upper phase (organic) from a whiteish lower phase. The upper one is the one utilized to perform the absorbance reads at 520 nm. Pro concentration and absorbance were linked via a standard curve designed with known increasing concentrations of this metabolite and results were expressed in mg g^{-1} fw.

2.4.5 Determination of reduced glutathione (GSH)

To quantify glutathione (GSH) levels, a protocol adapted from Soares and colleagues (2019) was used. Briefly, 1 mL of 3% (w/v) sulfosalicylic acid was used to homogenize 100 mg of frozen tissue in the Bead Ruptor 12 (Omni, International) homogeniser, followed by a centrifugation at 16 000 x *g* at 4 °C for 10 min. To prevent overheating of the samples, three homogenization cycles (5 m s^{-1}; 20 s) were performed with a 1-min period on ice between each. The SN was collected and 50 µL of it were added to 200 µL ddH_2O and 750 µL of a reaction mixture, containing 100 mM PK (pH 7.0), 10 mM EDTA and 1.5 mg mL^{-1} 5,5-dithio-bis-(2-nitrobenzoic acid) (DTNB). The mixture was vortexed and incubated in the dark for 10 min. The absorbance was read at 412 nm, and the levels of GSH were quantified according to a standard curve prepared with known concentrations of this AOX. The results were expressed in µmol g^{-1} fw.

2.4.6 Determination of catalase (CAT) and ascorbate peroxidase (APX) activity

2.4.6.1 Quantification of soluble proteins

To quantify total soluble proteins, aliquots of 100 mg of frozen tissue were homogenised, with the aid of Bead Ruptor 12 (Omni International), in 2 mL of potassium phosphate buffer (100 mM, pH7.3) (PK), supplemented with 1 mM EDTA, 1 mM phenylmethylsulphonyl fluoride (PMSF), 5 mM L-ascorbic acid, 8% (v/v) glycerol and 1% (w/v) polyvinylpolypyrrolidone (PVPP). To prevent overheating of the samples, three homogenization cycles (5 m s^{-1}; 20 s) were performed with a 1-min period on ice between each one. The homogenates were centrifuged at 4 °C for 25 min at 16000 x *g* and the SN was collected. Total protein was quantified based on the protocol described by Bradford (1976). For that, a 1:100 dilution of each SN was obtained. Then, 75 µL of diluted sample was mixed with 750 µL of Bradford Solution (PanReac AppliChem), followed by a 15 min incubation in the dark. Finally, the absorbance was read at 595 nm. A standard curve, prepared with known concentrations of bovine serum albumin (BSA), was determined, as a way to establish a link between obtained absorbances and protein content. Final results were expressed in mg g^{-1} fw.

2.4.6.2 Determination of CAT and APX acticity

For the determination of CAT and APX activity, frozen aliquots of tissue, with ca. 200 mg, were homogenized in 2 mL of extraction solution, composed by PK buffer (100 mM, pH 7.3), 8% (v/v) glycerol, 1 mM PMSF, 1 mM EDTA, 5 mM L-ascorbic acid and 1% (w/v) PVPP. The homogenisation procedure was carried out in the Bead Ruptor 12 (Omni, International), as previously described. Then, extracts were centrifuged for 25 min at 16000 x *g* at 4 °C and the SNs were recovered. Prior to enzyme activity assays, total protein content was assessed as described earlier (2.6.2).

Regarding APX, its activity was evaluated based on the protocol of Nakano and Asada (1981), adapted for UV-microplates by Murshed and colleagues (2008). Briefly, 20 µL of the protein extract was mixed with 170 µL PK (50 mM, pH 7), containing 0.6 mM AsA. Immediately before the measurement, 10 µL H_2O_2 (254 mM) were added to each well of the UV-microplate. APX-mediated AsA oxidation was followed at 290 nm each 5 s, with a 2 min interval. Utilizing AsA molar extinction coefficient (0.49 mM/cm), final activity values were expressed as µmol AsA min^{-1} mg protei^{-1}.in/mg.

Concerning CAT, the original procedure of Aebi (1984) was used and adapted for microplates. The temporal catalase-mediated degradation of H_2O_2 was measured spectrophotometrically. In a UV-microplate, 20 µL of SN were mixed with 160 µL of PK

(50 mM, pH 7). Prior the absorbance reading, 20 µL of 100 mM H_2O_2 were added to each well. The CAT activity was followed in intervals of 5 s for 2 minutes, at 240 nm. Final activity values were determined with H_2O_2 molar extinction coefficient (39.4 mM^{-1} cm^{-1}) and expressed in µmol H_2O_2 min^{-1} mg $protein^{-1}$.

All the procedures were performed in the microplate reader MultiskanGo (Thermo Scientific), and the software used to analyse the data was SkanIt 6.1 (Thermo Scientific).

2.5 Production of cDNA constructs

To evaluate how abiotic stress may or may not affect the subcellular localisation of some endomembrane system effectors (VTI12, VTI11, VSR2, RMR1), a series of molecular biology techniques were performed to create chimeras with the fluorescent protein mNeonGreen (Shaner et al., 2013).

2.5.1 DNA amplification

The expression vector pMDC83 and pUNI51 carrying several endomembrane effectors, depicted in Table 5, were already available at the laboratory and maintained in *Escherichia coli* DH5α glycerol stocks. Plasmids were extracted using the NZYMiniprep kit (NZYTech®) following the manufacturers guidelines. In this study two cloning strategies were used:

- Classical cloning – The first strategy used to obtain the fluorescent chimeras resorted to classical cloning using restriction enzymes and DNA ligase. Specific primers were designed for each effector carrying an adaptor sequence for the restriction enzymes chosen (Table 6.). Then, the cDNA's were amplified so the adaptor region would be flanking the cDNA sequence. With this approach it was obtained pMDC83-mNeonGreen, pMDC83-VSR2-mNeonGreen, pMDC83-RMR1-mNeonGreen and pMDC83-VTI11-mNeonGreen;

- Gibson assembly – Since VTI12 has more than one restriction site for the chosen enzymes, Gibson assembly was the technique chosen to perform the cloning of this cDNA. Thereby, specific overlapping primers were designed to obtain the pMDC83-VTI12-mNeonGreen.

The primers for both techniques were designed with the objective of introducing a linker with neutral amino acids between the protein of interest and the fluorescent protein (mNeonGreen) to avoid coverage and malfunction of the main protein. All primers are presented in Supplementary Table 2.

Table 5 - List of the plasmids used

cDNAs	Obtained from
mNeonGreen-mRuby-FRET-10	AdGene
pUNI51-VSR2	TAIR
pUNI51-VTI12	TAIR
pUNI51-RMR1	TAIR
pUNI51-VTI11	TAIR
pMDC83-SP-mCherry	unpublished

Table 6 - Enzymes used for restriction cloning

DNA to be digested	Restriction Enzymes
VSR2	XbaI + SalI
VTI12	
VTI11	
mNeonGreen	SalI+SacI

All the cDNAs mentioned above were amplified with Phusion High-Fidelity PCR Master Mix (Thermo Scientific) using the PCR reaction mix and PCR program described in Tables 7 and 8, respectively. All PCR products were confirmed through electrophoresis in a horizontal system (Horizon 58, Life Technologies) at 100 V for 30-40 min, in a 1% (w/v) agarose gel prepared in 1x TAE. All PCR products were purified using NZYGelpure kit (NZYTech) according to the manufacturers procedure and quantified using 1 µL of DNA in a DS-11 microvolume Spectrophotometer (Denovix).

Table 7 - Component mix for the amplification of cDNAs of interest

Components	Concentration	Volume
Primer forward	0.5 µM	1.25 µL
Primer reverse	0.5 µM	1.25 µL

Template DNA	5 ng	variable
2x Phusion Master Mix	1x	25 µL
Nuclease-free water	-	variable
Final Volume	-	50

Table 8 - PCR Program for the amplification of cDNAs of interest

Steps		**Temperature (°C)**	**Time**
Initial Denaturation		98	3 min
35x	Denaturation	98	10 s
	Annealing	55	30 s
	Extension	72	15-30 s/kb
Final Extension		72	10 min
Hold		4	∞

2.5.2 Cloning

2.5.2.1 Restriction Enzyme cloning

To produce the constructs pMDC83-VSR2-mNeonGreen, pMDC83-RMR1-mNeonGreen and pMDC83-VTI11-mNeonGreen, the first step was to clone mNeonGreen in the vector pMDC83-SP-mCherry, by replacing SP-mCherry for mNeonGreeen using the enzymes SalI and SacI. The reaction to perform the digestion was prepared according to the instructions of the manufacturer (Anza line, Invitrogen). Briefly a mix of 10 µL of DNA, 2 µL of 10x Anza Red Buffer and 1 µL of each restriction enzyme were added to a final volume of 20 µL. Then, this reaction mixture was incubated for 15 min at 37 °C. The results of these digestions were cleaned up with using NZYGelpure kit (NZYTech) according to the manufacturers' instructions and quantified in a DS-11 microvolume Spectrophotometer (Denovix). Then, the ligation was performed with Anza T4 DNA Ligase Master Mix (Invitrogen), according to the company specifications. To this reaction a fixed quantity of 50 ng of vector was used, and the amount of insert was calculated through the following formula: $ng\ insert = \frac{ng\ insert\ x\ bps\ insert}{bps\ vector}$ in order to have a 1:5 ratio of vector:insert. After having the pMDC83-mNeonGreen the effectors cDNAs were inserted at the N-terminal end of mNeonGreen

using XbaI and SalI enzymes. The steps performed were similar to the ones already described.

2.5.2.2 *Gibson Assembly*

Since VTI12 has more than one recognition site for the enzymes chosen, Gibson Assembly technique, represented in the figure 5, was the method selected to perform the cloning of this cDNA. Thereby, a reaction mix was performed as showed in Table 9, in which the DNAs used were VTI12 and pMDC83:mNeonGreen, split in two pieces and the resistance gene, and the mix was incubated for 1 h at 50 °C (Gibson et al., 2009).

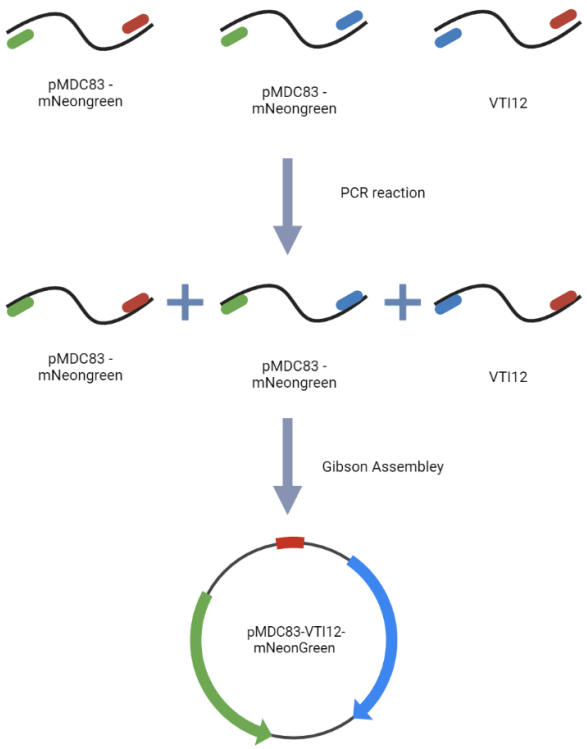

Figure 5 - Schematic representation of the Gibson Assembly cloning method designed for this study, where one cDNA was amplified and linked to an expression vector (pMDC83) linked with a fluorescent protein (mNeongreen).

Table 9 - Gibson Assembly Reaction

Components	Volumes
DNA to assemble	Equimolar volumes
5x IRB	4 µL
Taq DNA Ligase	2 µL

Phusion HF DNA Polymerase	0.25 µL
T5 Exonuclease (prediluted in 1:30 1x IRB)	0.25 µL
DdH_2O	Up to 20 µL

2.5.3 Preparation of competent cells

2.5.3.1 Chemical Escherichia coli competent cells

To prepare chemical competent cells, isolated colonies from NZYStar (NZYTech) were inoculated in 25 mL of Luria Broth medium (LB) (Duchefa Biochemie) supplemente with 10 µg/mL tetracycline (TET) and allowed to grow ON at 37 °C, with orbital shaking at 200 rpm. The cultures were added to 225 mL of LB medium supplemented with 1 M $MgCl_2$ and 1 M $MgSO_4$ (SOB) and were incubated at 37 °C with orbital shaking, until the optic density of the culture, at 600 nm (OD_{600}), were close of 0.7. When the optimal OD was achieved, the culture was incubated on ice for 10 min and centrifugated at 3000 x *g* for 5 min. The SN was removed, and the pellet was resuspended in 100 mL of RF1 (prepared with 1.51 g Rubidium Chloride (RbCL), 0.41 g Calcium chloride ($CaCl_2$), 21.55 mL 87% (v/v) glycerol, pH 5.8; after autoclaved 10 mL of 0.5 M Manganese Chloride ($MnCl_2$) and 10 mL of 0.3 M KAc were added) and left on ice for 15 min. Then, the mix was centrifuged at 3000 x *g* for 5 min, and the SN was discarded. The pellet was resuspended in 16 mL of RF2 (prepared with 0.019 g RbCl, 0.396 g $CaCl_2$, 0.033 g MOPS and 1.72 mL 87% (v/v) glycerol, pH 8.0). Finally, the mix was divided in 100 µL aliquots and stored at -80 °C.

2.5.3.2 Electrocompetent Agrobacterium tumefaciens cells

A culture of *Agrobacterium tumefaciens* GV3101 was inoculated in 5 mL of LB+Gen (LB supplemented with 50 µg/mL gentamycin) and was allowed to grow ON at 28 °C with orbital shaking. The total volume of the ON culture was inoculated in 200 mL of LB+Gen and was allowed to grow until an OD_{600} between 0.5 and 0.6. The culture was let on ice for 1 h and 200 mL of 1 mM HEPES, as well as 10 mL of 1 mM HEPES with 10% glycerol were prepared and left on ice. From this point, all the procedures were performed on ice and all the centrifugations were performed for 10 min at 2500 x *g* at 4 °C. The culture was then divided in 50 mL falcons and centrifuged once more. Afterwards, the pellet was resuspended in 25 mL of ice-cold 1 mM HEPES, combined into two 50 mL falcons, and centrifuged. This step was further repeated to wash the pellet, being finally resuspended in 20 mL of ice-cold 1 mM HEPES/10% glycerol. The mixture was centrifugated and the pellet was resuspended in 0.5 mL ice-cold 1 mM HEPES/10% glycerol, and aliquots of 50 µL were prepared and stored at -80 °C.

2.5.4 Bacteria transformation

2.5.4.1 Chemical Transformation

The entire volume of ligations or Gibson assembly mixes were used to transform E. Coli NZYStar chemically competent cells. In all the cases, the DNA was mixed with 100 µL of competent cells and incubated on ice for 15 min. Then all samples were transferred to a heating block at 42 °C for 1 min and further cooled down on ice for 5 minutes. To recover the bacteria from the heat shock, 1 mL of LB was added, followed by an incubation at 37 °C for 1 h, with orbital shaking. At the end, the cells were pelleted at 3 000 x g, 900 µL of the SN were discarded and the cell pellet resuspended in the remaining liquid and transferred to a plate with 1.5% (w/v) LB agar with 50 µg/mL kanamycin and 10 µg/mL tetracycline. The plate was left to incubate ON at 37 °C.

2.5.4.2 Electroporation Transformation

To transform *A. tumefaciens* competent cells, 2 µL of the plasmid DNAwere added to 50 µL electrocompetent cells, previously incubated on ice for 10 minutes in a electroporation cuvette. The cuvette with the mix was placed in the MicroPulser electroporator (Bio-Rad) and an electrical shock was delivered to the cells (1 pulse at 2.2 kV). To recover the cells, 1 mL of LB was added, followed by an incubation of 4 h at 28 °C. Afterwards, the cells were pelleted at 3 000 x g, 900 µL of the SN were discarded and the cell pellet resuspended in the remaining liquid and was transferred to a plate with 1,5% (w/v) LB agar with 50 µg/mL kanamycin, and 50 µg/mL gentamicin at, and left for incubation at 28 °C for 48 h.

2.5.5 Screening of positive colonies

The screening for positive colonies after the transformation was performed by Colony PCR. Fifteen colonies from the plates were selected and the PCR mix and protocol were performed using NZYTaq II 2x Green MasterMix (NZYTech) protocol, according to the Tables 2 and 3, respectively. Instead of DNA, a colony is partially used in the mix. Positive colonies were inoculated in 5 mL of LB with 50 µg/mL kanamycin and incubated ON at 37 °C with orbital shaking. The DNA was then extracted by using the NZYMiniprep kit (NZYTech) following the manufactures procedure. The plasmid DNA was then quantified using DS-11 microvolume Spectrophotometer (Denovix), sent to sequencing (https://eurofinsgenomics.eu/) and analyzed using SnapGene software (Dotmatics, https://www.snapgene.com/).

2.6 Vacuum infiltration for transient transformation of *Arabidopsis thaliana* seedlings

For transient expression of our constructs in *A. thaliana* by vacuum infiltration, the protocol established by Bernat-Silvestre and collaborators (2021) was adapted. Wildtype seedlings were let to grow for 7 days in a six well plate, where each one represented a different stress condition, as mentioned in the section 2.2.

Four days prior to the observation of the transformed plants one aliquot of *A. tumefaciens* GV3101 harbouring each construct was inoculated in 10 mL of LB medium with the appropriate antibiotics [Kanamycin (50 µg/mL) and Gentamicin (50 µg/mL)] and incubated for 24 h in agitation at 28 °C. This allowed the culture to reach an OD_{600} of 2.2, approximately. When the OD_{600} reached this value, SN was removed, and the pellet resuspended in liquid MS medium [2,2 g/L MS, 1,5 % (w/v) sucrose and pH 5.7]. Then, the OD_{600} of this bacterial suspension was measured in a 1:20 dilution and the bacterial suspension was diluted with infiltration buffer (liquid MS medium at RT with 0.005 % (v/v) Tween and 200 µM acetosyringone) to an OD_{600} of 2.2 to improve the transfection efficiency. This last suspension was kept at room temperature for 30-45 min, so the acetosyringone was assimilated by the bacteria and its virulence genes were activated. This suspension was poured into the wells (4 mL/well) so all the seedlings were completely covered. The plates were placed individually and opened into the vacuum desiccator and vacuum was applied at 300 mbar for 1 min. After this, the pressure was slowly increased to 400 mbar and vacuum applied for another minute. Afterwards, all bacteria suspension was removed carefully, and the wells were washed with liquid MS to remove all the remaining bacteria. The plates were reclosed with gas-permeable surgical tape and covered with aluminium foil for 45 min to 1 h to improve agroinfection. The aluminium foil was then removed, and the plates were kept for 3 days under the previously mentioned growth conditions.

The seedlings were then examined using a confocal laser scanning microscope Leica TCS-SP5 AOBS (Leica Microsystems CMS GmbH, Germany) equipped with a 40x water immersion objective. mNeonGreen was detected within short 505-530 nm wavelength range, assigning the green colour. All the acquisitions were performed in Leica LAS AF Lite software and image processing and analysis in Fiji Software.

2.7 Confocal analysis of plants expressing fluorescent markers

Transgenic plants provided by Prof. GianPietro Di Sansebastiano, namely *A. thaliana* lines transformed with SYP51-GFP and TUA6-GFP were grown in the same

conditions as mentioned in chapter 2.2 for 5 days. Afterwards they were analysed through a confocal laser scanning microscope LSM 710 Zeiss (ZEN Software, GmbH, Germany) equipped with 40X and 40X immersion oil objectives. Green fluorescent protein (GFP) was detected within the short 505-530 nm wavelength range, assigning the green colour.

2.8 Real-time qPCR

To evaluate the expression of genes that encode for proteins involved in the same trafficking pathways as the genes targeted in the T-DNA lines, RNA was extracted, cDNA produced and then qPCR assays were performed.

2.8.1 RNA extraction

To extract RNA from the *Arabidopsis* T-DNA lines, the kit Total RNA Isolation kit (NZYTech) was used. The manufacturer protocol was used, however the mass of plant tissue used was 150 mg and was previously frozen with liquid nitrogen, and the elution volume was down to 20 µL. After the extraction, the RNA was quantified in DS-11 microvolume Spectrophotometer (Denovix) and stored at -80 °C. The RNA integrity was confirmed by an horizontal electrophoresis system using a bleach gel [1% (w/v) agarose supplemented with 1% (v/v) bleach, with TAE 1x].

2.8.2 cDNA production

To produce cDNA from the isolated RNA, the NZY First-Strand cDNA Synthesis kit (NZYTech) was used according to the manufacturers protocol. The reaction components present in Table 10 were added to a PCR tube, and then transferred to the thermocycler to perform the program mentioned in Table 11. Then, 1 µL of NZY RNase H was added and an incubation of 20 min at 37 °C was performed. This step is crucial to remove the RNA from the cDNA. The cDNA solution was stored at -20 °C.

Table 10 - Reaction mix for cDNA production according to NZY First-Strand cDNA Synthesis kit

Components	Volumes
NZYRT 2x Master Mix	10 µL
NZYRT Enzyme Mix	2 µL
RNA	Calculated based on RNA quantification 1 µg
DEPC-treated H_2O	Up to 20 µL

Table 11 - Thermocycler program used according to manufacturer's protocol

Temperature (°C)	Time (min)
25	10
50	30
85	5

2.8.3 Real-time assays

All the selected genes belong to the protein sorting/defence mechanisms of the cell, as they are described in table 12. The genes encoding proteins involved in protein sorting were tested using the cDNA from the T-DNA plants affecting *VSR2*, and the genes encoding proteins involved in the cell defence were evaluated in the T-DNA plants affecting *EXO70*.

All the primers were already available in the laboratory, and were already optimized, according to Neves et al. (2021), as well other reaction optimizations like dilution tests, efficiency studies and the validation of the reference genes (*UBC9* and *SAND*), all presented in supplementary table 3.

The experimental plate design was made, and it was decided that each plate would be to one gene to test, where each line (A, B, C, D, E and F) would represent a stress situation, and each triplet of columns one biological replicate, where each well of the triplet would correspond to one technical replicate. The plate design was performed with the software Bio-Rad CFX Maestro 1.0, and is represented in supplementary figure 1.

The qPCR reaction included 8 µL of a master mix composed by 315 µL of NZYSupreme qPCR Green Master Mix (2x), 400 nM of each primer (forward and reverse), and 163.8 µL of water, and 2 µL of cDNA previously diluted 1:8, performing a reaction volume of 10 µL. The plates used were the Hard-Shell PCR plates (Bio-Rad) of 96 wells. The protocol used is described in Table 12, and the equipment where the assays were performed was CFX96 Real-Time System (BioRad). Using Bio-Rad CFX Maestro (version 1.0) software, cycle threshold (Ct) and expression tests were calculated, by comparing with control condition. Based on the research of Czechowski and associates (2005) the UBQ9 and SAND were selected as housekeeping genes.

Table 12 - qPCR program

Step	Temperature (°C)	Time
1	95	3 min
2	95	10 s
3	56	10 s
4	72	30 s
	Plate read	
5	Repeat 39x from step 2	
6	95	10 s
7	65-95 Gradient	5 s
	Plate Read	
	End	

2.9 Statistical analysis

All the parameters mentioned in the section 2.4 were submitted to statistical analysis to confirm significant differences. All biometrical and biochemical procedures were performed in, at least, three independent biological replicates (n ≥ 3). Prior to any statistical treatment, variances homogeneity was checked by the Brown–Forsythe test. Analysis with only one variable were examined through a one-way ANOVA, while the ones comparing two variables (genotype and stress) used a two-way ANOVA. All statistical analyses were performed in Prism 8 (GrahPad®, San Diego, CA, USA).

3. Results

3.1 Characterisation of *Arabidopsis* mutant lines

3.1.1 Genotypic evaluation of *Arabidopsis thaliana* T-DNA mutant lines

All the lines mentioned in Table 1 (section 2.1.1) were germinated and grown until the rosette state under controlled conditions. Afterwards, a leaf fragment was collected to extract gDNA, and PCRs were performed to check if the lines were homozygous for the T-DNA insertions. In the agarose gel, every three wells represent samples from the same plant, where three different PCRs were performed so it could be possible to check for the wild type or the insertion band. Therefore, 3 samples were loaded and separated, allowing to identify wild type plants by the presence of a band in the gel, and two allowing

to identify the T-DNA insertions. The combinatory analysis of all three PCRs allows to identify wild type, heterozygous or homozygous plants for the T-DNA insertions. Of the 9 lines tested only two were homozygous for the *vsr2* and *exo70*, as it is possible to observe in Figures 6 and 7, respectively (red rectangles). These plant lines were selected for use along the rest of the work.

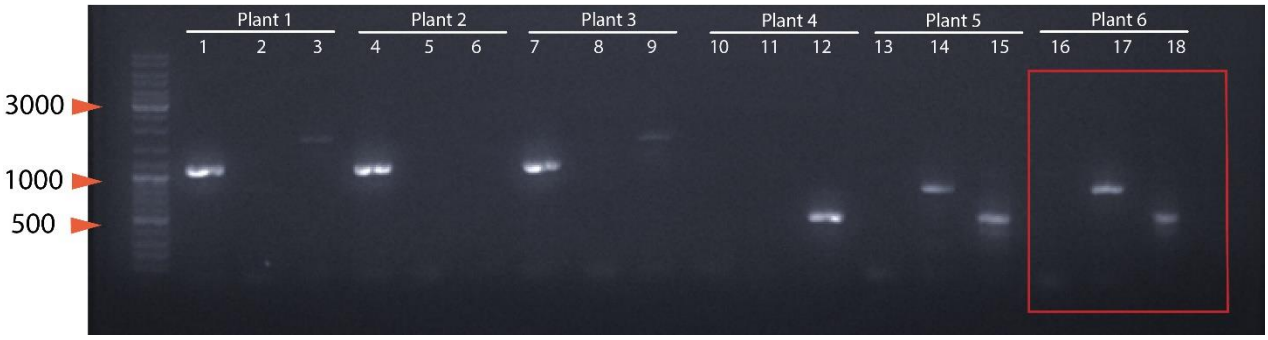

Figure 6 – Electrophoretic analysis of different gDNA's from *vsr2* mutant lines. Each plant was loaded in 3 wells due to the 3 different PCRs performed to identify the bands. First well is for the wt band, while the other two represent a T-DNA insertion. The samples that were used in well 13-15, 16-18 represent homozygous mutants. Ladder: GeneRuler DNA Ladder Mix (Thermofisher). Orange arrows indicate DNA ladder bands of 3000 bp, 1000 bp and 500 bp.

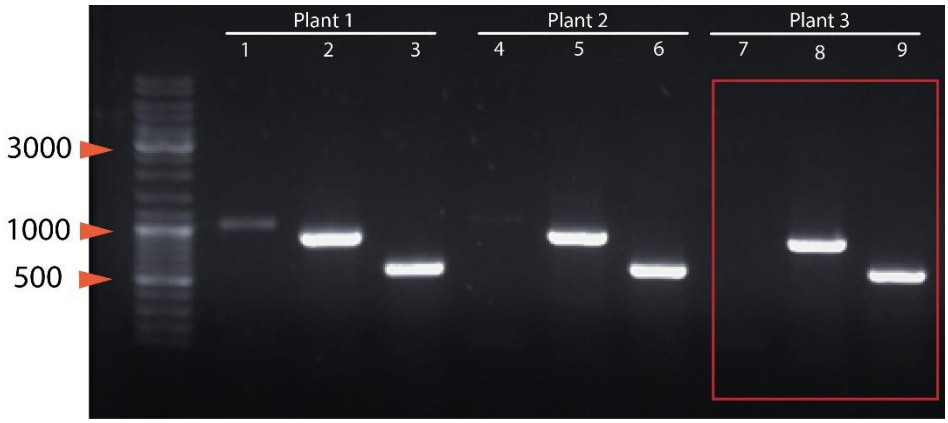

Figure 7 - Electrophoretic analysis of different gDNA's from *exo70* mutant lines. Each sample is constituted by 3 wells, first well is for the wt band, while the other two represent a T-DNA insertion. The sample that was used in well 16, 17 and 18 represent a homozygous mutant. Ladder: GeneRuler DNA Ladder Mix (Thermofisher). Orange arrows indicate DNA ladder bands of 3000 bp, 1000 bp and 500 bp.

3.1.2 Biometric parameters of T-DNA mutants under abiotic stress

After obtaining *exo70* and *vsr2* homozygous mutants, seedlings were grown under different abiotic stresses (salinity, osmotic, oxidative and metal toxicity), as mentioned in Section 2.2. In the *vsr2* line, morphologic changes are notorious when comparing control and stress situations (Figure 8). In saline (S1) and osmotic stresses (H1 and H2) the alteration in seedling growth is very similar, showing some developmental delay (figure 8A S1, H1, H2). The oxidative (Ox) situation did not show notorious morphological changes (figure 8A Ox), as these seedlings were quite similar to the control. The metal-induced stress by Zn, besides inducing a delay in seedling

development, also led to the appearance of chlorotic areas on leaves (figure 8A Zn). Concerning root length, a significant growth inhibition was found for H1 (35%), H2 (56%), Ox (48%) and Zn (46%) situations when compared to the control (figure 8C). When compared with the wt plants, significant differences were found in all stress situations, except H1, showing an increase in root length in C (54%) and S1 (126%), and decreases in H2 (38%), Ox (41%) and Zn (28 (figure 8B).

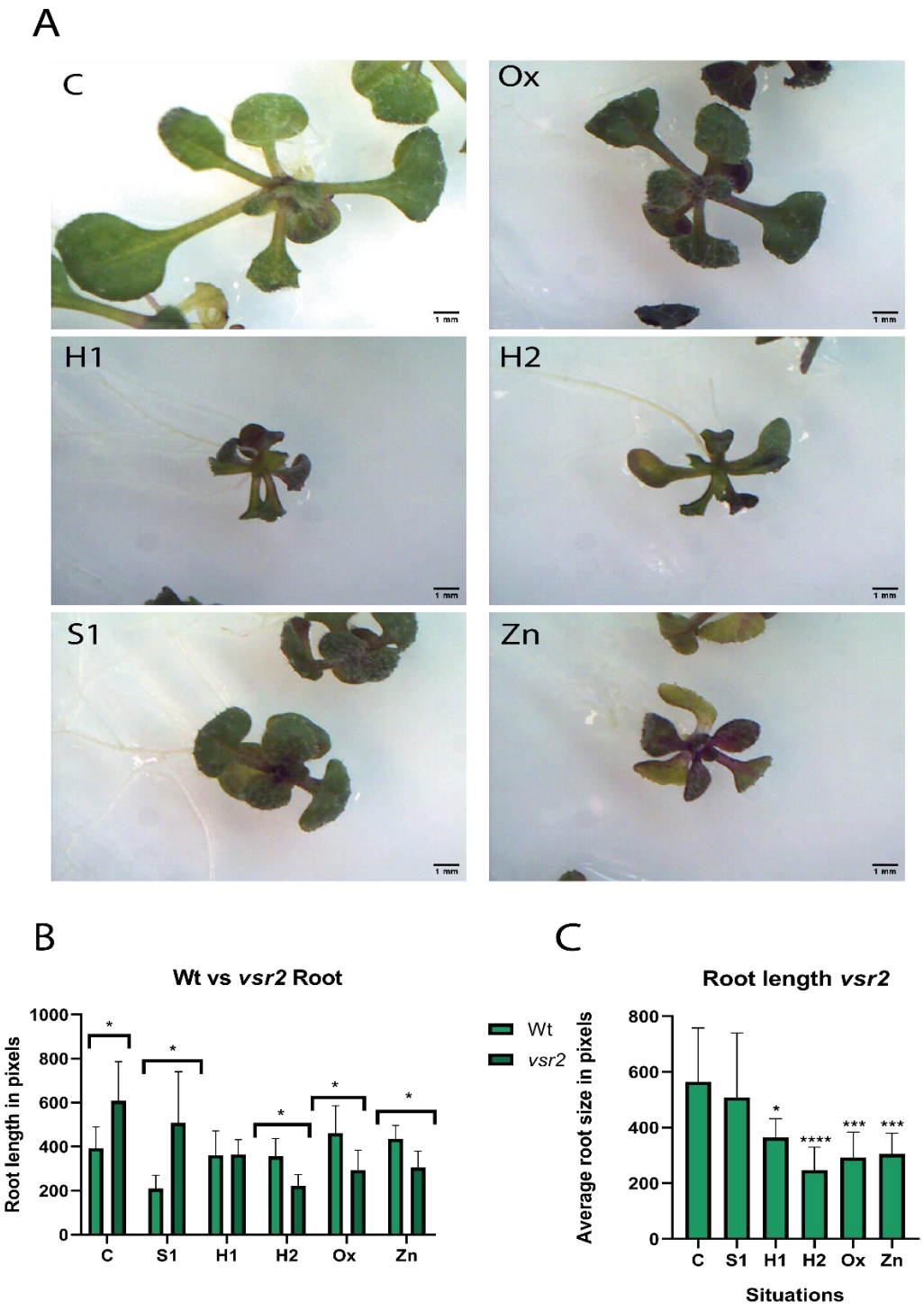

Figure 8 - Biometric analysis of vsr2 line
A - Size comparison of Arabidopsis thaliana seedlings in stress conditions B - Bar plot of the average root size in stress conditions relative to wt; C -Bar plot of the average root size in stress conditions relative to control;; The statistically experimental from One-way ANOVA values are represented by:* (pvalue ≤0.05), ** (pvalue ≤0.01); ***(pvalue ≤0.001);****(pvalue <0.0001), according with the One-way ANOVA.

In the *exo70* T-DNA line, morphological changes were also found. In control seedlings it was already possible to notice some changes comparatively to *vsr2,* by the appearance of purple stains that can be areas accumulating anthocyanins and even the seedling structure. In this genotype, S1, H1 and H2 had similar morphological responses as *vsr2*, such as signs of developmental delay (figure 9A S1, H1 and H2), being this aspect more evident in H2 situation. In addition, a different response was observed when seedlings were under oxidative stress, where a developmental delay was registered (figure 9A Ox). Moreover, Zn-exposed seedlings presented more evident symptoms of leaf chlorosis, compared to the control (Figure 9A Zn). The root length had a significant increase in H1 (51%), and a significant decrease in H2 (37%) and Ox (38%) (Figure 9C). When comparing the root length of the mutant with wt, significant differences were not observed in the control situation. However a decrease was found in H2 (40%) and Ox (67%) (Figure 9B).

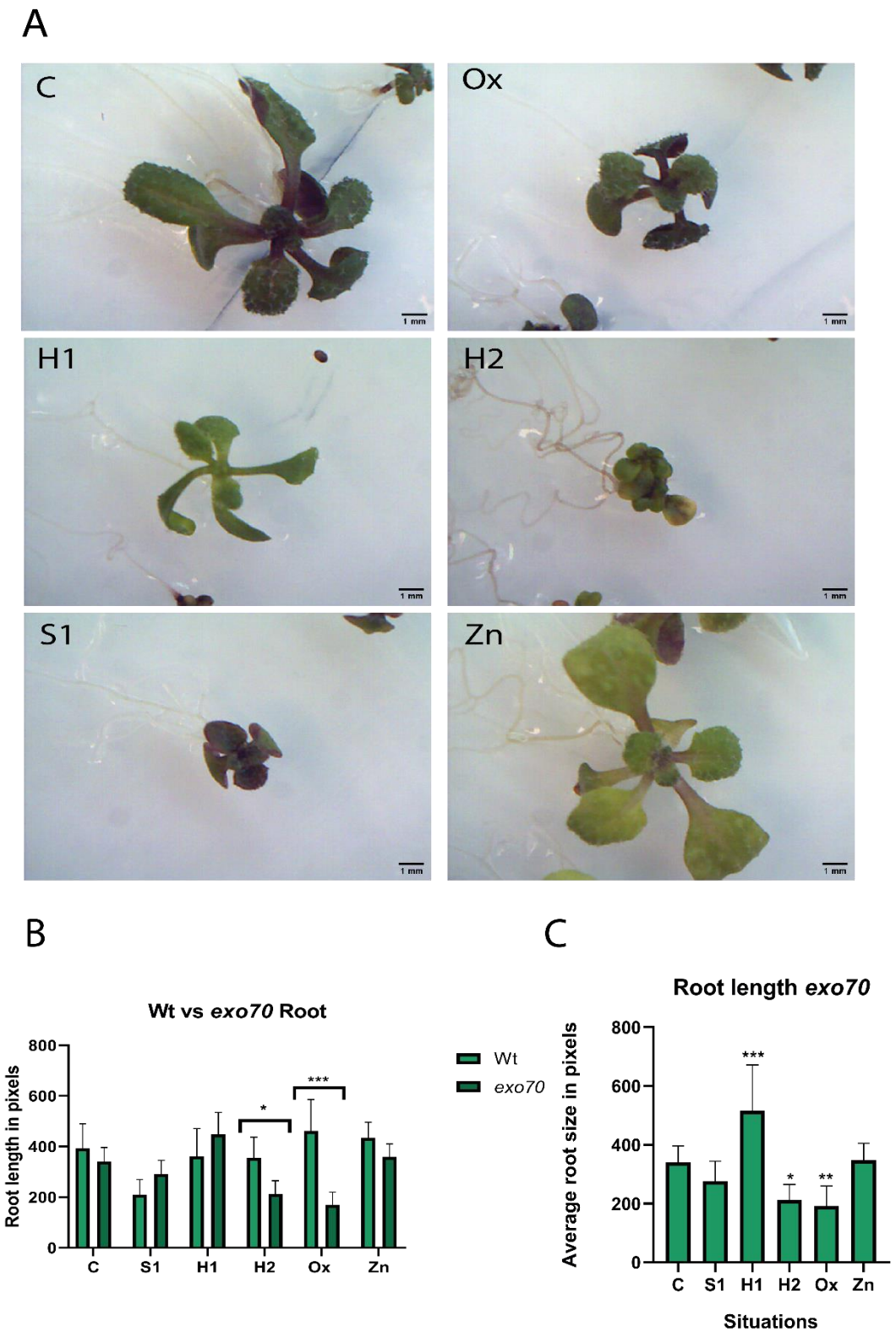

Figure 9 - Biometric analysis of exo70 line
A – Size comparison of Arabidopsis thaliana seedlings in stress conditions B - Bar plot of the average root size in stress conditions relative to wt; C-Bar plot of the average root size in stress conditions relative to control;; The statistically experimental values were performed by a One-way ANOVA are represented by:* (pvalue ≤0.05), ** (pvalue ≤0.01); ***(pvalue ≤0.001);

3.2 Biochemical assessment of wt and mutant seedlings

To analyse how the seedlings from different genotypes reacted to the different stress conditions, several biochemical assays were performed to evaluate the physiological performance and the oxidative status, along with the response of the AOX system.

3.2.1 Photosynthetic pigments

The photosynthetic pigments (total chlorophylls and carotenoids) were quantified in leaves of all studied genotypes. Both pigments showed very similar responses among the lines tested. In the wt plants, chlorophylls and carotenoids exhibited a significant decrease in S1 (26% and 17%), H2 (20% on both) and Zn (51% and 40%) stress situations (Figure 10 A and B). Regarding *vsr2* similar results were observed; however, the chlorophylls and carotenoids reduction was significant in all stress situations (S1- 26% and 28%; H1- 45% and 43%; Ox- 47% and 43%; Zn - 30% and 26%), apart from Ox (Figure 10 C and D). *Exo70* plants were no exception, demonstrating a decrease in the amount of both pigments under Ox (38% and 36%) and Zn (67% and 59%) situations. Plants under H1 only showed a significant decrease in the carotenoids (29%), and plants under H2 showed a decrease in chlorophylls (45%) (Figure 10 E and F).

3.2.2 H_2O_2 content and Lipid Peroxidation peroxidation (LP) content

Wild type plants showed a decrease in the amount of H_2O_2 across treatments, though statistical relevance was only achieved for H1(50%) and H2 (45%) treated plants. However, in Ox treated plants there was a significant increase (36%) in the amount of H_2O_2 (Figure 11C). Regarding *vsr2* plants, there was significant decreases in all stress situations: S1 (32%), H1(28%), H2(43%), Ox (35%) and Zn (28%), when compared with control situation (Figure 11E). In the *exo70* plants although a general tendency for decreased values of H_2O_2 were found in all treatments compared with the control, a significant reduction of about 56% was only recorded upon exposure to Zn (Figure 11G). The H_2O_2 contents for the three genotypes (wt, *vsr2, exo70*) under control conditions were compared, but no significant changes were found (Figure 11A).

Concerning LP levels and comparing control plants, there were significant differences between the T-DNA lines (Figure 11B). Regarding the behaviour wt plants under the stress treatments, only the oxidative stress (Ox) induced a significant increase of MDA (123%). H1 and H2 treatments did not change this parameter; however, MDA levels showed a tendency to increase in S1 treated plants and to decrease in Zn treated

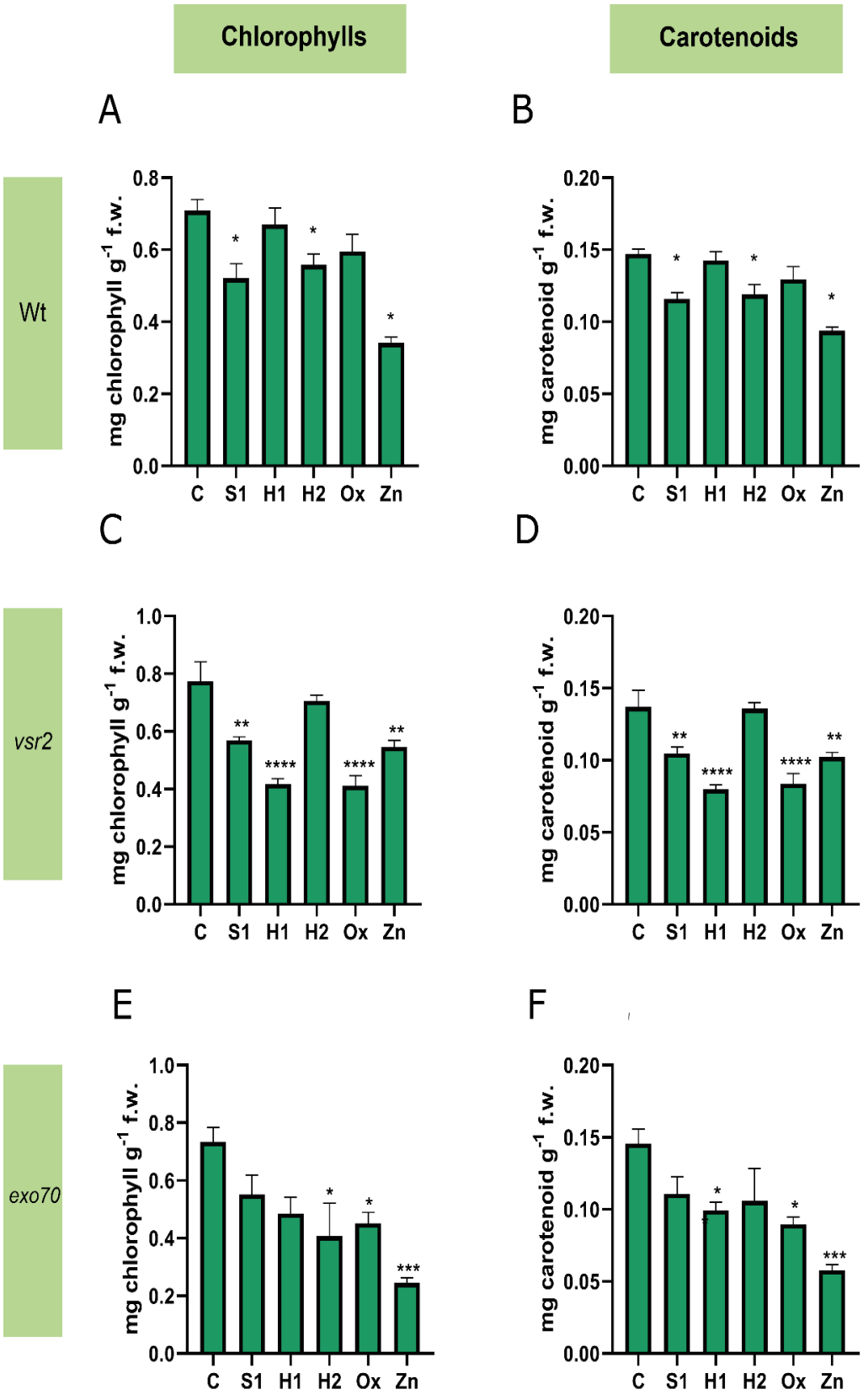

Figure 10 -Quantification of total chlorophylls and carotenoids. A, C and E show the Chlorophylls related results from, wt, *vsr2* and *exo70* plants. B, D and F show the carotenoids content from Wt, *vsr2* and *exo70* plants. Results are presented as mean ± standard deviation (SD) and result from the evaluation of at least three experimental replicates (n ≥ 3). * (pvalue ≤0.05), ** (pvalue ≤0.01); ***(pvalue ≤0.001);****(pvalue <0.0001), according to the one-way ANOVA

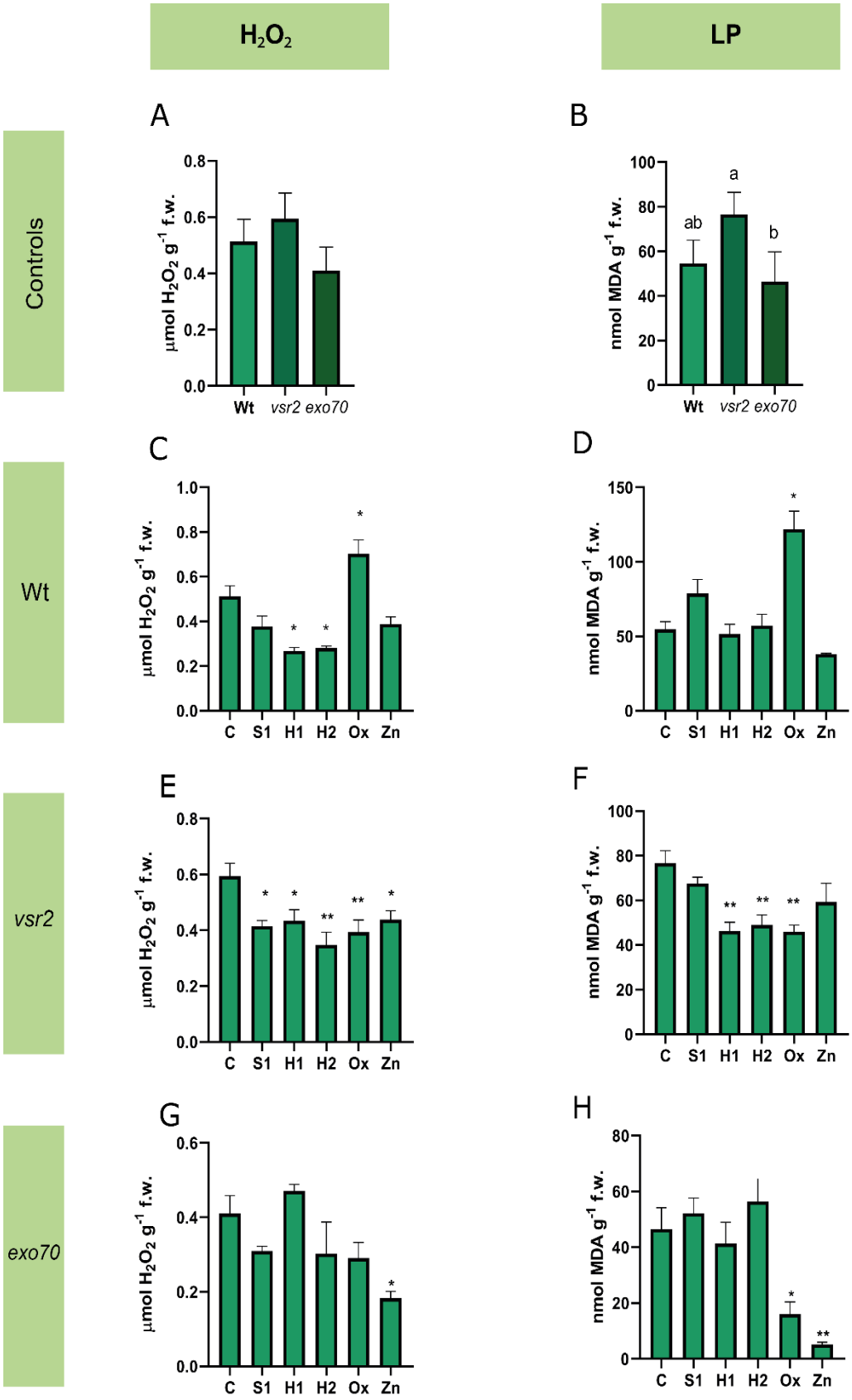

Figure **11** - Quantification of H_2O_2 and LP activity (measured as nmol MDA g^{-1} f.w.). A and B represent comparisons between the control plants (wt, *vsr, exo70*). C, E and G are H_2O_2related results from, wt, *vsr2* and *exo70* plants. D, F and H show the LP activity from wt, *vsr2* and *exo70* plants. Results are presented as mean ± standard deviation (SD) and result from the evaluation of at least three experimental replicates (n ≥ 3). * (pvalue ≤0.05), ** (pvalue ≤0.01), according to the one-way ANOVA; a and b refer to significant differences between them, according to the one-way ANOVA

plants, in relation to the control plants (Figure 12D). In *vsr2* plants, the LP was reduced by 40%, 36% and 40% respectively when compared with the control seedlings (Figure 11F). In *exo70* plants, there were no significant changes between the MDA amounts in S1, H1, and H2 treated plants; however, in the Ox treated plants, there was a significant reduction in MDA amounts (65%) and an even higher decrease (88%) in the Zn treated plants when compared with the control (Figure 11H).

3.2.3 Non-enzymatic AOX system

From several components of the non-enzymatic AOX system, proline (Pro) and GSH contents were chosen for this work. Comparing the Pro values from wt and the mutants, there were significant changes between mutants, namely an increase of 90% of proline levels in *vsr2* plants (Figure 12A). Wild type (wt) plants under stress situations showed an increased accumulation of Pro when compared to the control (C), apart from H1 treatment that did not alter. Thereby, the S1 as well as the H2 treated plants presented a 1.5-fold increase. In the Ox treated plants, the increase was of 0.84-fold and in Zn treated plants 1-fold (Figure 12C). The mutant *vsr2* showed a tendency to increase the values of Pro, presenting significant changes in the S1, with an increase of almost 3.5-fold, when compared with the control situation, and a 1.27-fold increase In H2 (Figure 12E). In *exo70* plants significant mutant increases were detected in the Pro amount, compared with control, since S1 and H2 significantly increased by 1.73-fold and 3-fold, respectively (Figure 12G).

Regarding GSH on control plants (wt, *vsr2* and *exo70*) a significant decrease was perceived in *vsr2* (77%) and *exo70* (91%) plants (Figure 12B), in relation with wt. Interestingly, wt plants under stress conditions only showed a significant change of GSH upon Zn exposure, where an increase of 50% was recorded, when compared with the control (Figure 12D). Seedlings from the mutant *vsr2* also followed this pattern, as Zn-treated plants were the only ones enhancing the production of this metabolite, which rises to 47% (Figure 12F). Regarding *exo70* more alterations in GSH levels were observed since the levels in H2, Ox and Zn increased significantly by 170%, 112% and 210%, respectively (Figure 12H).

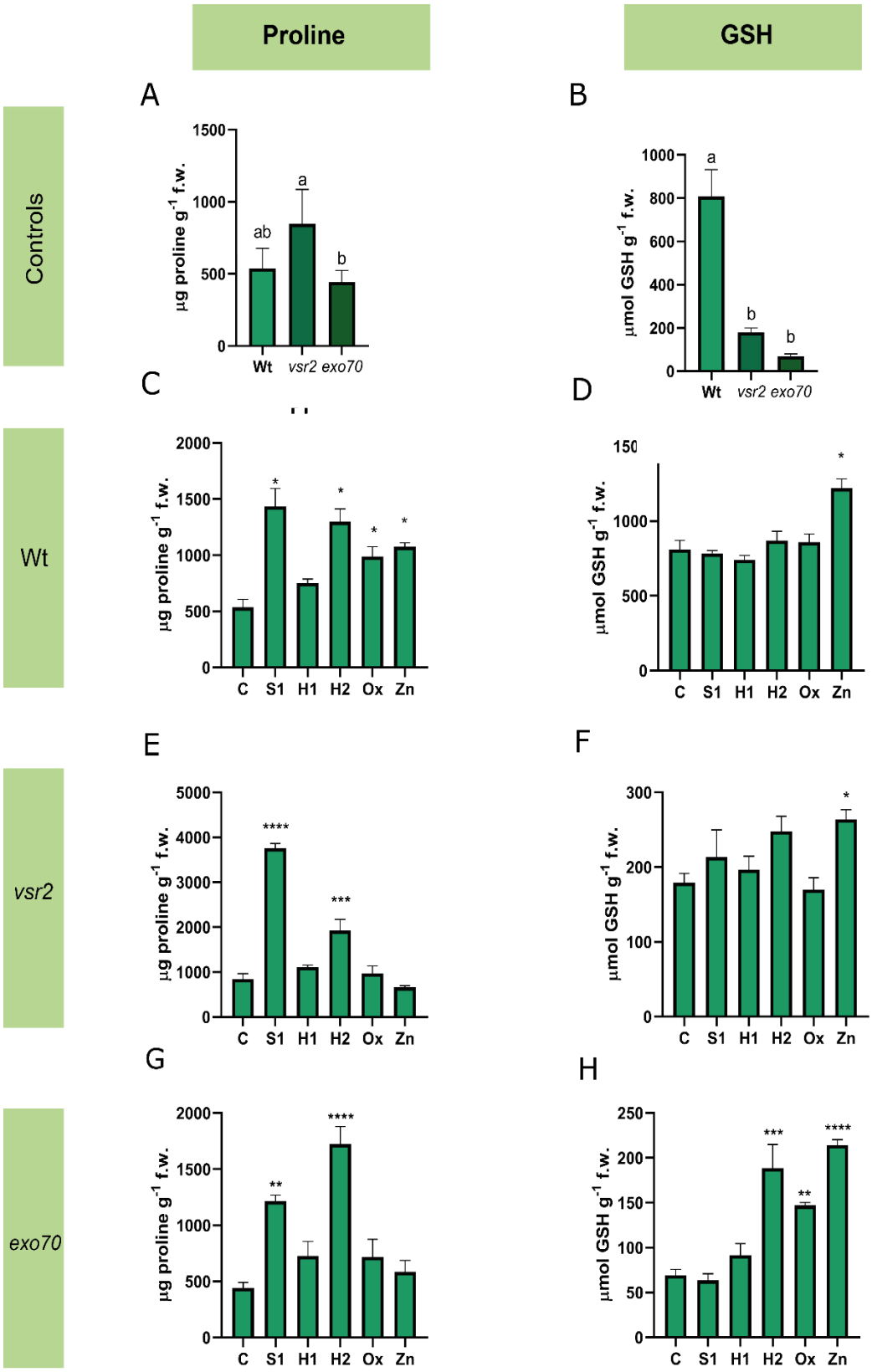

Figure 12 - Quantification of Proline (Pro) and GSH. A and B represent comparisons of Pro and GSH values between control plants (wt, *vsr2 and exo70*). C, E and G SHOW Pro results from, wt, *vsr2* and *exo70*, respectively. D, F and H depict GSH quantification from wt, *vsr2* and *exo70*, respectively. Results are presented as mean ± standard deviation (SD) of at least three experimental replicates (n ≥ 3). * (pvalue ≤0.05), ** (pvalue ≤0.01); ***(pvalue ≤0.001);****(pvalue

<0.0001), according to the one-way ANOVA; a and b refer to significant differences between them, according to the one-way ANOVA

3.2.4 AOX enzymatic system – APX and CAT activities

Significant changes in APX were found when comparing control plants (wt, *vsr2* and *exo70*) between them, *vsr2* showed a decrease of 74% and *exo70* a decrease of 66%, in relation with wt (Figure 13A). Wildtype seedlings showed a significant increase of APX activity in H1 (29%), and significant decreases in H2(71%), Ox (64%) and Zn (55%) (Figure 13C). In relation to *vsr2* plants, APX activity has significantly increased in all stress situation (S1- 82%, H1 - 134%, Ox - 109%, Zn- 148%), when compared with control, reaching its maximum values in H2 (161%) (Figure 13E). Concerning *exo70* plants, no significant alterations were observed, excluding S1 which showed a reduced APX activity of 40%, compared to the control (Figure 13G).

Regarding CAT in control plants, significant changes were found between mutants, namely an increase of 127% in *exo70* (Figure 13B). In the wt plants under stress conditions CAT activity showed a significant increase in H1(26%), and decreases in H2 (55%), Ox (37%) and Zn (65%) (Figure 13D). Interestingly enough in the *vs2* plants CAT activity increased significantly in all stress situations, apart from S1, that had no significant changes (H1-62%, H2-79%, Ox-69%, Zn-79%), when compared to the control plants (Figure 13F). Relative to *exo70* plants, a significant reduction of CAT activity was found in S1 (47%), but no major changes were found in the other treatments (Figure 13H).

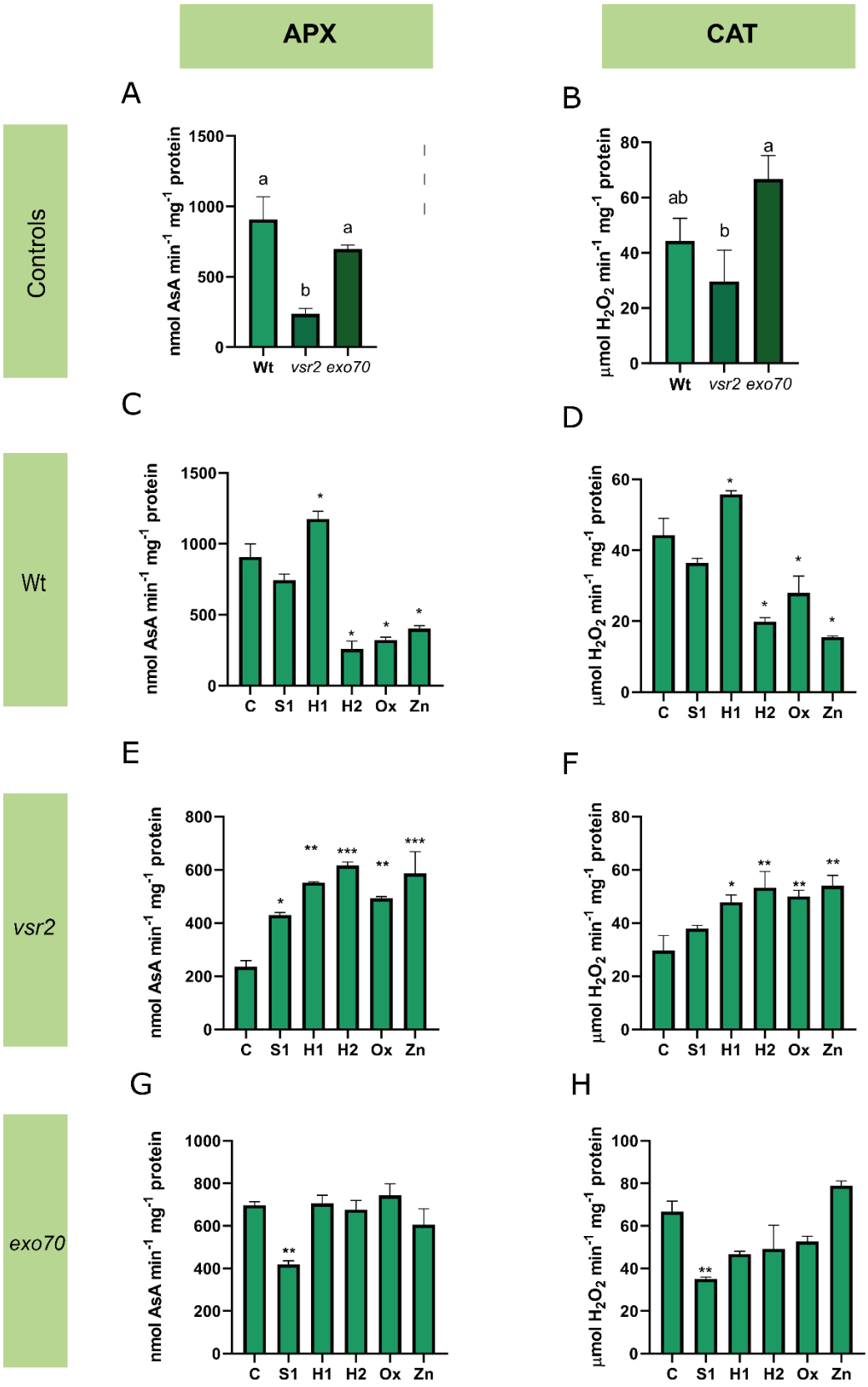

Figure 13 - Quantification of APX and CAT activity. A, C and E represent APX activity from, wt, *vsr2* and *exo70*, plamts. B, D and F depict CAT activity from wt, *vsr2* and *exo70* plants. Results are presented as mean ± standard deviation (SD) from the evaluation of at least three experimental replicates (n ≥ 3). * (pvalue ≤0.05), ** (pvalue ≤0.01); ***(pvalue ≤0.001);****(pvalue <0.0001), according to the one-way ANOVA

3.3 Localisation of endomembrane system effectors under stress

3.3.1 Isolation of the cDNA's – classical cloning

One of the objectives of this study was to evaluate the localisation of several endomembrane system effectors under stress conditions, to check if there are alterations in their sorting and accumulation. The first step to do so, was to obtain fluorescent fusions of the selected effectors and mNeonGreen. Therefore, cDNA's of the effectors had to be isolated from plasmids already available in the laboratory, namely VSR2 (Figure 14A – blue arrow), RMR1 (Figure 14B – red arrow) and VTI11 (Figure 14C – green arrow). Also, the fluorescent protein, mNeongreen, had to be isolated and inserted in the expression plasmid pMDC83 (Figure 14D). These isolations were performed through PCR with primers that added adaptors to the restriction enzymes, as mentioned in section 2.5.1.

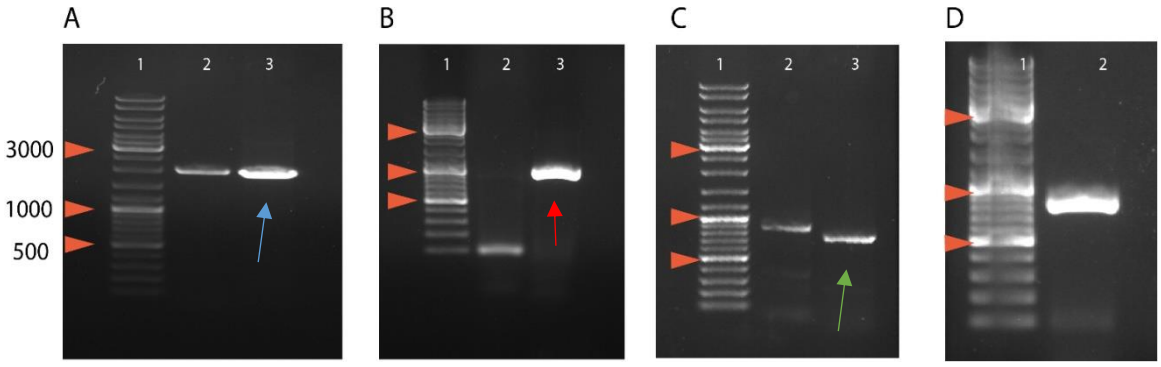

Figure 14 - Electrophoretic analysis of different isolated cDNA's. A – VSR2; B- RMR1; C – VTI11; D- mNeonGreen. Ladder: GeneRuler DNA Ladder Mix (Thermofisher) Orange arrows indicate DNA ladder bands of 3000 bp, 1000 bp and 500 bp.

Through restriction cloning, mNeongreen was inserted in pMDC83 by cutting off the mCherry gene that was in the initial construct and replaced with the new fluorescent protein gene. Screening for the positive colonies was performed through PCR and DNA sequencing, where was obtained the pMDC83-mNeonGreen (Figure 15). Then all the cDNA's were inserted in the pMDC83-mNeongreen (Supplementary Figure 2) through restriction cloning. Screening for the positive colonies was performed through PCR and DNA sequencing using the primers described in supplementary table 2. Positive colonies with the correct insert were only obtained for pMDC83-VTI11-mNeongreen (Figure 16, Supplementary figure 3) and pMDC83-RMR1-mNeongreen (Figure 17, Supplementary figure 4).

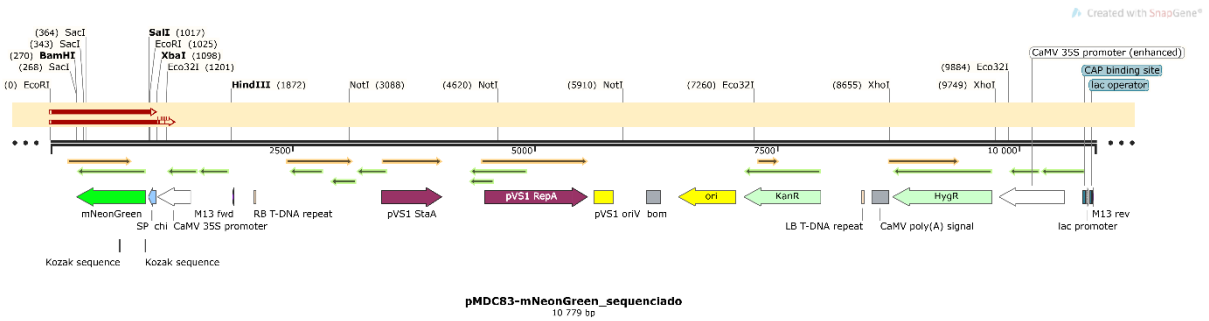

Figure 15 - Alignment of the sequencing results of pMDC83-mNeongreen. The sequencing results with M13Uni primer (Supplementary table x) were aligned with the expected DNA sequence of pMDC83 -mNeonGreen. The sequence alignment was performed resorting to Snapgene software (https://www.snapgene.com/). Red portions of the arrows represent sequence match and alignment, whereas white portions represent no alignment.

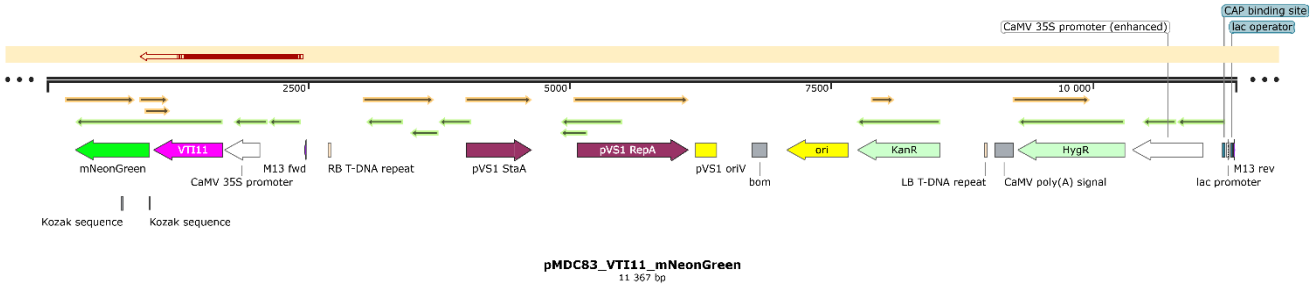

Figure 16 - Alignment of the sequencing results of pMDC83-VTI11-mNeongreen. The sequencing results with M13Uni primer (Supplementary table x) were aligned with the expected DNA sequence of pMDC83- VTI11-mNeonGreen. The sequence alignment was performed resorting to Snapgene software (https://www.snapgene.com/). Red portions of the arrows represent sequence match and alignment, whereas white portions represent no alignment.

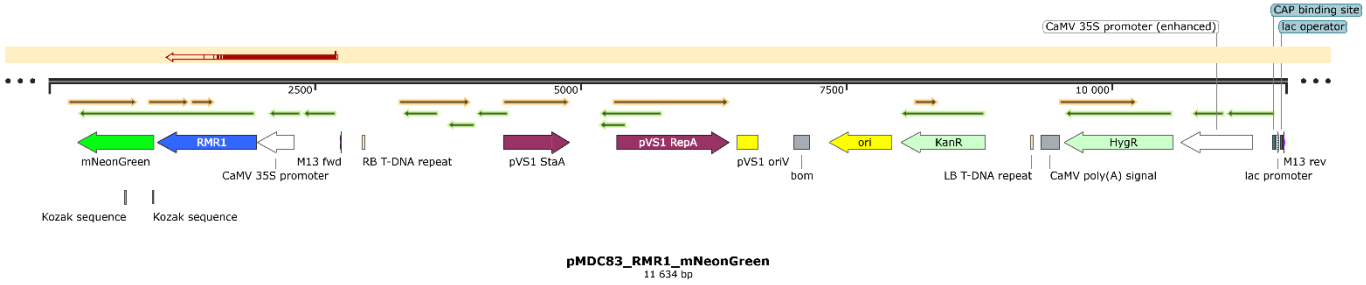

Figure 17 - Alignment of the sequencing results of pMDC83- RMR1-mNeonGreen. The sequencing results with M13Uni primer (Supplementary table x) were aligned with the expected DNA sequence of pMDC83- RMR1-mNeonGreen. The sequence alignment was performed resorting to Snapgene software (https://www.snapgene.com/). Red portions of the arrows represent sequence match and alignment, whereas white portions represent no alignment.

3.3.2 Gibson Assembly

For VTI12 cloning, Gibson assembly method was performed. Specific primers were designed to VTI12 and pMDC83-mNeongreen to perform this reaction. Following Gibson assembly, the same strategies to check for positive colonies were used as in classical cloning. Positives clones after sequencing of pMDC83-VTI12-mNeongreen were selected (Figure 18, Supplementary figure 5).

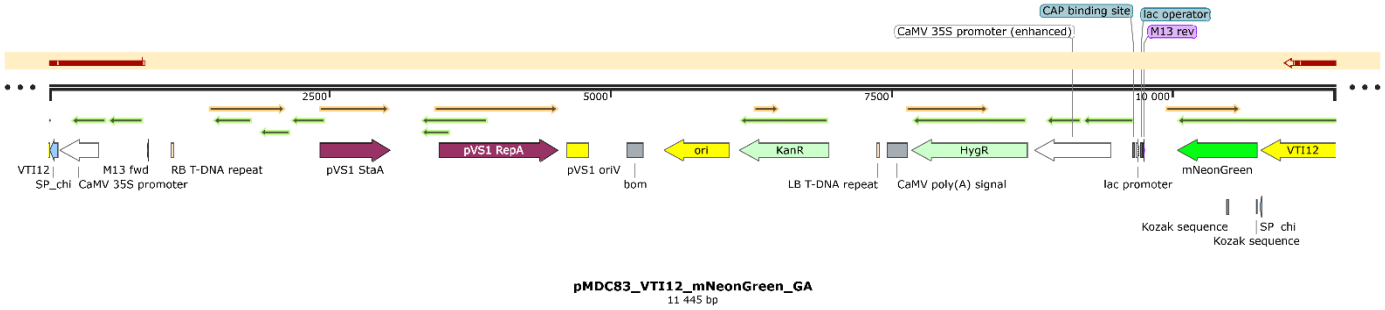

Figure 18 - Alignment of the sequencing results of pMDC83- VTI12-mNeonGreen. The sequencing results with M13Uni primer (Supplementary table x) were aligned with the expected DNA sequence of pMDC83- VTI12-mNeonGreen. The sequence alignment was performed resorting to Snapgene software (https://www.snapgene.com/). Red portions of the arrows represent sequence match and alignment, whereas white portions represent no alignment.

3.3.3 Localisation of the Endomembrane system effectors under abiotic stress

After obtaining all the constructs, *A. thaliana* seedlings, grown under abiotic stress conditions, were transformed through vacuum infiltration (section 2.6). This part of the work was performed under an Erasmus+ internship, supervised by Doctor Gian Pietro Di Sansebastiano, in Lecce, Italy. Despite being a technique routinely performed in the lab, the fluorescent signal obtained for the endomembrane effectors was not optimal and did not allow to see differences between the different types of stress. There we compared the signal from stable transformed plants, available in Dr. Di Sansebastiano lab, (with SYP51-GFP, Figure 19) with the signal from our transient transformed plants (Figure 19 RMR1-mNeonGreen and VTI11-mNeonGreen) and confirmed that the fluorescence detected after transient expression was rather lower, than the one detected in stably transformed plants, and did not allow for a proper analysis. Therefore, and since the signal is better in the plants that stably express the fluorescent fusion, we decided to produce transgenic plants to have better and more conclusive results. Nevertheless, and despite SYP51 was not in the initial set of effectors to approach in this work, we decided to perform the stress localization analysis using these plants. The acquisition of these images was only performed in osmotic stresses, since SYP51 localises majorly at the tonoplast. Since no differences were noticed in

leaves (data not shown), we decided to analyse root tissue. Here differences are noted. In S1 the formation of vesicles was observed, increasing in number and size in H1 situation (Figure 20 white arrows). Some tonoplast shrinkage is also observed in the osmotic stresses.

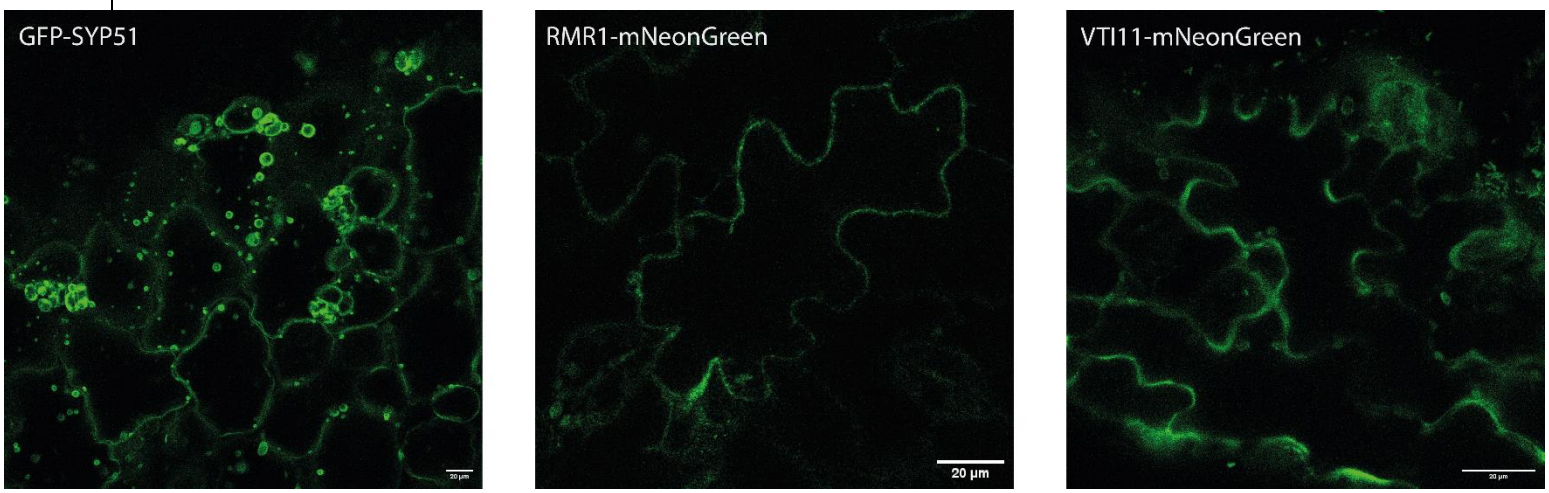

Figure 19 – Diferences between signals from stable expression (GFP-SYP51) and transient expression (RMR-mNeonGreen and VTI11-mNeonGreen).

Furthermore, and still under the supervision of Doctor Di Sansebastiano, it was evaluated the distribution of the cytoskeleton microtubules under abiotic stress. So, plants stably expressing TUA6 (Tubulin alpha-6 chain) fused with GFP, were allowed to grow under the abiotic stress conditions mentioned before in this study. The results showed no visible alterations in the organization of microtubules in plants exposed to stress. In all cases, the microtubule network is visible as a mesh of tubules, particularly at the cell surface (figure 21). It is not possible to exclude subtle alterations in the microtubule's organization or dynamics, however more sensitive techniques and super-resolution technology must be used.

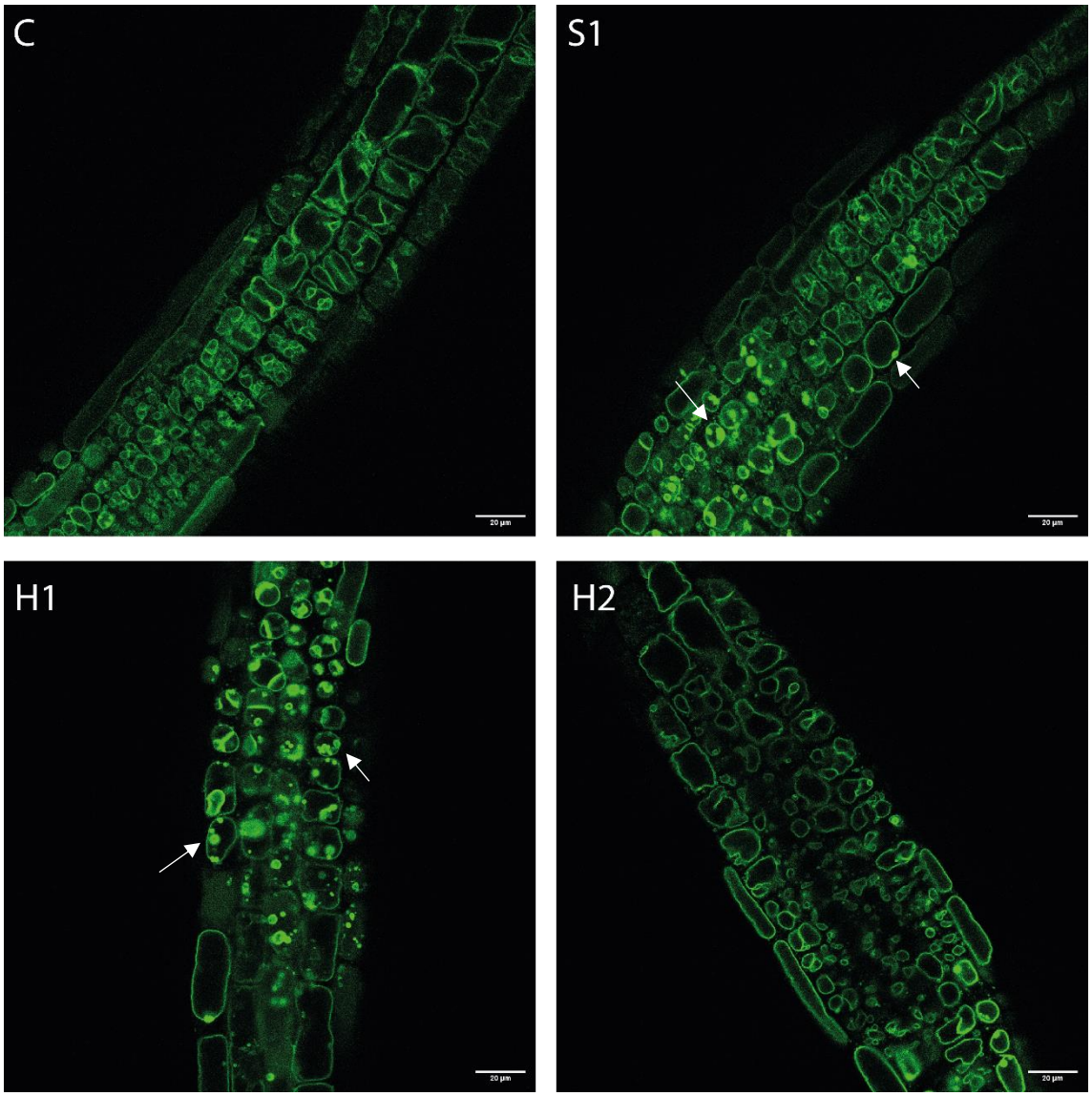

Figure 20 -SYP51-GFP expression in routes under osmotic stresses. The white arrows represent vesicles tagged with SYP51-GFP that are increased under the stress situations.

3.5 Different genes behave differently under abiotic stress

Genes involved in protein sorting, namely LV and PSV routes, were selected to evaluate if their expression would alter in the *vsr2* mutant. The results obtained show that PSV trafficking related genes (*AtRMR1, AtVTI12, AtSYP51, AtVSR1* and *AtVPS45*) behave differently: *AtRMR1* expression shows significant decrease in H2, and a tendency to increase in Ox; *AtVTI12* shows a tendency to be upregulated under salt stress and downregulated on H1 and H2, while in Ox shows significant downregulation; *AtVPS45* expression tends to decrease in S1, H2 and Zn, while in Ox has a significant increased expression (figure 22A); *AtSYP51* is significantly upregulated in all stress conditions, except for H1; *AtVSR1* is significantly downregulated in all stress conditions (Figure 22B).

Similarly, LV sorting-related genes (*AtVTI11* and *AtSYP52*) also demonstrate to have different responses to the different stresses: *AtVTI11* expression shows tendence to increase in S1 and Zn, and to decrease in H1 and H2; *AtSYP52* is upregulated for Zn situation, while in H2 is downregulated (Figure 23A).

Two SYPs that play a part in the vacuolar trafficking routes, *AtSYP22* and *AtSYP23* were also tested. The first one shows a tendency to be downregulated in H1, H2 and Zn, while the second is downregulated for H2 and Zn, and demonstrates a tendency to be downregulated in the other stress conditions (Figure 23 B).

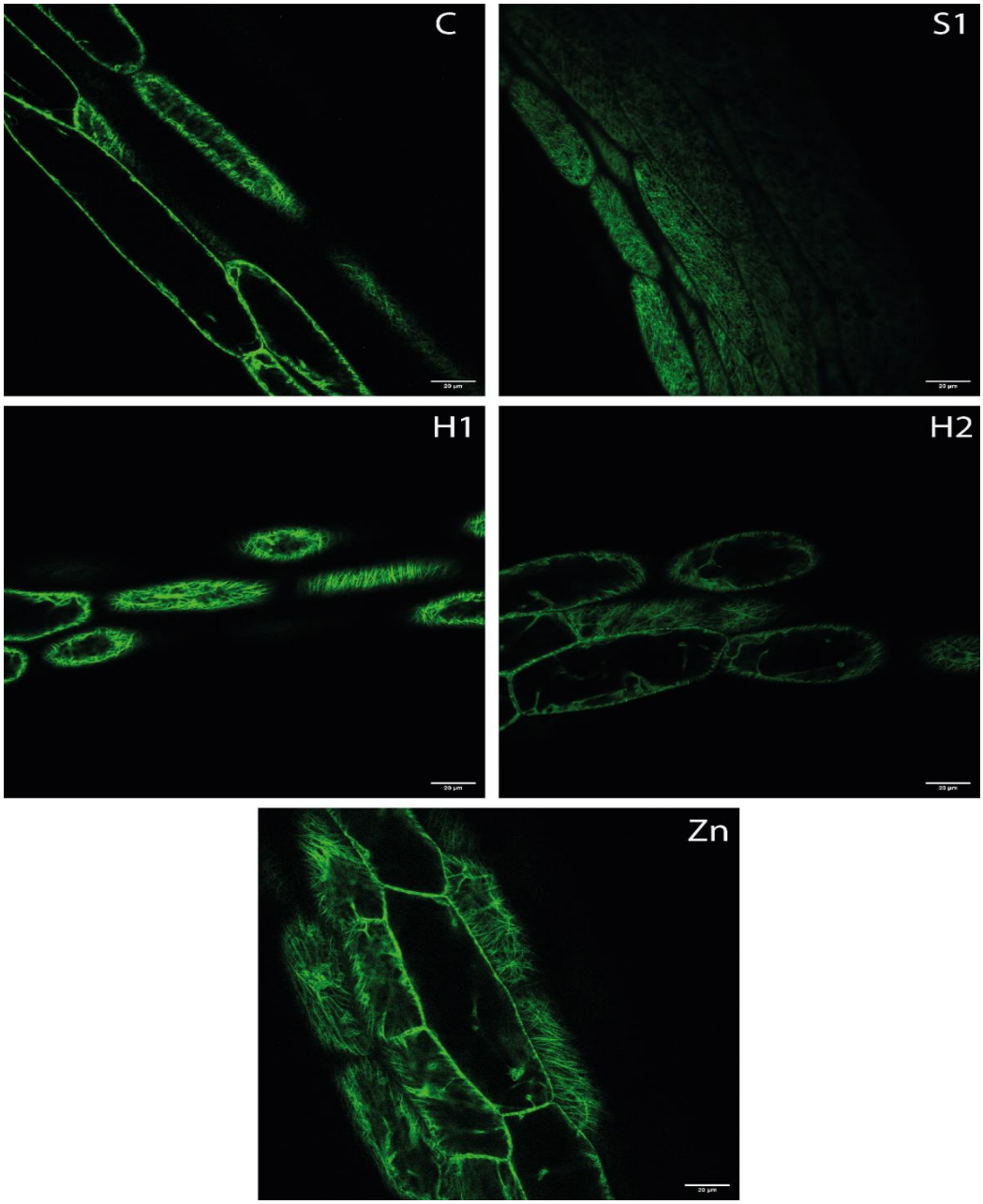

Figure 21 - TUA6-GFP expression under several abiotic stress conditions

Regarding the *exo70* mutant, genes involved in the defence system were selected for analysis, namely *AtATG8* and *AtVTI12*. The first only showed significant alterations in oxidative stress, where its expression is significantly reduced. The second one, had a significant increase in its expression in S1 and Zn conditions, and a significant decrease in expression in Ox (Figure 24).

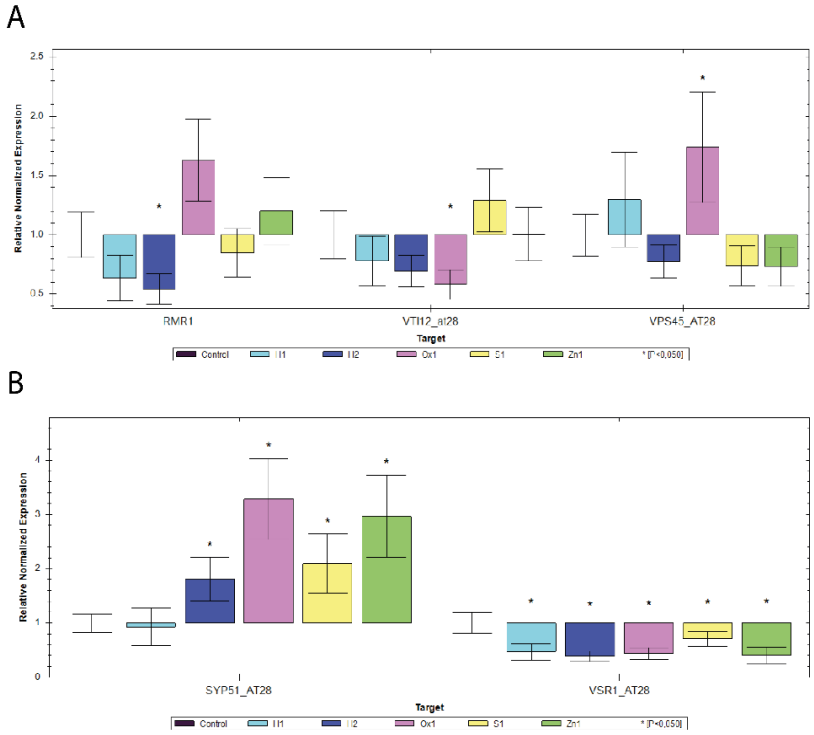

Figure 23- Expression analysis by qRT-PCR of genes involved in vacuolar routes, in *vsr2* mutant. A- Bar chart analysis of AtRMR1, AtVTI12 and AtVPS45 genes involved in trafficking to the protein storage vacuole in different stress conditions relative to control; B - Bar chart analysis of AtSYP51 and AtVSR1 genes involved in trafficking to the protein storage vacuole in different stress conditions relative to control. * Indicates statistically experimental values ($p < 0.05$)

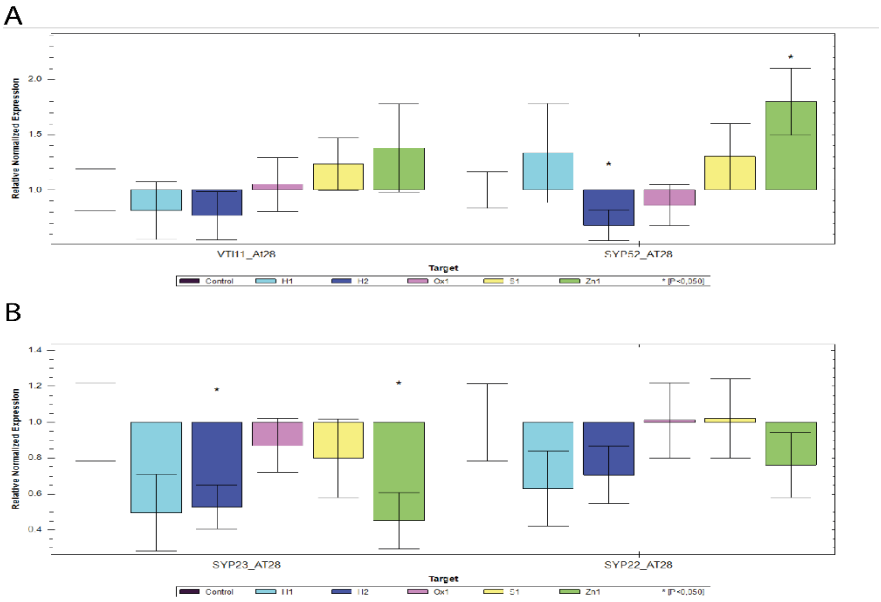

Figure 22 - Expression analysis by qRT-PCR of genes involved in vacuolar routes, in *vsr2* mutant. A - Bar chart analysis of AtVSR2, AtVTI11 and AtSYP52 genes involved in trafficking to the lytic vacuole in different stress conditions relative to control; B- Bar chart analysis of AtSYP23 and AtSYP22 genes in different stress conditions relative to control. * Indicates statistically experimental values ($p < 0.05$)

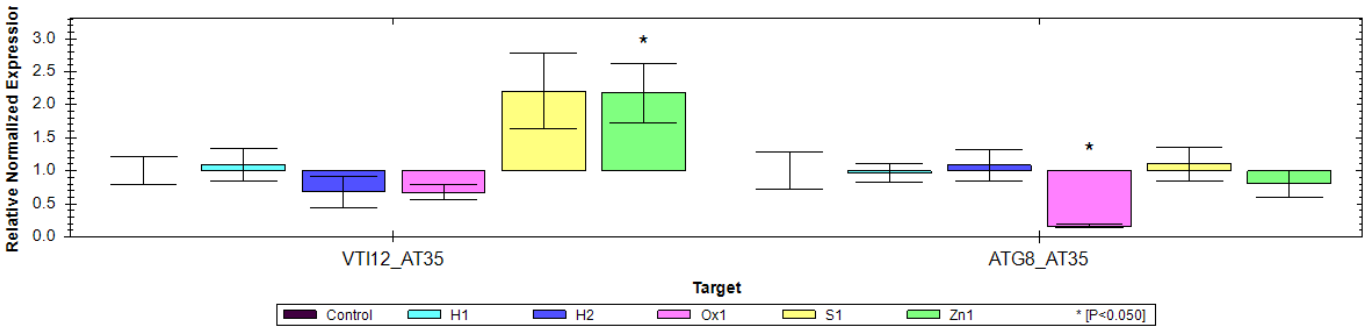

Figure 24 - Expression analysis by qRT-PCR of genes involved in defense mechanisms, in *exo70* mutant. Bar chart analysis of AtVTI12, AtATG8 genes involved in defense mechanisms in different stress conditions relative to control; * Indicates statistically experimental values ($p < 0.05$)

4. Discussion

Nowadays, agriculture is frequently confronted with new and stronger challenges triggered by climatic alterations and human activities, which can substantial impact the agroecosystems, affecting the natural development of crops (Abberton et al., 2016; Mousavi-Derazmahalleh et al., 2019). Thereby, plants must adapt and take all the advantages possible from stressful situations to thrive by promoting metabolic, molecular and cellular adjustments such as protein trafficking and accumulation, and the activation of powerful AOX networks (Zhu, 2016; Soares et al., 2019; Sampaio et al., 2022).

In a recent study from our lab (Neves et al., 2021) plants grown under abiotic stress conditions identical to those explored in this study (*i.e* osmotic, metal induced toxicity, saline and oxidative stresses) were analysed to see how the protein trafficking machinery respond. Interestingly it was found that upon exposure to stressful conditions the plants shifted their protein trafficking to the PSV, instead to the LV, which is the typical route for a developing plant. Actually, this finding was the starting point of the current research, which firstly aimed to study how the protein sorting machinery would respond to the absence of some key players in this process, either under control or stress conditions, and how the cellular oxidative metabolism would adapt to these challenging environments. Primarily, seeds from T-DNA lines were ordered and then analysed to find homozygous plants to be used in this study. Two homozygous lines were found, namely *vsr2* and *exo70*, that correspond to genes involved in the LV trafficking (Lee et al., 2013) and in the exocyst formation (Synek et al., 2006; Žárský et al., 2013), respectively. Thus, after performing their biometrical assessment under stress conditions, a set of biochemical assays were performed to analyse the cellular redox status, along with gene

expression studies to unravel what genes involved in protein sorting were being differentially expressed.

4.1 Downregulation of *VSR2* and *EXO70* significantly impacts Arabidopsis abiotic stress tolerance

Biometric and growth-related parameters

The evaluation of the macroscopic phytotoxicity, along with different growth endpoints, such as organ elongation and biomass production is a common tool to estimate the negative effects of different stress factors (Soares et al., 2016), including salt, osmotic, oxidative and metal induced toxicity.

Our former study found that wt seedlings exposed to identical stress conditions exhibited developmental delays and chlorosis in the leaves, especially under salt and metal induced stress, respectively (Neves et al., 2021). When working with mutant plants and abiotic stress, attention must be drawn not only to the stress response, but also to the observed effects under control conditions between the different genotypes. Actually, in *vsr2* mutant, and despite of being macroscopically smaller than the wt, some responses are within the same range of responses as wt seedlings under the same conditions. Concerning stress treatments, a developmental delay in S1 (salinity), H1 and H2 (osmotic) could be observed. As these situations disrupt the osmotic potential and can block the water uptake, these results were fairly expected outcomes; also, leaf chlorosis was observed upon media supplementation with Zn, suggesting that the photosynthetic apparatus is being conditioned by the presence of the metal, as previously reported for the wt seedlings under the same stress treatment (Neves et al., 2021). Regarding oxidative stress, no differences were noticed for seedlings under the Ox situation (Neves et al., 2021), probably because H_2O_2 is a signal involved in plant development and growth (Taiz et al., 2017). Thus, in an initial timepoint it can be assimilated as a signal and not a stress factor, which correlates with the fact that the aerial part of seedlings from Ox situations are quite similar to control ones.

Regarding the root length of the *vsr2* mutant and comparing the control and stress treatments, roots were generally short among experimental groups, reaching maximum reduction values upon exposure to H2; curiously, only salt-stressed seedlings did not show any effect on the elongation of the radicular system. This finding is well described in literature, as frequently root length increases in situations of water scarcity or salinity (Pedroso et al., 2014; Negrão et al., 2017; Moles et al., 2018), as a way to reach zones with a higher water potential. Moreover, it is also important to stress out that, under the

same stress conditions, wt and *vsr2* seedlings not always responded the same way. Actually, mutant seedlings showed an increased root length in the C and S1 groups, but a decrease in H2, Ox and Zn treatments, suggesting that the genotype significantly impacts root growth at both control and stress conditions. Curiously, this is in accordance with the observations regarding the leaf rosette, as this decrease in root length in H2, Ox and Zn groups is accompanied with a delay in leaf development.

Concerning the seedlings of the *exo70* line great differences were observed regarding the stress treatments and the control. The aerial part of the seedlings in the C situation was smaller than wt, and even more than *vsr2* line seedlings. In general, all stress treatments impacted the normal development of the seedlings, especially S1 and H2, where an extreme developmental delay was recorded. Regarding Zn-mediated stress, the same pattern previously described was also found for *exo70* seedlings, where a growth inhibition took place accompanied by the appearance of chlorotic spots. Interestingly, in the case of this mutant, the presence of H_2O_2 in the medium caused a delay in the development, which was not observed earlier for the wt (Neves et al., 2021) and the other mutant. An overall reduction of the root length was found among treatments, with the exception of salinity, as in the other genotypes and H1 treatment, where a significant increment was found. The EXO70 is the protein responsible for the exocyst assembly (Žárský et al., 2013). It was already demonstrated by Neves and collaborators (2021) that the expression of the gene encoding this protein is overexpressed under the same abiotic stress situations. Therefore, the data presented by the biometric parameters corroborates what already exists in the literature, that the exocyst is an important stress response mechanism, since there are notorious developmental delays in its absence.

Photosynthetic activity

Symptoms associated with adverse environmental conditions, like toxicity induced by ion excess, metals, and ROS can occur at different levels, affecting the photosynthetic machinery and photosynthesis itself. For this reason, the levels of total chlorophylls and carotenoids were evaluated as photosynthetic markers. Starting with the wt seedlings, significant differences were found when seedlings were exposed to salinity (S1), mannitol (H2) and Zn, though in terms of macroscopic manifestations, chlorosis was only found upon exposure to Zn. Metals may induce a reduction in the photosynthetic pigments by negatively affecting the main source of energy production in plants, by restraining photosystem II activity, through inhibition the reduction of chloroplast enzymes and inhibiting the photoreaction (Lin and Aarts, 2012; Sousa et al., 2020). Also,

Na and Cl interfere with photosynthesis by affecting stomatal behaviour and through a combination of osmotic and ionic components, reducing the photosynthetic kinetics and photosynthetic capacity, respectively (Zhang et al., 2022). Overall, similar results were found for the other genotypes, though specific differences could be noticed – while *vsr2* seedlings have their pigments reduced by all tested stresses, *exo70* seedlings did not show any reduction in total chlorophylls upon media supplementation with salt. Yet, both mutants were affected by H_2O_2 exposure, contrary to the wt. It is known that the lower levels of pigments in response to oxidative stress may be related to ROS action in the chloroplasts, namely H_2O_2, that will inhibit photosynthetic machinery and their counterparts (Foyer, 2018).

Oxidative stress and AOX defence mechanisms

Upon adverse environmental conditions ROS generation is enhanced, leading to an overaccumulation of these compounds (Mittler, 2017; Soares et al., 2019). Although they can act as important intracellular signalling agents at low doses, ROS become phytotoxic at high concentrations, affecting the overall plant cell homeostasis. Therefore, to regulate the cellular concentrations of ROS, the AOX system is activated to re-establish redox homeostasis (Gill and Tuteja, 2010; Sharma et al., 2012).

In this study several biochemical assays were conducted to evaluate some oxidative stress indicators (H_2O_2 and LP), along with the AOX system's response, to better understand how the protein sorting machinery directly affects the oxidative stress response.

From all ROS, H_2O_2 is regarded as one of the primary ROS, being also considered as a key signal in different physiological mechanisms (Soares et al., 2019). In general, different responses were found between genotypes and stress conditions, revealing that H_2O_2 levels were modulated by both factors. First, under control conditions, no major changes were found between the genotypes, revealing that, at least under homeostasis-promoting conditions, ROS content does not seem to be altered. Moreover, in wt seedlings, no major changes in this ROS content were found in response to stress, except in the osmotic treatment, where its levels decreased, and in the Ox stress, where, expectedly, its content rose significantly. This result suggests an uptake of H_2O_2 from the nutritive medium and/or an intracellular overproduction in response to the external stimuli. As a result of ROS overproduction, LP can occur, damaging the biological membranes. Indeed, this process may aggravate the cellular redox imbalance, since radicals derived from the LP can react with proteins and DNA (Sharma et al., 2012). Following the pattern registered for H_2O_2, MDA levels in wt seedlings were only

enhanced in response to the Ox treatment, revealing the occurrence of great redox disorders. On the contrary, *vsr2* and *exo70* plantlets showed no increase in H_2O_2 content and LP degree; actually, their content was even reduced in almost all situations. In fact, when under stress, both mutant lines behave similarly regarding the H_2O_2 levels and decreasing the MDA levels in all abiotic stress situations. Minimal levels were observed in *exo70* mutant line exposed to Ox and Zn, which represented a surprise since peroxidation of lipids is a common metabolic event resulting from plant's exposure to metal excess (Dimkpa et al., 2012). Here, a new hypothesis can be raised - the AOX system is being more actively activated in the mutants than in the wt, helping to lower the overaccumulation of ROS and the lipid peroxidation degree. Indeed, this seems to be the case, as the mutant genotypes exhibited a general decrease in H_2O_2 and LP content in almost all stress conditions. Different works dealing with water stress, metal toxicity and oxidative damage, reporting decreases in ROS content are often related to improved efficiency of the AOX system, allowing a better acclimation of the plants to the stress (Branco-Neves et al., 2017; Fujita and Hasanuzzaman, 2022; Sousa et al., 2022)

To cope with oxidative stress, plants developed a complex and coordinated antioxidant system throughout the evolution process, comprising both non-enzymatic and enzymatic mechanisms (Soares et al., 2019). To explore the involvement of the non-enzymatic AOX system, the accumulation of Pro and GSH were quantified. Proline accumulation is a common response of plants to a large range of stress factors due to its multiple biological functions. The proteinogenic amino acid can act like an osmoprotectant, conferring tolerance to water-related stresses, but is also involved in the stabilising biological membranes, scavenging of ROS and metal sequestration (Soares et al., 2019). Thus, changes in Pro levels are often considered as early warning signals of oxidative stress and provide an overall assessment of the cellular responses to different stressors (Soares et al., 2019; Sousa et al., 2020; Spormann et al., 2022). The results showed that the levels of this amino acid in control situations are higher in *vsr2* than *exo70* line, but none differ significantly from the wt. When referring to each genotype, and starting with the wt, substantial rises of Pro were expected, especially under S and H treatments, given its well-recognized functions as osmolyte and compatible solute (Hayat et al., 2012). Still, even in other stresses, such Ox and Zn, Pro accumulation also took place, indicating that induction of Pro production is a typical response for *Arabidopsis* plants under stress. Equivalent findings were also reported by Spormann and colleagues (2022), when studying tomato plants exposed to nickel and drought stress. However, the mutants behave somewhat differently: *vsr2* and *exo70* only increased the levels of Pro in S1 and H2 treatments, revealing that, for the other stresses,

further AOX mechanisms are being activated to balance ROS overproduction. In fact, it can be suggested that a shift is occurring between the mutants under the Ox and Zn treatments – while wt seedlings greatly rely on Pro accumulation to face ROS and LP, mutant seedlings do not seem to invest in this non-enzymatic mechanism. Still, since LP and H_2O_2 significantly decreased upon exposure to H_2O_2 and Zn in the two mutants, other players, such as GSH and ascorbate, must have been acting to prevent oxidative damages.

GSH is an important cellular redox buffer, since it plays a role in different components of the AOX system like AsA-GSH cycle, GR activity, besides participating in processes linked to protein synthesis, enzymatic regulation, and expression of stress-responsive genes (Soares et al., 2019). Curiously, the levels of GSH in control were very distinctive between genotypes, since the GSH content in wt was 4-fold higher than in the mutans. Moreover, within the studied lines, the three genotypes showed an increase of GSH levels in Zn, a result expected since this molecule is also a metal chelator (Soares et al., 2019). Additionally, exo*70* line also showed big GSH increases under H2 and Ox stresses, situations where Pro were not enhanced; however, in the *vsr2* line GSH remained unchanged in these treatments, suggesting that, even within the mutants, there are quite differences recorded regarding the AOX response. Overall, by analysing the levels of the oxidative stress markers with this data, it is possible to observe that *exo70* seedlings have a higher amount of non-enzymatic components working in ROS detoxification, while *vsr2* seedlings did not seem to activate this component as much. Thereby, quantifying the activity of the enzymatic part of the AOX system was an important step to achieve a solid conclusion and help to unravel physiological differences between the genotypes.

So, to have a better insight of the full picture of the ROS detoxification, enzymatic players of the AOX system were evaluated under control and abiotic stress conditions. For this purpose, CAT and APX, both related to H_2O_2 detoxification, were analysed. Under control conditions, *vsr2* mutant seedlings appear to have lower levels of both enzymes, which agrees with the tendency for this mutant to present increased levels of H_2O_2. However, when these seedlings were exposed to stress conditions, a curious result was obtained - the activity of APX and CAT were greatly enhanced in all stressed conditions, suggesting that these plants, though not particularly increasing Pro and GSH content uniformly, are clearly activating the enzymatic component the AOX system, lowering the oxidative damage, even in the situation of H_2O_2 and Zn stresses. On the other hand, the opposite occurred in *exo70* seedlings since there was a clear tendency

to decrease the activity of APX and CAT enzymes, which became significant in S1 treated seedlings. In this case, it is also important to recall the previous hypothesis – the AOX enzymes in this mutant, contrary to *vsr2* mutant, are not particularly relevant to the seedling's response, which appear to be investing in the non-enzymatic players, such as Pro and GSH. Moreover, the inhibition of CAT and APX activity in the *exo70* mutant can also be linked to H_2O_2-mediated impairment of enzyme activity, as these seedlings – though decreasing H_2O_2 content – appear to be more sensitive in terms of growth than *vsr2* mutant. Either way, especially in terms of physiological performance and redox status, mutant plants seem to be able to better cope with the stressful conditions than wt. However, big differences were found among the responses – while *vsr2* mutant preferentially invests on enzymatic mechanisms, the *exo70* mutant relies on the action of non-enzymatic AOX to prevent oxidative-induced damages.

Overall, with all the data presented so far, it is possible to observe that the mutant lines had a better response to adverse environmental conditions, than the wt plants, through the levels of the oxidative stress indicators were higher in the wt plants. It is very interesting that besides both mutants demonstrated redox imbalances in all stress situations, they respond differently to them. In fact, it is possible to establish a pattern for each one of the mutants: *vsr2* seedlings invest more on the enzymatic AOX system, as the APX and CAT have more pronounced responses than the non-enzymatic system; while *exo70* seedlings demonstrated a preference for the non-enzymatic AOX system, since there was a tendency to lower the levels of the stress markers and no differences were observed in the enzymes activity.

4.2 Protein sorting is affected

All eukaryotic cells require endomembrane trafficking because numerous proteins are continually generated and must be carried to the proper location to perform their functions. Plant's endomembrane system must continually change in order to meet morphological requirements for development or a changing environment. As a result, the *de novo* production and/or relocalisation of stress-related proteins through trafficking routes, and the associated machinery, are intimately tied to stress signalling pathways (Kwon et al., 2008; Rosquete and Drakakaki, 2018; Wang et al., 2020). In this work we analysed the expression of some endomembrane system effectors, that participate in LV and PSV routes, in case of *vsr2*, and defence mechanisms, when working with *exo70*.

PSV trafficking is no longer a priority

Under abiotic stress conditions, *AtRMR1, AtVTI12, AtVPS45, AtSYP51* and *AtVSR1*, all genes encoding for proteins involved in the PSV trafficking are upregulated in wt plants under abiotic stress (Neves et al., 2021). However, in the *vsr2* line this response is not so linear, demonstrating that the knock-down of a gene involved in these pathways induces some changes in one of the most important cell processes. RMR1 is a vacuolar sorting receptor localised in Golgi, TGN and PSVs, and contribute to the transport of proteins carrying a C-terminal vacuolar sorting determinant (ctVSD). It mediates trafficking through PACs vesicles to the PSV(Shen et al., 2011; Xiang et al., 2013). In the absence of *VSR2*, a gene that encodes a protein related to LV route, upregulation of genes involved in the PSV could be expected since there would be more proteins to translocate to PSV; however, that did not happen. In fact, the opposite occurred, as *AtRMR1* was found to be downregulated or did not alter its expression (Figure 25). This result may imply that PSV is not the preferred route in the absence of *AtVSR2*, indicating that there could be some overlapping between the routes, as described in the literature, yet. In fact, intracellular pathways, particularly the vacuolar ones, have been compartmentalized over the years with intermediate players being addressed to one or the other. However, in recent years, an integrated vision of the endomembrane system as a dynamic and continuous process started to be discussed where the trafficking pathways and organelle biogenesis are closely related (Pereira and Di Sansebastiano, 2021). To corroborate this, other genes involved in PSV route were tested. *AtVTI12* encodes a protein involved in many cell processes like defence and protein trafficking, and mediates clathrin independent transport (Surpin et al., 2003; Sanmartín et al., 2007). In wt plants the gene *AtVTI12* was abundantly overexpressed in all stress conditions (Neves et al., 2021), probably due to the multiple functions that the protein has, so similar response was expected in this study. However, and like *AtRMR1*, *AtVTI12* gene only showed significant alterations in the Ox treatment, being downregulated (Figure 25). Moreover, when comparing the relative expression of this gene in the wt and in the mutant line (Supplementary Figure 4A and B), a decrease in its expression is very clear, revealing a tight connection between the genes coding for proteins belonging to the PSV route. In fact, the results suggest that in the absence/decrease of one intervenient, their partners are also affected, instead of replacing their roles.

Another SNARE that participates in the PSV trafficking is SYP51, a positive regulator of the PSV route for proteins with a ctVSD, as demonstrated with Chitinase A (Ebine et al., 2008; Di Sansebastiano et al., 2009; Barozzi et al., 2019). The gene

encoding this protein is the only one that maintains the upregulation (observed in wt) for all the abiotic stress situations, apart from H1 treatment where it does not alter its expression (Figure 25). However, the expression levels of *AtSYP51* showed a tendency to be higher in the *vsr2* than the wt seedlings for Ox and Zn treatments (Supplementary figure 4E). The protein encoded by this gene, SYP51, has a specific interaction with NIP1.1, an ER aquaporin, in the tonoplast (Barozzi et al., 2019). Structures like the ones observed in this study are also observed in the other studies available in the literature, but in less amount in the cell tonoplast, and both makers are colocalized in them, although they have different intracellular localisation (Barozzi et al., 2019). Therefore, the interaction between these two proteins can be related to stress response, since the number of these vesicles increases under adverse conditions. However, this interaction is not entirely understood and why it happens, but it is speculated that it can be related to unconventional protein trafficking (Barozzi et al., 2019). To prove this hypothesis, similar tests with *AtNIP1.1* should be conducted. Moreover, SYP51 may also be part of the exocytosis (De Benedictis et al., 2013), a process that is more pronounced process in stressful situations, since the expression of *AtEXO70* increases under stress conditions.

The other two endomembrane system effectors participating in the transport to the PSV are VPS45 and VSR1. The first protein, mediates the recycling of VSRs in TGN (Zouhar et al., 2009). Since VSR2 is absent in *vsr2* mutant, a lower expression was expected and, despite an upregulation in Ox, no other alterations were observed (Figure 25). Since VPS45 also regulates the complex formed by VTI12 and other proteins, like SYP61 (Zouhar et al., 2009), this result stays in frame with the data obtained so far, as a lower expression of *AtVTI12* is observed, resulting in less number of complexes formed by VTI12 protein. VSR1 is a vacuolar sorting receptor that interacts with proteins that in turn mediate PSV transport (Yamazaki et al., 2008; Xiang et al., 2013). The gene that encodes this protein, *AtVSR1*, is the only one among all the mentioned genes that is downregulated for all stress conditions (Figure 25). The protein encoded by this gene is a positive regulator for the PSV route (Xiang et al., 2013). This is a surprising this observation as one would expect little or no interference between genes that code for proteins participating in opposite pathways. As so, this seems to be a good result to further explore in more detail the relationship between different genes of the VSR family in Arabidopsis. Even so, we can argue that the downregulation for *AtVSR1* might be related with the biogenesis of this vacuolar receptor and may be related with the vacuolar transport of this protein, that can be mediated by VSR2 (Zouhar et al., 2010). Also, when comparing with wt expression, a clear tendency to lower the expression of *AtVSR1* gene

is observed (Supplementary figure 4D). This demonstrates that despite VSR1 and VSR2 proteins work in different routes, they can share paths in prior stages.

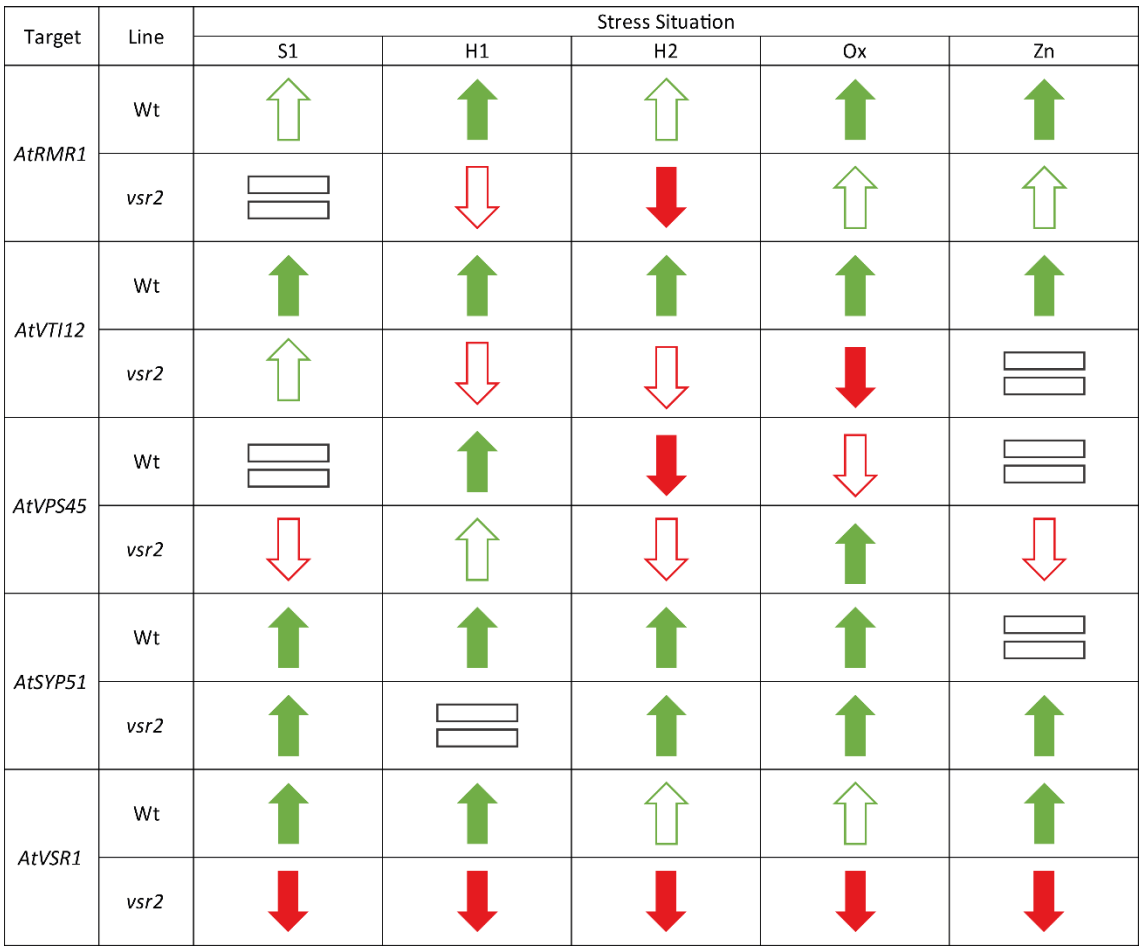

Figure **25** – Expression of genes coding for PSV effectors, comparison between between wt (data from Neves et al 2021) and *vsr2* seedlings. Green arrows represent significant overexpression, while green and white arrows represent an overexpression tendency Red arrows represent significant downregulation, while green and white arrows represent an downregulation tendency.
Equal signs represent that no alterations are observed. All the data is compared with the controls of each line.

Due to the scenario that was presented at this point, we decided to test the expression of genes involved in the LV route, namely *AtVTI11, AtSYP52* and *AtSYP22* (SNvti11complex). The proteins encoded by these genes form a complex that is responsible for the clathrin dependent protein trafficking for the LV (Sanderfoot et al., 2001; Sanmartín et al., 2007; Shirakawa et al., 2010). The gene that encodes VTI11 did not show any significant alteration in its expression in the *vsr2* line (Figure 26). However, when comparing the values with those of the wt a tendency to be more expressed was observed (Supplementary figure 5A). Upregulation of this gene could be expected since VTI11 protein mediates the same route as the VSR2, however that does not happen,

demonstrating that *AtVTI11* gene can't rescue VSR2 roles in the of LV route. *AtSYP52* showed a downregulation in H2 stress and an overexpression in Zn treatment (Figure 26), but when compared with the wt, its expression had a tendency to be lower than in the wt situation (Supplementary Figure 5B). The protein SYP52, besides mediating the LV route, is linked with endocytosis (De Benedictis et al., 2013), therefore a downregulation on the gene that encodes this protein may be related with the decrease in endocytosis, as the cell is struggling against environmental conditions. The last gene that codes for a protein of the SNvti11complex, *AtSYP22*, had only a downregulation in H2 situation (Figure 26). This was expectable since *AtVTI11* did not show any alterations, and the two are part of the same complex. Another process that may be involved in the lower expression of *AtSYP22* is the overexpression of *AtSYP51*. Since SYP51 is a partner element. a titration may be happening because SYP22 and SYP51 interact with each other (Foresti and Denecke, 2008). However, the functions of SYP22 protein are not yet well understood, so a brighter picture can't be achieved.

The last gene studied in this work is *AtSYP23*. Despite how the SYP23 protein operates in the cell being still not clear, it is known that it is a cytosolic form of SYP22. The results showed that *AtSYP23* gene in *vsr2* mutant has a clear tendency to be

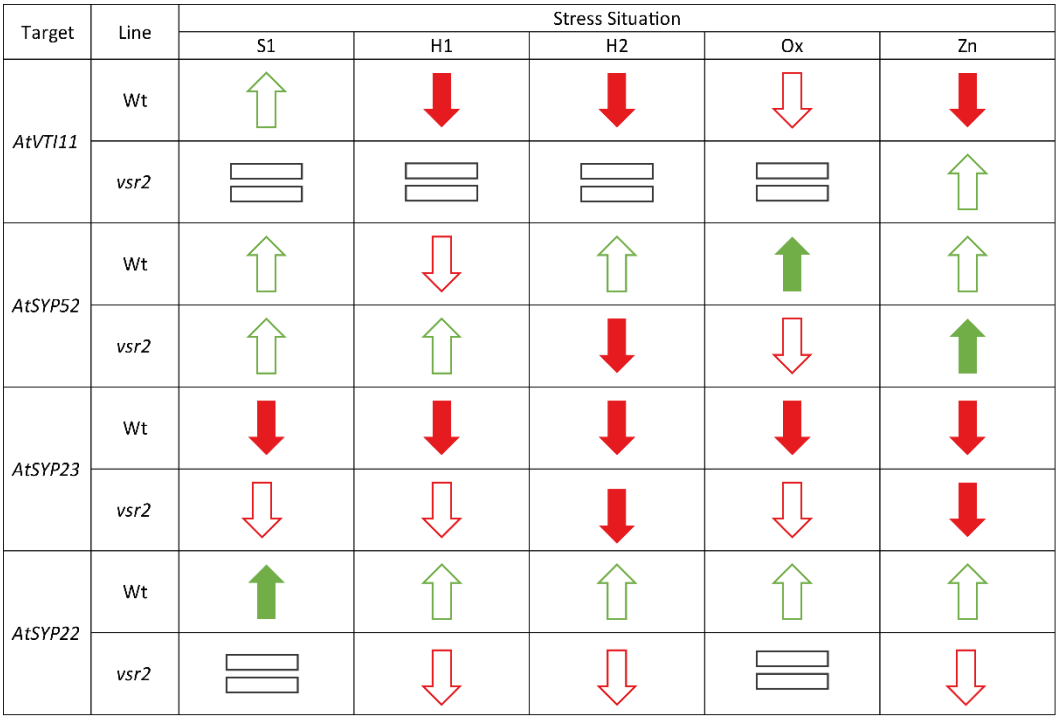

Figure **26** - Comparison between LV effectors and SYP22/23 encoding genes between wt (data from Neves et al 2021) and *vsr2*. Green arrows represent significant overexpression, while green and white arrows represent an overexpression tendency Red arrows represent significant downregulation, while green and white arrows represent an downregulation tendency. Equal signs represent that no alterations are observed. All the data is compared with the controls of each line.

downregulated; indeed, it presented significative downregulation in the H2 and Zn treatments (Figure 26). When comparing with the expression in wt, it is overexpressed in all stress treatments, despite being downregulated in the mutant line (Supplementary Figure 5C). It has been discussed that this cytosolic form may also assist in LV fusion and docking of vesicles assisting SYP22 in its function (Shirakawa et al., 2010). We previously showed that *AtSYP22* is downregulated in the mutant when compared to wt plants. As so, it is possible to speculate that At*SYP23* upregulation comparing with wt may be related to a decreased function of SYP22 in the same conditions.

The results obtained so far demonstrates that PSV trafficking, in *vsr2* mutant, is no longer a priority route for protein transport. It is also clear that the different vacuolar routes cannot be seen as independent as has been described and the same players may participate in common processes or regulate each other.

Exocyst and autophagy

Under stress conditions the autophagic pathway is linked with the cell endomembrane system. A recently autophagic pathway, mediated by the exocyst, has been described as having a major role in plant tolerance to the adverse conditions(Kalinowska and Isono, 2018). In the present work. we observed how the autophagic pathway responded to the absence of one of the essential factors for the formation of the exocyst, the EXO70, since in a previous study in our lab, it was shown that the exocyst pathway was enhanced in relation to the autophagic route, when seedlings were facing abiotic stress (Neves et al., 2021). Thereby, the expression of *AtATG8*, a well-known marker for cellular autophagy (Shpilka et al., 2011), and *AtVTI12*, which protein is responsible for the fusion of the vesicles of both pathways with the vacuole, were evaluated in this mutant background.

Given the results obtained previously, upregulation of both genes was expected, especially because this defence mechanism is highly necessary for the plant survival. However, *AtATG8* did not alter its expression, except in the Ox situation (Figure 27). This can be explained by the fact that selective autophagy processes, like pexophagy, are being preferred (Su et al., 2020). The levels of the stress markers and the inhibition of the enzymatic activity on *exo70*, corroborate it, since peroxisomes contain multiple AOX enzymes (Su et al., 2018). *AtVTI12* also did not change its behaviour, apart from being upregulated in the Zn condition, (Figure 27). Comparing the expression of both *AtATG8* and *AtVTI12* with the results obtained in the wt plants (Supplementary figure 6A and B), *AtATG8* expression did not present a massive change in its behaviour, indicating that autophagic processes are completely independent of exocyst. On the other hand,

AtVTI12 had its expression very reduced when compared with the wt plants, which can be related to the absence of exocyst vesicles. It is possible to speculate that some proteins present in the exocyst pathway could be positive regulators for VTI12 expression when plants face adverse conditions.

Combining these results with the morphological traits of the *exo70*, namely the delayed development, a clearer image of the importance of the exocyst-mediated transport for stress response is obtained. However, other genes regarding this process should be further tested to evaluate how the exocyst formation may or may not occur or if other non-conventional pathways are preferred.

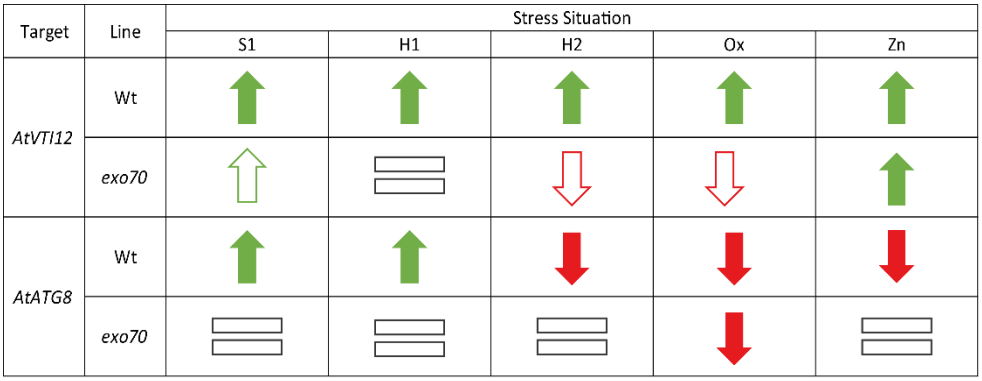

Figure **27** - Comparison between defence proteins encoding genes between wt (data from Neves et al 2021) and *exo70*. Green arrows represent significant overexpression, while green and white arrows represent an overexpression tendency Red arrows represent significant downregulation, while green and white arrows represent an downregulation tendency. Equal signs represent that no alterations are observed. All the data is compared with the controls of each line.

Correlation between biochemical and molecular traits

Many studies devoted to understanding how protein sorting affects the stress response or is involved in it do not draw a clear picture on how this process impacts the plant behaviour as the responses of other metabolic pathways are important for plant adaptation. By combining functional genetics, biochemistry and gene expression data, this work is pioneer as it presents a first overview on how sorting machinery directly affects the plant at the physiological and molecular levels. Although working on such topic is quite important, it is also challenging since no major conclusions can be drawn at the moment, without further studies. Yet, from the datasets obtained so far, it is clear that mutants lacking important trafficking players, such as VSR2 and EXO70, were able to better cope with the stress conditions than the wt, though the mechanisms involved were quite different from each other. The thorough analysis of the redox metabolism strongly suggested that assumption. Nevertheless, the importance of these genes, and

therefore the endomembrane trafficking pathways, in plant responses to stress is obvious in the analysis of the biological growth parameters analysed, since both lines had a bigger developmental delay than wt.

The main results of this study rely on the fact that one mutant preferred the enzymatic pathway (*vsr2)* and the other preferred the non-enzymatic component (*exo70)*. The correlation between the mutants and the response from the AOX system is not immediate, as little is known regarding the trafficking of these molecules, especially in what concerns the vacuolar routes. Nevertheless, one can speculate that the exocyst may have a role in the transport of antioxidative enzymes from the cytoplasm towards other locations in the cell. In its absence it is fair to assume an impairment of these transport in the EXO70 mutant. In fact, more than two decades ago, Mullen and co-workers (1999) demonstrated that plant peroxisomal APX is sorted to peroxisomes via a side pathway including a preperoxisomal compartment with traits of a distinctive ER subdomain, potentially a peroxisomal ER subdomain. The exocyst was only discovered many years later, so it would be important to revisit the biogenesis and trafficking of these enzymes and cross it with the vast knowledge and tools now available for the study of endomembrane trafficking.

5. Conclusion

In a world where climate changes start to dictate the way of living, it is urgent to develop new ways to prevent crop failures, avoiding food scarcity. Plants, as sessile organisms, have mechanisms to thrive or prevent further damage under adverse conditions, such as the AOX system, defence mechanisms and protein sorting itself. Therefore, under abiotic stress conditions, plants activate enzymes and produce metabolites that will reduce the amount of ROS intracellularly, impairing an extension of irreversible cellular damages, or even cell death. In addition, the endomembrane system shifts their protein trafficking from the LV to the PSV, and even unconventional defence systems, like the exocyst, are activated to help cells and, therefore, tissues and the plant to fight adverse conditions.

This study aimed to further understand how protein trafficking is directly linked to the stress response by using T-DNA lines for genes involved in the protein trafficking and correlating the data retrieved with biochemical markers that quantify the AOX system response.

The results of this study showed that both mutants behave very differently under abiotic stress conditions. Expression analysis of endomembrane-related genes from *vsr2* mutant plants demonstrated that PSV is no longer a priority in protein sorting and AOX system invested more in an enzymatic response. Regarding *exo70* mutant, the expression analysis showed that the exocyst plays an important role in stress response, and in this case, a non-enzymatic response is preferred by AOX system.

This is an innovative study involving two areas that are not immediately related and poorly addressed in the literature. Even so, it is possible to conclude that endomembrane trafficking and the response from the AOX system may be two interconnected pathways for plant's responses to stress. It is clear from the work presented here that the integrity of plant endomembrane routes is important for the plant to thrive under adverse conditions, as in the mutants, a delay in development was observed under stress; and that different mutants activate different responses from the AOX system. As a whole, and despite the data already produced with this project, this study demonstrates promising results for future research and opens doors for bringing these two areas together in the study on plants' adaptation/tolerance to stress.

As future perspectives the work will be developed with other mutant lines so it can be possible to have a better picture of how the protein sorting mechanisms interact with the stress response and how plants cope with stress without other key players in this process.

6. References

Abbasi H, Jamil M, HAQ A, Ali S, Ahmad R, Malik Z (2016) Salt stress manifestation on plants, mechanism of salt tolerance and potassium role in alleviating it: a review. Zemdirbyste **103**: 229–238

Abberton M, Batley J, Bentley A, Bryant J, Cai H, Cockram J, Costa de Oliveira A, Cseke LJ, Dempewolf H, De Pace C, et al (2016) Global agricultural intensification during climate change: A role for genomics. Plant Biotechnol J **14**: 1095–1098

Ahmed SU, Rojo E, Kovaleva V, Venkataraman S, Dombrowski JE, Matsuoka K, Raikhel N V (2000) The plant vacuolar sorting receptor AtELP is involved in transport of NH(2)-terminal propeptide-containing vacuolar proteins in Arabidopsis thaliana. J Cell Biol **149**: 1335–1344

Alonso JM, Stepanova AN, Leisse TJ, Kim CJ, Chen H, Shinn P, Stevenson DK, Zimmerman J, Barajas P, Cheuk R, et al (2003) Genome-wide insertional mutagenesis of Arabidopsis thaliana. Science (80-) **301**: 653–657

Aniento F, de Medina Hernández VS, Dagdas Y, Rojas-Pierce M, Russinova E (2022) Molecular mechanisms of endomembrane trafficking in plants Get access. Plant Cell **34**: 146–173

Barozzi F, Papadia P, Stefano G, Renna L, Brandizzi F, Migoni D, Fanizzi FP, Piro G, Di Sansebastiano G Pietro (2019) Variation in membrane trafficking linked to SNARE AtSYP51 interaction with aquaporin NIP1;1. Front Plant Sci. doi: 10.3389/fpls.2018.01949

Bassham DC, Sanderfoot AA, Kovaleva V, Zheng H, Raikhel N V (2000) AtVPS45 complex formation at the trans-Golgi network. Mol Biol Cell **11**: 2251–2265

De Benedictis M, Bleve G, Faraco M, Stigliano E, Grieco F, Piro G, Dalessandro G, Di Sansebastiano G Pietro (2013) AtSYP51/52 functions diverge in the post-golgi traffic and differently affect vacuolar sorting. Mol Plant **6**: 916–930

Bolte S, Lanquar V, Soler MN, Beebo A, Satiat-Jeunemaître B, Bouhidel K, Thomine S (2011) Distinct lytic vacuolar compartments are embedded inside the protein storage vacuole of dry and germinating arabidopsis thaliana seeds. Plant Cell Physiol **52**: 1142–1152

Bradford MM (1976) A rapid and sensitive method for the quantitation of microgram quantities of protein utilizing the principle of protein-dye binding. Anal Biochem **72**:

248–254

Branco-Neves S, Soares C, Sousa A De, Martins V, Azenha M, Gerós H, Fidalgo F (2017) An efficient antioxidant system and heavy metal exclusion from leaves make Solanum cheesmaniae more tolerant to Cu than its cultivated counterpart. 123–133

Brandizzi F (2018) Transport from the endoplasmic reticulum to the Golgi in plants: Where are we now? Semin Cell Dev Biol **80**: 94–105

Cvrčková F, Grunt M, Bezvoda R, Hála M, Kulich I, Rawat A, Zárský V (2012) Evolution of the land plant exocyst complexes. Front Plant Sci **3**: 159

Czechowski T, Stitt M, Altmann T, Udvardi MK, Scheible WR (2005) Genome-wide identification and testing of superior reference genes for transcript normalization in arabidopsis. Plant Physiol **139**: 5–17

daSilva LLP, Taylor JP, Hadlington JL, Hanton SL, Snowden CJ, Fox SJ, Foresti O, Brandizzi F, Denecke J (2005) Receptor salvage from the prevacuolar compartment is essential for efficient vacuolar protein targeting. Plant Cell **17**: 132–148

Demidchik V (2015) Mechanisms of oxidative stress in plants: From classical chemistry to cell biology. Environ Exp Bot **109**: 212–228

Dimkpa CO, McLean JE, Latta DE, Manangón E, Britt DW, Johnson WP, Boyanov MI, Anderson AJ (2012) CuO and ZnO nanoparticles: Phytotoxicity, metal speciation, and induction of oxidative stress in sand-grown wheat. J Nanoparticle Res. doi: 10.1007/s11051-012-1125-9

Ding Y, Robinson DG, Jiang L (2014) Unconventional protein secretion (UPS) pathways in plants. Curr Opin Cell Biol **29**: 107–115

Driouich A, Faye L, Staehelin A (1993) The plant Golgi apparatus: a factory for complex polysaccharides and glycoproteins. Trends Biochem Sci **18**: 210–214

Dupree P, Sherrier DJ (1998a) The plant Golgi apparatus. Biochim Biophys Acta - Mol Cell Res **1404**: 259–270

Dupree P, Sherrier DJ (1998b) The plant Golgi apparatus. Biochim Biophys Acta - Mol Cell Res **1404**: 259–270

Ebine K, Okatani Y, Uemura T, Goh T, KeikoShoda, Niihama M, Morita MT, Spitzer C, Otegui MS, Nakano A, et al (2008) A SNARE complex unique to seed plants is

required for protein storage vacuole biogenesis and seed development of arabidopsis thaliana. Plant Cell **20**: 3006–3021

Fidalgo F, Azenha M, Silva AF, de Sousa A, Santiago A, Ferraz P, Teixeira J (2013) Copper-induced stress in Solanum nigrum L. and antioxidant defense system responses. Food Energy Secur **2**: 70–80

Foresti O, Denecke J (2008) Intermediate organelles of the plant secretory pathway: identity and function. Traffic **9**: 1599–1612

Foyer CH (2018) Reactive oxygen species, oxidative signaling and the regulation of photosynthesis. Environ Exp Bot **154**: 134–142

Fujita M, Hasanuzzaman M (2022) Approaches to Enhancing Antioxidant Defense in Plants. Antioxidants (Basel, Switzerland). doi: 10.3390/antiox11050925

Gibson DG, Young L, Chuang RY, Venter JC, Hutchison CA, Smith HO (2009) Enzymatic assembly of DNA molecules up to several hundred kilobases. Nat Methods **6**: 343–345

Gill SS, Tuteja N (2010a) Reactive oxygen species and antioxidant machinery in abiotic stress tolerance in crop plants. Plant Physiol Biochem **48**: 909–930

Gill SS, Tuteja N (2010b) Reactive oxygen species and antioxidant machinery in abiotic stress tolerance in crop plants. Plant Physiol Biochem PPB **48**: 909–930

Hawes C, Satiat-Jeunemaitre B (2005a) The plant Golgi apparatus—Going with the flow. Biochim Biophys Acta - Mol Cell Res **1744**: 93–107

Hawes C, Satiat-Jeunemaitre B (2005b) The plant Golgi apparatus—Going with the flow. Biochim Biophys Acta - Mol Cell Res **1744**: 93–107

Hayashi Y, Yamada K, Shimada T, Matsushima R, Nishizawa NK, Nishimura M, Hara-Nishimura I (2001) A proteinase-storing body that prepares for cell death or stresses in the epidermal cells of arabidopsis. Plant Cell Physiol **42**: 894–899

Hayat S, Hayat Q, Alyemeni MN, Wani AS, Pichtel J, Ahmad A (2012) Role of proline under changing environments: a review. Plant Signal Behav **7**: 1456–1466

Howell SH (2013) Endoplasmic Reticulum Stress Responses in Plants. doi: 10.1146/annurev-arplant-050312-120053

Jiang L, Phillips TE, Rogers SW, Rogers JC (2000) Biogenesis of the Protein Storage Vacuole Crystalloid. J Cell Biol **150**: 755–770

Jiang L, Rogers JC (2018) Sorting of Lytic Enzymes in the Plant Golgi Apparatus. Annu Plant Rev online 128–156

Kalinowska K, Isono E (2018) All roads lead to the vacuole — autophagic transport as part of the endomembrane trafficking network in plants. J Exp Bot **69**: 1313–1324

Kang B-H, Anderson CT, Arimura S-I, Bayer E, Bezanilla M, Botella MA, Brandizzi F, Burch-Smith TM, Chapman KD, Dünser K, et al (2022) A glossary of plant cell structures: Current insights and future questions. Plant Cell **34**: 10–52

Kim H, Kang H, Jang M, Chang JH, Miao Y, Jiang L, Hwang I (2010) Homomeric interaction of AtVSR1 is essential for its function as a vacuolar sorting receptor. Plant Physiol **154**: 134–148

Kim S-H, Kwon C, Lee J-H, Chung T (2012) Genes for plant Autophagy: Functions and interactions. Mol Cells **34**: 413–423

Kintlová M, Blavet N, Cegan R, Hobza R (2017) Transcriptome of barley under three different heavy metal stress reaction. Genomics Data **13**: 15–17

Koizumi N, Martinez IM, Kimata Y, Kohno K, Sano H, Chrispeels MJ (2001) Molecular characterization of two Arabidopsis Ire1 homologs, endoplasmic reticulum-located transmembrane protein kinases. Plant Physiol **127**: 949–962

Kriechbaumer V, Brandizzi F (2020) The plant endoplasmic reticulum: an organized chaos of tubules and sheets with multiple functions. J Microsc **280**: 122–133

Kwon C, Bednarek P, Schulze-Lefert P (2008) Secretory Pathways in Plant Immune Responses. Plant Physiol **147**: 1575–1583

Kwon C, Lee JH, Yun HS (2020) Snares in plant biotic and abiotic stress responses. Mol Cells **43**: 501–508

Lee Y, Jang M, Song K, Kang H, Lee MH, Lee DW, Zouhar J, Rojo E, Sohn EJ, Hwang I (2013) Functional identification of sorting receptors involved in trafficking of soluble lytic vacuolar proteins in vegetative cells of Arabidopsis. Plant Physiol **161**: 121–133

Li S, van Os GMA, Ren S, Yu D, Ketelaar T, Emons AMC, Liu C-M (2010) Expression and Functional Analyses of EXO70 Genes in Arabidopsis Implicate Their Roles in Regulating Cell Type-Specific Exocytosis. Plant Physiol **154**: 1819–1830

Lin YF, Aarts MGM (2012) The molecular mechanism of zinc and cadmium stress

response in plants. Cell Mol Life Sci **69**: 3187–3206

Liu JX, Howell SH (2016) Managing the protein folding demands in the endoplasmic reticulum of plants. New Phytol **211**: 418–428

Liu L, Li J (2019) Communications between the endoplasmic reticulum and other organelles during abiotic stress response in plants. Front Plant Sci. doi: 10.3389/fpls.2019.00749

Liu Y, Bassham DC (2012) Autophagy: Pathways for self-eating in plant cells. Annu Rev Plant Biol **63**: 215–237

Mimura T, Kura-Hotta M, Tsujimura T, Ohnishi M, Miura M, Okazaki Y, Mimura M, Maeshima M, Washitani-Nemoto S (2003) Rapid increase of vacuolar volume in response to salt stress. Planta **216**: 397–402

Mittler R (2017) ROS Are Good. Trends Plant Sci **22**: 11–19

Moles TM, Mariotti L, De Pedro LF, Guglielminetti L, Picciarelli P, Scartazza A (2018) Drought induced changes of leaf-to-root relationships in two tomato genotypes. Plant Physiol Biochem **128**: 24–31

Mousavi-Derazmahalleh M, Bayer PE, Hane JK, Valliyodan B, Nguyen HT, Nelson MN, Erskine W, Varshney RK, Papa R, Edwards D (2019) Adapting legume crops to climate change using genomic approaches. Plant Cell Environ **42**: 6–19

Mullen RT, Lisenbee CS, Miernyk JA, Trelease RN (1999) Peroxisomal membrane ascorbate peroxidase is sorted to a membranous network that resembles a subdomain of the endoplasmic reticulum. Plant Cell **11**: 2167–2185

Munns R, Tester M (2008a) Mechanisms of Salinity Tolerance. Annu Rev Plant Biol **59**: 651–681

Munns R, Tester M (2008b) Mechanisms of Salinity Tolerance. Annu Rev Plant Biol **59**: 651–681

Negrão S, Schmöckel SM, Tester M (2017) Evaluating physiological responses of plants to salinity stress. Ann Bot **119**: 1–11

Neves J, Sampaio M, Séneca A, Pereira S, Pissarra J, Pereira C (2021) Abiotic stress triggers the expression of genes involved in protein storage vacuole and exocyst-mediated routes. Int J Mol Sci. doi: 10.3390/ijms221910644

Paris N, Stanley CM, Jones RL, Rogers JC (1996) Plant Cells Contain Two

Functionally Distinct Vacuolar Compartments. Cell **85**: 563–572

Park CJ, Park JM (2019) Endoplasmic reticulum plays a critical role in integrating signals generated by both biotic and abiotic stress in plants. Front Plant Sci. doi: 10.3389/fpls.2019.00399

Pedroso FKJ V, Prudente DA, Bueno ACR, Machado EC, Ribeiro R V (2014) Drought tolerance in citrus trees is enhanced by rootstock-dependent changes in root growth and carbohydrate availability. Environ Exp Bot **101**: 26–35

Pereira C, Pereira S, Satiat-Jeunemaitre B, Pissarra J (2013) Cardosin A contains two vacuolar sorting signals using different vacuolar routes in tobacco epidermal cells. Plant J. doi: 10.1111/tpj.12274

Pereira C, Di Sansebastiano G Pietro (2021) Mechanisms of membrane traffic in plant cells. Plant Physiol Biochem **169**: 102–111

Piotto FA, Carvalho MEA, Souza LA, Rabêlo FHS, Franco MR, Batagin-Piotto KD, Azevedo RA (2018) Estimating tomato tolerance to heavy metal toxicity: cadmium as study case. Environ Sci Pollut Res **25**: 27535–27544

Queval G, Jaillard D, Zechmann B, Noctor G (2011) Increased intracellular H2O2 availability preferentially drives glutathione accumulation in vacuoles and chloroplasts. Plant, Cell Environ **34**: 21–32

Rengasamy P (2006) World salinization with emphasis on Australia. J Exp Bot **57**: 1017–1023

Robinson DG, Ding Y, Jiang L (2016) Unconventional protein secretion in plants: a critical assessment. Protoplasma **253**: 31–43

Robinson DG, Neuhaus J (2016) Receptor-mediated sorting of soluble vacuolar proteins : myths , facts , and a new model. **67**: 4435–4449

Rogers JC (2008) Multiple vacuoles in plant cells. Plant Physiol **146**: 1024–1025

Rosquete MR, Drakakaki G (2018) Plant TGN in the stress response: a compartmentalized overview. Curr Opin Plant Biol **46**: 122–129

Sampaio M, Neves J, Cardoso T, Pissarra J, Pereira S, Pereira C (2022) Coping with Abiotic Stress in Plants—An Endomembrane Trafficking Perspective. Plants 1–15

Sanderfoot AA, Kovaleva V, Bassham DC, Raikhel N V (2001) Interactions between syntaxins identify at least five SNARE complexes within the Golgi/prevacuolar

system of the Arabidopsis cell. Mol Biol Cell **12**: 3733–3743

Sanmartín M, Ordóñez A, Sohn EJ, Robert S, Sánchez-Serrano JJ, Surpin MA, Raikhel N V., Rojo E (2007) Divergent functions of VTI12 and VTI11 in trafficking to storage and lytic vacuoles in Arabidopsis. Proc Natl Acad Sci U S A **104**: 3645–3650

Di Sansebastiano GP, Faraco M, Zouhar J, Dalessandro G (2009) The study of plant SNAREs specificity in vivo. Plant Biosyst **143**: 621–629

Shabala S, Cuin TA (2008) Potassium transport and plant salt tolerance. Physiol Plant **133**: 651–669

Shaner NC, Lambert GG, Chammas A, Ni Y, Cranfill PJ, Baird MA, Sell BR, Allen JR, Day RN, Israelsson M, et al (2013) A bright monomeric green fluorescent protein derived from Branchiostoma lanceolatum. Nat Methods **10**: 407–409

Sharma P, Jha A, Dubey R, Pessarakli M (2012a) Reactive Oxygen Species, Oxidative Damage, and Antioxidative Defense Mechanism in Plants under Stressful Conditions. J Bot. doi: 10.1155/2012/217037

Sharma P, Jha AB, Dubey RS, Pessarakli M (2012b) Reactive Oxygen Species, Oxidative Damage, and Antioxidative Defense Mechanism in Plants under Stressful Conditions. J Bot **2012**: 1–26

Shen Y, Wang J, Ding Y, Lo SW, Gouzerh G, Neuhaus JM, Jiang L (2011) The rice RMR1 associates with a distinct prevacuolar compartment for the protein storage vacuole pathway. Mol Plant **4**: 854–868

Shimada T, Kuroyanagi M, Nishimura M, Hara-Nishimura I (1997) A Pumpkin 72-kDa Membrane Protein of Precursor-Accumulating Vesicles Has Characteristics of a Vacuolar Sorting Receptor. Plant Cell Physiol **38**: 1414–1420

Shimada T, Watanabe E, Tamura K, Hayashi Y, Nishimura M, Hara-Nishimura I (2002) A Vacuolar Sorting Receptor PV72 on the Membrane of Vesicles that Accumulate Precursors of Seed Storage Proteins (PAC Vesicles). Plant Cell Physiol **43**: 1086–1095

Shirakawa M, Ueda H, Shimada T, Koumoto Y, Shimada TL, Kondo M, Takahashi T, Okuyama Y, Nishimura M, Hara-Nishimura I (2010) Arabidopsis Qa-SNARE SYP2 proteins localized to different subcellular regions function redundantly in vacuolar protein sorting and plant development. Plant J **64**: 924–935

Shomer I, Novacky AJ, Pike SM, Yermiyahu U, Kinraide TB (2003) Electrical Potentials of Plant Cell Walls in Response to the Ionic Environment. Plant Physiol **133**: 411–422

Shpilka T, Weidberg H, Pietrokovski S, Elazar Z (2011) Atg8: an autophagy-related ubiquitin-like protein family. Genome Biol **12**: 226

Soares C, Branco-Neves S, de Sousa A, Pereira R, Fidalgo F (2016) Ecotoxicological relevance of nano-NiO and acetaminophen to Hordeum vulgare L.: Combining standardized procedures and physiological endpoints. Chemosphere **165**: 442–452

Soares C, Carvalho MEA, Azevedo RA, Fidalgo F (2019) Plants facing oxidative challenges—A little help from the antioxidant networks. Environ Exp Bot **161**: 4–25

Sousa B, Rodrigues F, Soares C, Martins M, Azenha M, Lino-Neto T, Santos C, Cunha A, Fidalgo F (2022) Impact of Combined Heat and Salt Stresses on Tomato Plants—Insights into Nutrient Uptake and Redox Homeostasis. Antioxidants **11**: 1–21

Sousa B, Soares C, Oliveira F, Martins M, Branco-Neves S, Barbosa B, Ataíde I, Teixeira J, Azenha M, Azevedo RA, et al (2020) Foliar application of 24-epibrassinolide improves Solanum nigrum L. tolerance to high levels of Zn without affecting its remediation potential. Chemosphere **244**: 1–11

Spormann S, Soares C, Martins V, Azenha M, Gerós H, Fidalgo F (2022) Early Activation of Antioxidant Responses in Ni-Stressed Tomato Cultivars Determines Their Resilience Under Co-exposure to Drought. J Plant Growth Regul. doi: 10.1007/s00344-022-10595-4

Staehelin A (1997) The Plant ER: a dynamic organelle composed of a large number of discrete functional domains. Plant J **11**: 1151–1165

Stefano G, Brandizzi F (2018) Advances in Plant ER Architecture and Dynamics. Plant Physiol **176**: 178–186

Stigliano E, Faraco M, Neuhaus J-MM, Montefusco A, Dalessandro G, Piro G, Di Sansebastiano G-P Pietro (2013) Two glycosylated vacuolar GFPs are new markers for ER-to-vacuole sorting. Plant Physiol Biochem **73**: 337–343

Stigliano E, Sansebastiano G-P, Neuhaus J-M (2014) Contribution of Chitinase A's C-Terminal Vacuolar Sorting Determinant to the Study of Soluble Protein Compartmentation. Int J Mol Sci **15**: 11030–11039

Su T, Li X, Yang M, Shao Q, Zhao Y, Ma C, Wang P (2020) Autophagy: An Intracellular Degradation Pathway Regulating Plant Survival and Stress Response. Front Plant Sci **11**: 1–16

Su T, Wang P, Li H, Zhao Y, Lu Y, Dai P, Ren T, Wang X, Li X, Shao Q, et al (2018) The Arabidopsis catalase triple mutant reveals important roles of catalases and peroxisome-derived signaling in plant development. J Integr Plant Biol **60**: 591–607

Suo J, Zhao Q, David L, Chen S, Dai S (2017) Salinity Response in Chloroplasts: Insights from Gene Characterization. Int J Mol Sci . doi: 10.3390/ijms18051011

Surpin M, Zheng H, Morita MT, Saito C, Avila E, Blakeslee JJ, Bandyopadhyay A, Kovaleva V, Carter D, Murphy A, et al (2003) The VTI Family of SNARE Proteins Is Necessary for Plant Viability and Mediates Different Protein Transport Pathways. Plant Cell **15**: 2885–2899

Synek L, Schlager N, Eliás M, Quentin M, Hauser M-T, Zárský V (2006) AtEXO70A1, a member of a family of putative exocyst subunits specifically expanded in land plants, is important for polar growth and plant development. Plant J **48**: 54–72

Taiz L, Zeiger Ian Max Møller E, Murphy A Fisiologia e Desenvolvimento Vegetal.

Taiz L, Zeiger Ian Max Møller E, Murphy A (2017) Fisiologia e Desenvolvimento Vegetal, 6ª.

Tang RJ, Zhao FG, Garcia VJ, Kleist TJ, Yang L, Zhang HX, Luan S (2015) Tonoplast CBL-CIPK calcium signaling network regulates magnesium homeostasis in Arabidopsis. Proc Natl Acad Sci U S A **112**: 3134–3139

Viotti C, Krüger F, Krebs M, Neubert C, Fink F, Lupanga U, Scheuring D, Boutté Y, Frescatada-Rosa M, Wolfenstetter S, et al (2013) The endoplasmic reticulum is the main membrane source for biogenesis of the lytic vacuole in Arabidopsis. Plant Cell **25**: 3434–3449

Walter P, Ron D (2011) The unfolded protein response: From stress pathway to homeostatic regulation. Science (80-) **334**: 1081–1086

Wang H, Rogers JC, Jiang L (2011) Plant RMR proteins: Unique vacuolar sorting receptors that couple ligand sorting with membrane internalization. FEBS J **278**: 59–68

Wang J, Ding Y, Wang J, Hillmer S, Miao Y, Lo SW, Wang X, Robinson DG, Jiang L (2010) EXPO, an exocyst-positive organelle distinct from multivesicular endosomes

and autophagosomes, mediates cytosol to cell wall exocytosis in arabidopsis and tobacco cells. Plant Cell **22**: 4009–4030

Wang P, Hawes C, Hussey PJ (2017a) Plant Endoplasmic Reticulum–Plasma Membrane Contact Sites. Trends Plant Sci **22**: 289–297

Wang P, Mugume Y, Bassham DC (2018) New advances in autophagy in plants: Regulation, selectivity and function. Semin Cell Dev Biol **80**: 113–122

Wang R, Wang J, Zhao L, Yang S, Song Y (2015) Impact of heavy metal stresses on the growth and auxin homeostasis of Arabidopsis seedlings. BioMetals **28**: 123–132

Wang X, Chung KP, Lin W, Jiang L (2017b) Protein secretion in plants: Conventional and unconventional pathways and new techniques. J Exp Bot **69**: 21–37

Wang X, Xu M, Gao C, Zeng Y, Cui Y, Shen W, Jiang L (2020) The roles of endomembrane trafficking in plant abiotic stress responses. J Integr Plant Biol **62**: 55–69

Wu H, Zhang X, Giraldo JP, Shabala S (2018) It is not all about sodium: revealing tissue specificity and signalling roles of potassium in plant responses to salt stress. Plant Soil **431**: 1–17

Xiang L, Etxeberria E, Van Den Ende W (2013) Vacuolar protein sorting mechanisms in plants. FEBS J **280**: 979–993

Yamazaki M, Shimada T, Takahashi H, Tamura K, Kondo M, Nishimura M, Hara-Nishimura I (2008) Arabidopsis VPS35, a retromer component, is required for vacuolar protein sorting and involved in plant growth and leaf senescence. Plant Cell Physiol **49**: 142–156

Žárský V, Kulich I, Fendrych M, Pečenková T (2013) Exocyst complexes multiple functions in plant cells secretory pathways. Curr Opin Plant Biol **16**: 726–733

Zhang X, Li H, Lu H, Hwang I (2021) The trafficking machinery of lytic and protein storage vacuoles: How much is shared and how much is distinct? J Exp Bot **72**: 3504–3512

Zhang Y, Kaiser E, Li T, Marcelis LFM (2022) NaCl affects photosynthetic and stomatal dynamics by osmotic effects and reduces photosynthetic capacity by ionic effects in tomato. J Exp Bot **73**: 3637–3650

Zhao C, Zhang H, Song C, Zhu JK, Shabala S (2020) Mechanisms of Plant Responses and Adaptation to Soil Salinity. Innov **1**: 100017

Zhu D, Zhang M, Gao C, Shen J (2020) Protein trafficking in plant cells : tools and markers. **63**: 343–363

Zhu J, Lee B-H, Dellinger M, Cui X, Zhang C, Wu S, Nothnagel EA, Zhu J-K (2010) A cellulose synthase-like protein is required for osmotic stress tolerance in Arabidopsis. Plant J **63**: 128–140

Zhu JK (2016) Abiotic Stress Signaling and Responses in Plants. Cell **167**: 313–324

Zouhar J, Muñoz A, Rojo E (2010) Functional specialization within the vacuolar sorting receptor family: VSR1, VSR3 and VSR4 sort vacuolar storage cargo in seeds and vegetative tissues. Plant J **64**: 577–588

Zouhar J, Rojo E, Bassham DC (2009) AtVPS45 is a positive regulator of the SYP41/SYP61/VTI12 SNARE complex involved in trafficking of vacuolar cargo1[OA]. Plant Physiol **149**: 1668–1678

7. Appendix

	1	2	3	4	5	6	7
A	Unk-1 Gene to study Control	Unk-1 Gene to study Control	Unk-1 Gene to study Control	Unk-2 Gene to study Control	Unk-2 Gene to study Control	Unk-2 Gene to study Control	Unk-3 Gene to stud Control
B	Unk-4 Gene to study S1	Unk-4 Gene to study S1	Unk-4 Gene to study S1	Unk-5 Gene to study S1	Unk-5 Gene to study S1	Unk-5 Gene to study S1	Unk-6 Gene to stud S1
C	Unk-7 Gene to study H1	Unk-7 Gene to study H1	Unk-7 Gene to study H1	Unk-8 Gene to study H1	Unk-8 Gene to study H1	Unk-8 Gene to study H1	Unk-9 Gene to stud H1
D	Unk-10 Gene to study H2	Unk-10 Gene to study H2	Unk-10 Gene to study H2	Unk-11 Gene to study H2	Unk-11 Gene to study H2	Unk-11 Gene to study H2	Unk-12 Gene to stud H2
E	Unk-13 Gene to study Ox	Unk-13 Gene to study Ox	Unk-13 Gene to study Ox	Unk-14 Gene to study Ox	Unk-14 Gene to study Ox	Unk-14 Gene to study Ox	Unk-15 Gene to stud Ox
F	Unk-16 Gene to study Zn	Unk-16 Gene to study Zn	Unk-16 Gene to study Zn	Unk-17 Gene to study Zn	Unk-17 Gene to study Zn	Unk-17 Gene to study Zn	Unk-18 Gene to stud Zn
G							
H							

Supplementary Figure 1 - Plate Design to the gene expression
Wells 1,2,3 – technical replicate sample 1; Wells 4,5,6 – technical replicate sample 2; Wells 7,8,9 – technical replicate sample 3
Line A – Control; Line B – S1; Line C- H1; Line D – H2; Line E – Ox; Line F – Zn

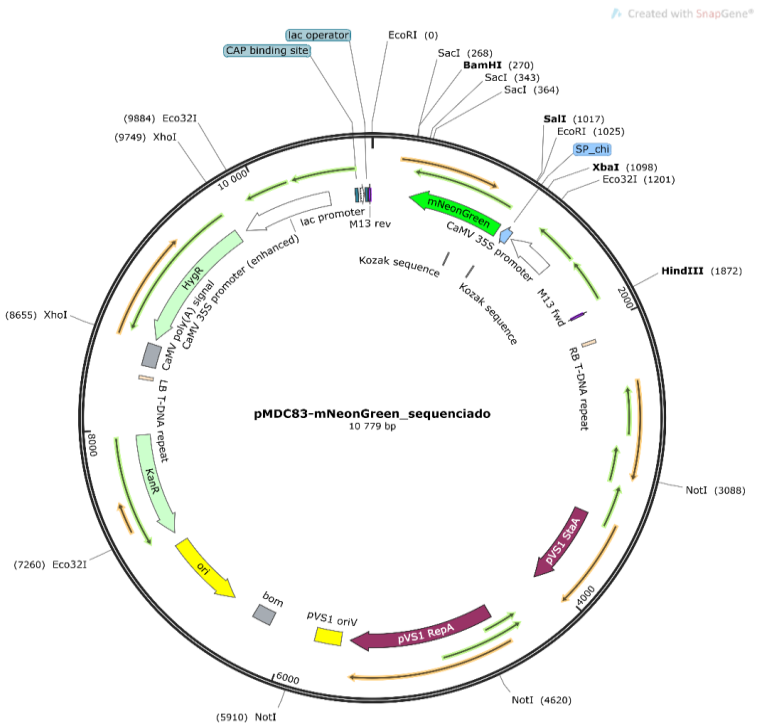

Supplementary Figure 2 – pMDC83-mNeongreen map used for cloning

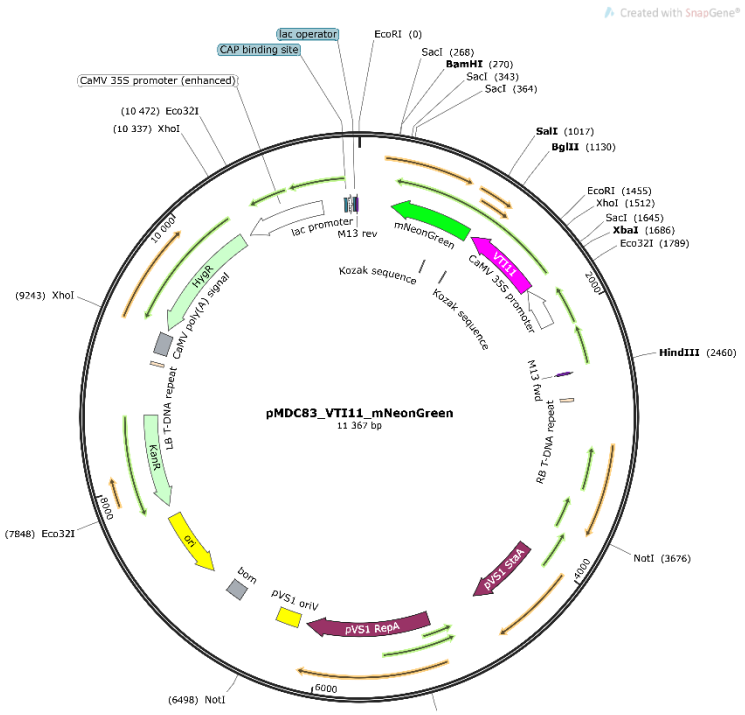

Supplementary Figure 1 - pMDC83-VTI11-mNeonGreen Map

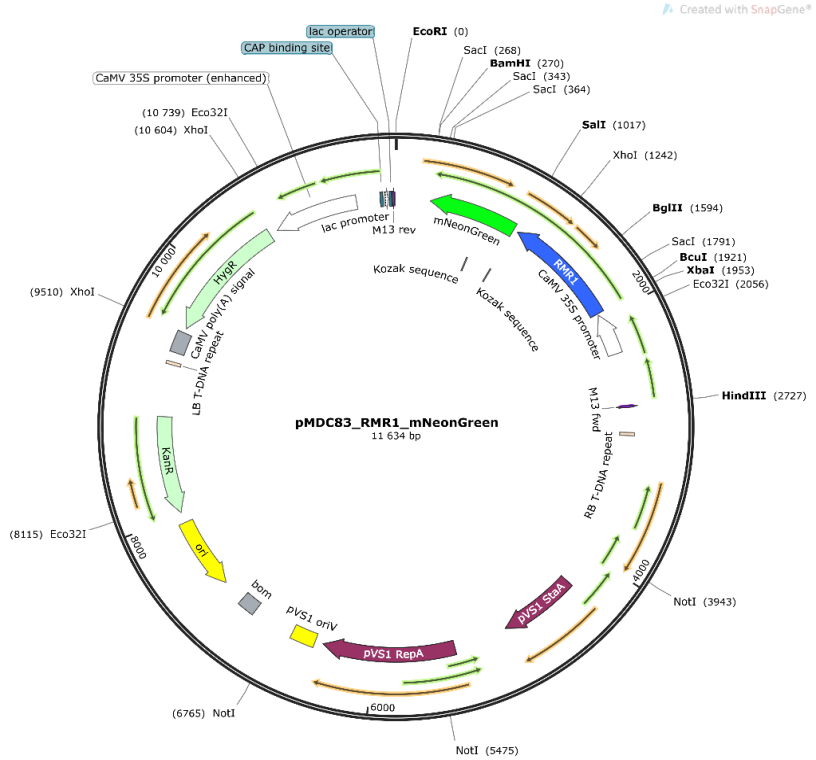

Supplementary Figure 2 - pMDC83-RMR1-mNeongreen map

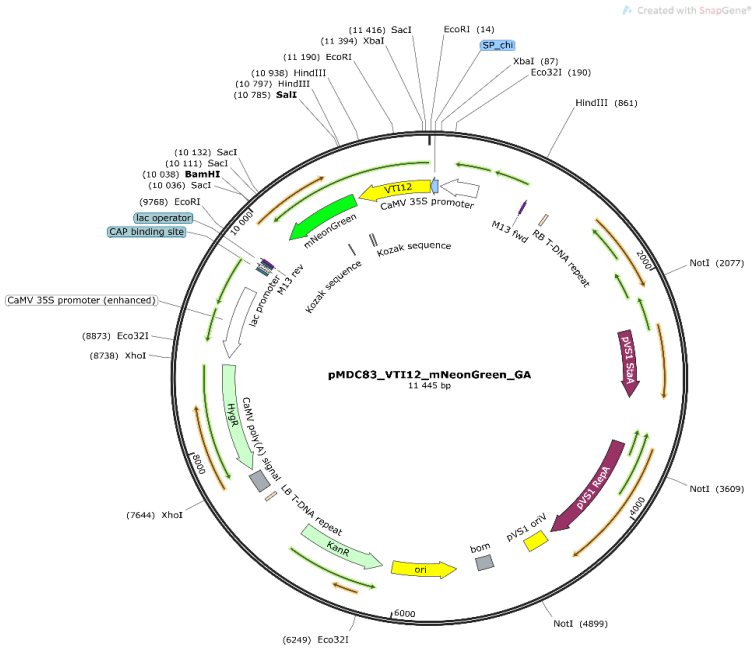

Supplementary Figure 3 - pMDC83-VTI12-mNeongreen map

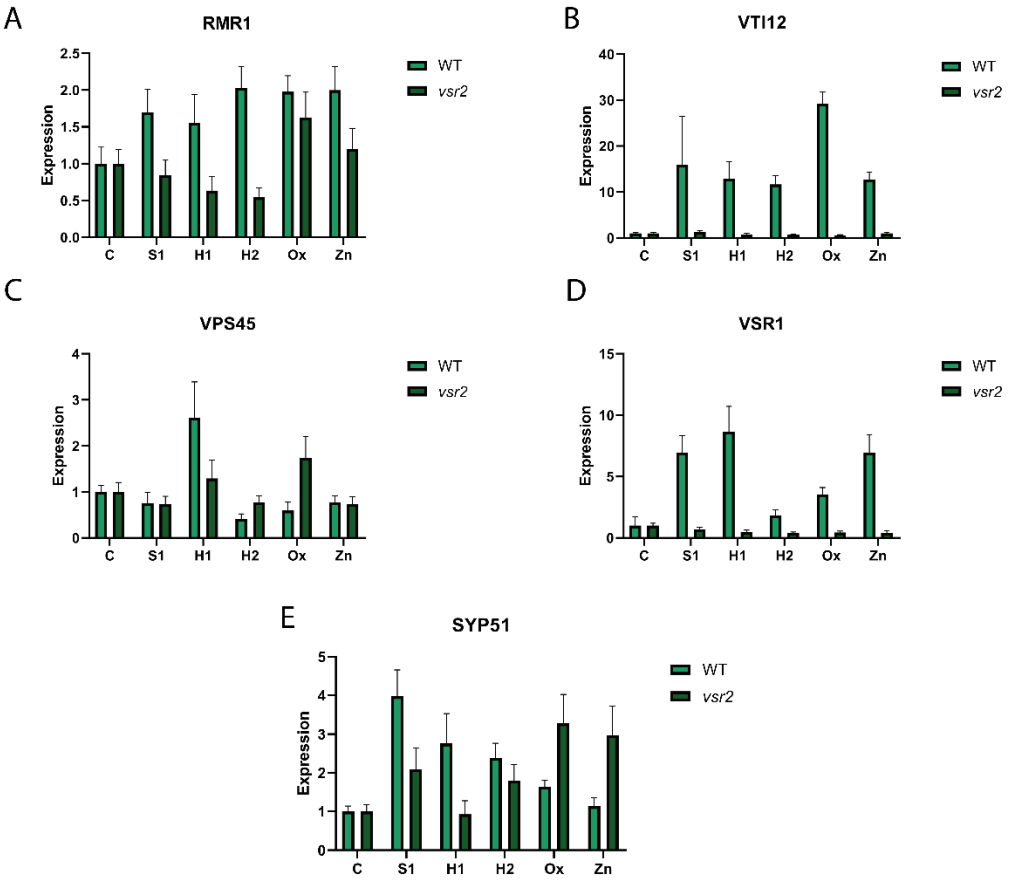

Supplementary Figure 4 – Comparison between qPCR results obtained in wt with *vsr2* line.

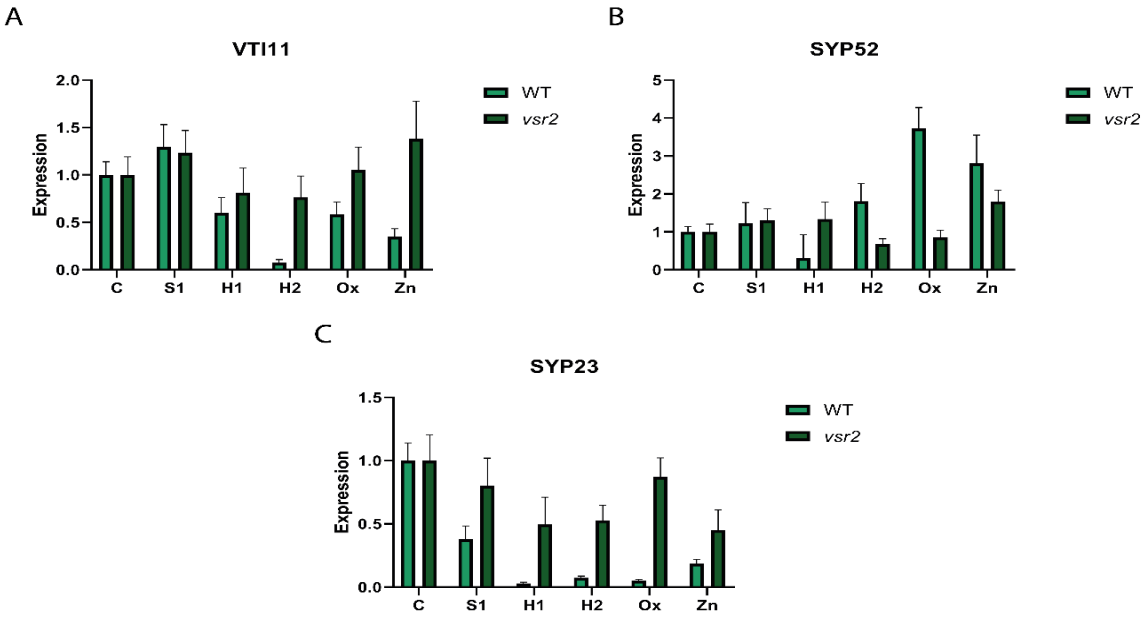

Supplementary Figure 5 - Comparison between qPCR results obtained in wt with *vsr2* line.

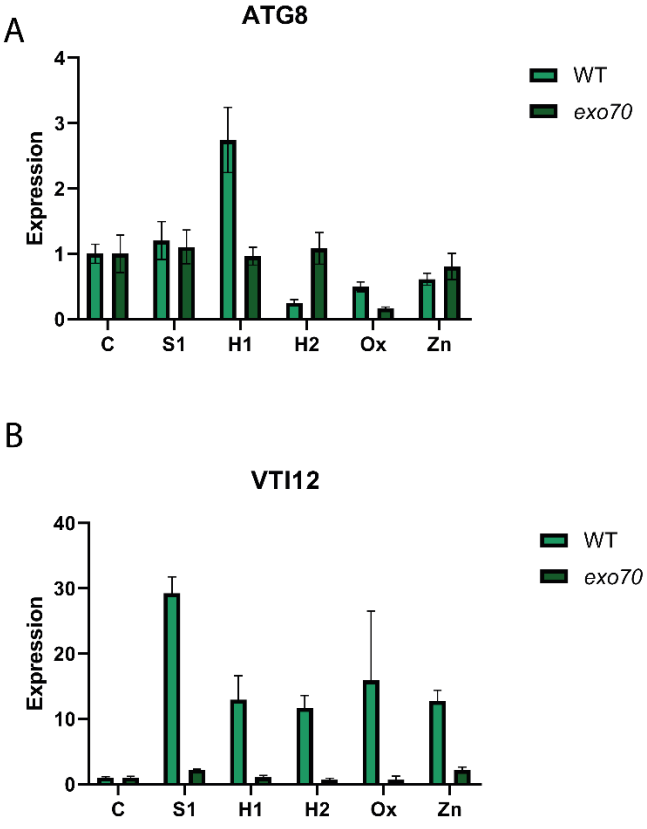

Supplementary Figure 6 - Comparison between qPCR results obtained in wt with *exo70* line.

Supplementary Table 1 – Primers used for genptyping T-DNA lines

Targerts	Primer	Sequence (5'-3')
SYP51	LP	CCATGAGAAAGCTTCGCTATG
	RP	GCCTCGTTGTATGCTCTCATC
VTI12	LP	TTTCATGCTCTGACGTGACAG
	RP	CTTGAGGCAAGAAGTTTGCAG
RMR1	LP	CCAAGACTACTTTCCGTTCCC
	RP	TCGAATCATATACAGGGCCAG
VTI11	LP	TTGTCTGAAATAAAATCCGGG
	RP	GCGAGATGTAGACCTCGATTG
EXO-70	LP	CCAGGATCAAAATCAAACACC
	RP	CCCCAAACTATAAGCTCCCAC
VSR2	LP	TTGTTAATCTCATTTAAACCCAAGC
	RP	TCCTCTGTGATTTGCACTCATC
RMR2	LP	CTGCACGGATACTCAACTTCC
	RP	GAAATTGACACGTCAGCTTCC
SYP22	LP	TGCATCAACAATCAAGCAAAG
	RP	TTGGCAAGAAAAACAGAAACG
SYP23	LP	GCTTGGCAGTAACAGTTGCTC
	RP	ATGAGATTGCGTTCAATGAGG
Line specific	LBb1.3 Salk	ATTTTGCCGATTTCGGAAC
	LB1 SAIL	GCCTTTTCAGAAATGGATAAATAGCCTTGCTTCC

Supplementary Table 2 – List of genes and primers used for qPCR assyas

Targets	Primers	Sequence (5'-3')
SAND	Fwd	AACTCTATGCAGCATTTGATCCACT
	Rev	
UBC9[1]	Fwd	TCACAATTTCCAAGGTGCTGC
	Rev	TCATCTGGGTTTGGATCCGT
VSR2	Fwd	CGCTGGATTGCCCACATTCGT
	Rev	TTGCGCATTCCACGCCTTCA
RMR1	Fwd	GCGAGGGAGGCACACCAGGA
	Rev	TTTCCCCGGCCTTGTGGTGA
EXO70	Fwd	TCCCCGATGAAACAGGCTCGTC
	Rev	GCCTCCATGAAAGGGGCGTGT
SYP51	Fwd	TGGCGTCTTCATCGGATTCATGG
	Rev	AGCTGAAGCACGACGCTGAGCA
VTI12	Fwd	GCAATGTCCGTGGAGAGGCTTGA
	Rev	TGCGCATGAAGGAGGGTTTGG
VSR1	Fwd	GGGAGCGGCGCAGATTCTTG

	Rev	GCCGGTTTCATTCGCCACCTT
SYP23	Fwd	GCAGCGTGCCCTTCTTGTGG
	Rev	TCCTTGGGCAGTTGCAGCGTA
VTI11	Fwd	GATTTTCCGACTCCGACGTA
	Rev	CAAACGCGTCACTCATTGTT
SYP52	Fwd	ATGTGGTGGCAACTTGTGAA
	Rev	CTTTGCCTCACAGACACGAA
VPS45	Fwd	CAGTTGTCGATCCCTCTGGT
	Rev	TTTCAACGCCAGAAACACTG
ATG8	Fwd	TTGCTTGCTTGAAATTCGCA
	Rev	TTCACTCATCCTTGCCTCGA

[1] from (Czechowski et al., 2005)

Supplementary Table 3 -Primers used for Cloning techniques

Target	Primer	Sequence (5'-3')	Function
M13	Universal	TGTAAAACGACGGCCAGT	Sequencing
AtRMR1	oC359	aaaaTCTAGAATGAGACTCGTCGTCTCAAG	Add a XbaI site
	oC360	aaaaGTCGACACGGCTTTGACTGGATTG	Add a SalI site
VTI11	oC480	aaaTCTAGAATGAGTGACGTGTTTGATGG	Add a XbaI site
	oC481	aaaGTCGACCTTGGTGAGTTTGAAGTAC	Add a SalI site
pMDC83-mNeonGreen	oC416	cgcatacagctcgataatcttttcagggctttg	Gibson Assembley
	oC417	caaagccctgaaaagattatcgagctgtatgcg	Gibson Assembley
	oC548	ACGTCGCTCATGTGAATTCGGCCGAGGATAA	Gibson Assembley
	oC551	AGCTTTCTCATGTCGACTCCGGACTCAGATC	Gibson Assembley
VTI12	oC549	GCCGAATTCACATGAGCGACGTATTTGAAGG	Gibson Assembley
	oC550	CCGGAGTCGACATGAGAAAGCTTGTATGAGA	Gibson Assembley